

# **Lipid droplet formation drives pathogenic ILC2 responses in airway inflammation**

A thesis submitted for the degree of  
Doctor of Philosophy (PhD)  
in Experimental Medicine

Medical Faculty  
Rheinische Friedrich-Wilhelms-University Bonn

**Schekufe Kharabi Masouleh**  
Wuppertal, Germany

Bonn 2020

**1<sup>st</sup> corrector: Prof. Dr. Christoph Wilhelm**

Institute of Clinical Chemistry and Clinical Pharmacology  
University Hospital Bonn

**2<sup>st</sup> corrector: Prof. Dr. Christian Kurts**

Institute of Experimental Immunology  
University Hospital Bonn

Institute for Clinical Chemistry and Clinical Pharmacology  
University Hospital Bonn

Director: Prof. Dr. Gunther Hartmann

Made with permission of the Medical Faculty of the University of Bonn

Oral examination: 20.05.2020

<b>List of Abbreviations .....</b>	<b>1</b>
<b>1. Introduction.....</b>	<b>3</b>
1.1. Chronic inflammatory diseases .....	3
1.2. The immune system - innate and adaptive immunity .....	3
1.3. Discovery, development and phenotype of innate lymphoid cells .....	6
1.4. ILC2 as drivers of allergic lung inflammation.....	10
1.5. Role of metabolism in immune cell function .....	13
1.6. Ketogenic diet - a unique metabolic state .....	15
1.7. PPAR $\gamma$ - a regulator in energy metabolism .....	16
1.8. Lipid droplets - regulators of lipid metabolism .....	18
1.9. Aims of the thesis .....	22
<b>2. Material and Methods .....</b>	<b>23</b>
2.1. Animals.....	23
2.2. Intranasal administration of papain and alternaria alternata .....	23
2.3. Intranasal administration of IL-33, IL-25 and TSLP.....	24
2.4. Cell isolation from tissues.....	24
2.5. Flow cytometry analysis .....	24
2.6. Re-stimulation of cells for intracellular cytokine staining .....	25
2.7. Fluorescence-activated cell sorting .....	25
2.8. Purification of ILC2 .....	25
2.9. In vitro culture of ILC2 .....	25
2.10. Cytokine measurements.....	26
2.11. BODIPY $^{\text{®}}$ 493/503, BODIPY $^{\text{®}}$ FL C16 and 2-NBDG stainings.....	26
2.12. Alkyne labeled palmitic acid uptake and staining .....	26
2.13. Flow cytometric determination of apoptosis .....	27
2.14. Lipid peroxidation staining.....	27
2.15. In vivo inhibitor treatment .....	27
2.16. Diet studies.....	28
2.17. Antibiotic treatment.....	28
2.18. Measurement of free fatty acids, glucose and ketone bodies .....	28
2.19. Histology - PAS staining .....	28
2.20. Confocal microscopy .....	28
2.21. Real-time PCR. ....	29

2.22. Seahorse Analysis.....	29
2.23. Key resources table.....	32
<b>3. Results .....</b>	<b>38</b>
3.1. Activation of ILC2 increased external glucose and FA uptake and induces lipid droplet formation .....	38
3.2. IL-33 promotes acquisition of external FA and LD formation in activated ILC2.....	44
3.3 DGAT1 dependent LD formation protects ILC2 from lipotoxicity and allows for increased uptake of external lipids .....	48
3.4 PPAR $\gamma$ regulated FA uptake fuels proliferation and cytokine production.....	54
3.5 Glucose and external FA cooperate to control fatty acid metabolism in ILC2 ....	61
3.6 Ketogenic diet abrogates ILC2-driven airway inflammation .....	64
<b>4. Discussion .....</b>	<b>71</b>
<b>5. Summary .....</b>	<b>79</b>
<b>6. List of figures.....</b>	<b>80</b>
<b>7. Literature.....</b>	<b>82</b>
<b>8. Acknowledgements .....</b>	<b>97</b>

## List of Abbreviations

AAM	alternatively activated macrophages
RA	retinoic acid
APC	antigen presenting cell
ATGL	adipose triglyceride lipase
COPD	chronic obstructive pulmonary disease
CPT1	carnitin-acyltransferase-1
DC	dendritic cell
DGAT	diacylglycerol o-acyltransferase
ER	endoplasmic reticulum
FA	fatty acid
FAO	fatty acid oxidation
FFA	free fatty acid
IFN- $\gamma$	interferon- $\gamma$
Ig	immunoglobulin
IL	interleukin
ILC	innate lymphoid cells
KD	ketogenic diet
LD	lipid droplet
LPS	lipopolysaccharide
LTi	lymphoid tissue inducer
MHC	major histocompatibility complex
CLP	common lymphoid progenitor
mLN	mediastinal lymph node
mRNA	messenger ribonucleic acid
NK	natural killer
OXPPOS	oxidative phosphorylation
PBS	phosphate buffered saline
PPAR	peroxisome proliferation-activated receptors

PPP	pentose-phosphate-pathway
PRR	pattern recognition receptor
RAG	recombination activating gene
ROR $\alpha$	retinoic acid receptor- related orphan receptor alpha
TAG	Triacylglycerol
TCA	tricarboxylic acid
TCR	T cell receptor
T <sub>H</sub>	T helper
TLR	Toll-like receptors
TNF- $\alpha$	tumor necrosis factor- $\alpha$
Tregs	regulatory T cells
TSLP	thymic stromal lymphopietin
HDM	house dust mite
WT	wild type

# **1. Introduction**

## **1.1. Chronic inflammatory diseases**

Chronic inflammation plays a central role in some of the most challenging inflammatory diseases of our time. Inflammation is a response to damage and potential danger signals in the body. However, the immune system can turn against the body in diseases like rheumatoid arthritis, asthma, ulcerative colitis, Crohn's disease and lupus. An inflammation can be acute or chronic. An acute inflammation is the first and immediate response to injury or stress, infection or physical trauma to induce repair processes. When the inflammation sustains, it can become chronic. This state requires medical intervention for controlling and stopping further tissue damage caused by uncontrolled inflammation (1) (2) (3). A wide variety of factors associated with westernization, such as changes in diet, increase of pollution and decreased incidence of infections are considered to be important aspects for disease development (4) (5). Understanding processes involved in chronic inflammation can help to treat or prevent diseases and is a main focus in today's research.

## **1.2. The immune system - innate and adaptive immunity**

The immune system is a highly complex defense system that protects against pathogens such as parasites, bacteria or viruses and foreign substances. The first natural barriers for protection are the skin and the mucous membranes. Nevertheless, these mechanical and physical barriers are often breached and need further support, which is provided by specialized cell, such as macrophages and monocytes. These cells can recognize foreign materials or pathogen and react to protect the host from damage or infection.

The overall function of the immune system is not only limited to the protection of the host, but includes the regulation of the immune response to limit a possible self-damage, which results in the development of autoimmune diseases, and the identification and destruction of mutant cells, which can promote the formation of tumors. The immune system is classified into the innate and adaptive immunity (6) (7).

The nonspecific, **innate immune system** is the first line of defense against pathogens or foreign substances, before the adaptive immune system gets involved. The cellular components of the innate immune system include phagocytic cells such as macrophages, mast cells, granulocytes such as neutrophils, eosinophils and basophils, as well as natural killer (NK) cells, which are able to engulf and eliminate pathogens or cell debris by phagocytosis. In addition, isozyme, interferons and the complement system, which is activated for the elimination of bacteria, belong to the humoral mechanisms of the innate immune system (8). Macrophages are involved in the induction of an inflammatory response by releasing various cytokines and chemokines after their activation (9), which are used for the recruitment of neutrophils. Macrophages and neutrophils, as well as dendritic cells (DC) are able to phagocytose pathogens and degrade them by proteolytic enzymes present in their granules (10). Macrophages and DC are also defined as antigen presenting cells (APC) due to their ability to absorb foreign material or modified self-molecules by phagocytosis and present them as processed antigens on certain molecules on their surface. APC are of great relevance to the activation of the adaptive immune system (11). Another class of cells that belong to the innate immune system are innate lymphoid cells (ILC), a group of immune cells at barrier surfaces which have an important role in homeostasis and inflammation. Cells of the innate immune system are capable of binding molecules expressed by several pathogens, for example, lipopolysaccharides (LPS), expressed on the surface of gram-negative bacteria or DNA or RNA of bacteria or viruses via a series of pattern recognition receptors (PRRs). This occurs via the recognition of pathogen-associated molecular patterns (PAMPs) (12) (13). These structures are not expressed in higher eukaryotes and thus on the body's own cells (9)(14). Of great importance are the recognition receptors of the family of Toll-like receptors (TLRs). TLRs are signaling receptors present on DC and macrophages lead to the release of proinflammatory cytokines, such as interleukin IL-1, IL-6 and IL-8, upon recognition of pathogens (15). These cytokines can help to eliminate pathogens and result in the recruitment of additional phagocytic cells, such as monocytes and neutrophils (9).



The **adaptive immune system** plays an important role in the protection of the organism if the mechanisms of the innate immune system are insufficient to eliminate foreign substances and pathogens. It is characterized by antigen specificity and formation of an immunological memory. Immunological memory allows faster, more specific and thus more effective control upon reinfection (16). Antigen-specific T and B lymphocytes, which are generated in the bone marrow, are the main players of the adaptive immune system. They circulate in the blood and lymphatic system and are found mainly in the secondary lymphoid organs, like in the lymph nodes and in the spleen.

As already mentioned, APC are very important for the initiation of the adaptive immune response. Upon activation, they migrate to the lymph nodes where they present the previously encountered antigens to the T lymphocytes. The interaction between APC and T cells takes part by the binding of the major histocompatibility complex (MHC) molecules, expressed on APC and the T cell receptors (TCR) which, unlike cells of the innate immune system, cannot recognize pathogen patterns, but highly specific peptide fragments. These antigens are presented bound to MHC class I or II proteins on the surface of APC (17). T cells are differentiated into two classes: the cytotoxic T cells (CTL or TC cells) and T helper cell ( $T_H$  cells) (18).

The TC cells express a CD8 co-receptor which binds to MHC class I molecules found on almost all nucleated cells of the organism. The MHC class I molecules present peptide fragments that are consistently cleaved from the cell's own proteins. Thus, even in a viral infection, they present virus peptides, which are recognized as foreign by the CD8 T cells and finally leading to the lysis of the infected cell. The presentation of endogenous peptides on the MHC class I molecules result in a low affinity binding with CD8 molecules, which does not induce the killing of MHC class I expressing cells.  $T_H$  cells possess a CD4 co-receptor which can bind the MHC class II molecules, expressed only on APC. MHC class II molecules present extracellular peptides previously picked up by the APC (19)(17).  $T_H$  cells can be subdivided into four subpopulations (20). Effector helper T cells  $T_{H1}$  secrete interferon- $\gamma$  (IFN- $\gamma$ ) and tumor necrosis factor- $\alpha$  (TNF- $\alpha$ ) and activate macrophages and CTL to kill microbes and infected cells. They also stimulate B cells to secrete subclasses of immunoglobulin G (IgG) antibodies. In contrast, effector helper T cells  $T_{H2}$  secrete IL-4, IL-5, IL-10 and IL-13 and defend the body against extracellular pathogens. They are also able to stimulate B cells to produce IgE and IgG

antibodies, that bind to mast cells, basophils and eosinophils (21)( 22). T<sub>H</sub>17 cells produce IL-17 and are involved in stimulating a neutrophil-dependent immune responses. They are also crucial in maintaining mucosal barriers (23). Regulatory T cells (T<sub>regs</sub>) are of great importance for the inhibition of an immune response and thus have an anti-inflammatory effect by secreting IL-10 and TGF- $\beta$  (24).

B cells acquire antigens via receptors termed immunoglobulins (Ig) (25). These can be membrane-bound or in soluble form in the plasma as antibodies. These antibodies consist of a constant and a variable region: the constant region determines the antibody class (IgM, IgG, IgD, IgA, IgE) and the variable region represents the antigen-binding site (26). B cells are activated by previously activated T<sub>H</sub> cells. The proliferation and maturation of B cells to antibody-producing plasma cells is mediated by the release of various cytokines from activated T<sub>H</sub> cells. The soluble antibodies are released into the blood, where they can opsonize antigens and form the T-cell independent humoral adaptive immune response (25). After opsonization, the antibody-antigene complexes are recognized and phagocytized by macrophages or neutrophils.

A fraction of activated T and B cells differentiate into effector cells after antigen contact and migrate to the inflammatory site; another fraction differentiates to the so-called memory cells, which are specific of the adaptive immune system. These memory cells can be reactivated on renewed contact with the same antigen and mount a faster and more effective immune response (27) (16).

### **1.3. Discovery, development and phenotype of innate lymphoid cells**

The barrier surfaces of the lung, gut and skin are continually exposed to environmental insults, which can lead to infection, tissue damage and inflammation. ILC, which are important regulators for inflammation and innate immunity are located at these barrier sites. Their dysregulation can result in chronic activation and pathology (28). These cells lack the recombination activating gene (RAG) and thus are defined by the absence of antigene specific B or T cell receptor (29).

The Classification of ILC into three groups is based on the expression of specific transcription factors and cytokine release (30) (31) (32). In mice, ILC derive from the common lymphoid progenitor (CLP) in the bone marrow, which further gives rise to the early lymphoid progenitor under the impact of transcription factors: thymocyte selection-associated high-mobility group box (TOX), nuclear factor IL-3 dependent (NFIL3) and T-cell factor 1 (TCF1). This precursor can develop into three ILC populations named ILC1, ILC2 and ILC3 (33) (34). The transcription factors Id2 and GATA3 are necessary for the commitment to common helper ILC progenitor. This progenitor, through promyelocytic leukemia zinc finger (PLZF)-precursor, can give rise to helper ILCs subsets, under the influence of T-bet for ILC1, GATA3/Bcl11b/ROR $\alpha$  for ILC2 and ROR $\gamma$ t for ILC3 (35).

In human, ILC can be differentiated *in vitro* from CD34<sup>+</sup> progenitors isolated from the bone marrow, thymus, peripheral blood or cord blood (36). Human ILCs and *in vitro* NK cells can be differentiated from CD34<sup>+</sup> progenitor which expresses ROR $\gamma$ t, CD34, CD45A, CD117, CD161, integrin  $\beta$ 7, and IL1R1. The development of human ILCs is still not completely understood and further research is required to clarify the mechanism behind this process (37) (38).

### **Natural killer cells and group 1 innate lymphoid cells**

Group 1 ILC express the transcription factor T-bet and produce IFN- $\gamma$ , reflecting T<sub>H</sub>1 cells characteristics (39) (40). ILC1 express CD127 and participate in type 1 inflammation in both mice and humans, producing IFN- $\gamma$  in response to IL-12, IL-15 and IL-18 stimulation. IL-15 is a regulator for the development and differentiation of ILC1 (41). Functionally, ILC1 are crucial for the defense against intracellular bacteria, viruses and they are also involved in anti-tumor responses (40) (42). Furthermore, they might be involved in the pathogenesis of inflammatory bowel disease (IBD) and chronic obstructive pulmonary disease (COPD) through the production of pro-inflammatory IFN- $\gamma$  (42). Conventional NK cells and intraepithelial type 1 innate lymphoid cells (ieILC1) are also part of group 1 ILC and are defined as cytotoxic ILC (33).

## **Group 2 innate lymphoid cells**

Group 2 ILC (ILC2) require the transcription factors GATA3 and retinoic acid receptor-related orphan receptor alpha (ROR $\alpha$ ) for their development. GATA3 is important for activation and IL-7 signaling is needed for optimal function. IL-7 KO or IL-7R $\alpha$  KO have greatly reduced ILC2 numbers (41). ILC2 are activated by innate cytokines like IL-25, IL-33, and thymic stromal lymphopoietin (TSLP) (43) (44) (45) (29). IL-25 is produced mainly by epithelial cells, T<sub>H</sub>2 cells, eosinophils and basophils (46), whereas TSLP is expressed in epithelial cells, epidermal keratinocytes, DC and mast cells (47). The expression of IL-33 has been confirmed in different cell types like epithelial cells, endothelial cells, macrophages, DC, smooth muscle cells and mast cells (48). ILC2 activation leads to production of T<sub>H</sub>2 cell-associated cytokines, mostly IL-5 and IL-13, but also IL-4, IL-9 and IL-6 (49). Upon activation ILC2 promote a type 2 immune response and contribute to allergic lung inflammation (50) (51), chronic rhinosinusitis (33), atopic dermatitis (52). In other contexts, ILC2 can also provide defense against parasites like helminth in the gut (53). Moreover, ILC2 produce amphiregulin, which can bind the epidermal growth factor-receptor, which has a crucial role in tissue repair and wound healing (54) (55). ILC2 also seem to play a role in the development in obesity, since ILC2 numbers are reduced in obese human individuals (56) (57). The role of ILC2 in allergic lung inflammation will be described in detail in section 1.4.

## **Group 3 innate lymphoid cells**

Group 3 ILC produce IL-17A and/or IL-22 in response to IL-1 $\beta$  and IL-23 stimulation. They express and depend on the transcription factors ROR $\gamma$ t, Notch and Tcf1 for their development (58). iILC1, ILC2 and also ILC3 rely on IL-7 stimulation for their development (41).

Human ILC3 are further divided based on the expression of the natural cytotoxicity receptor (NCR) NKp44. NKp44<sup>-</sup> ILC3 produce IL-17 and little IL-22, whereas NKp44<sup>+</sup> ILC3 are IL-22 producers. NKp44<sup>+</sup> ILC3 are absent in human peripheral blood under

healthy conditions, and are present in the healthy human intestine, where they are crucial for the proliferation of intestinal stem cells and the maintenance of gut barrier by producing IL-22 (59) (60). ILC3 have an important role in the protection of the intestine against extracellular microbes, such as bacteria and fungi. Additionally, a specific subclass of ILC3, called lymphoid tissue inducer (LTi) cells, are responsible for the development of secondary lymphoid organs. Recent study from Dr. Mjösberg's group based on single cell RNA sequencing of sorted tonsil ILC revealed other subpopulations of ILC3 (NKp44<sup>+</sup>, CD62L<sup>+</sup> and HLA-DR<sup>+</sup>) (61) (62) (60) (63) (29) (64).

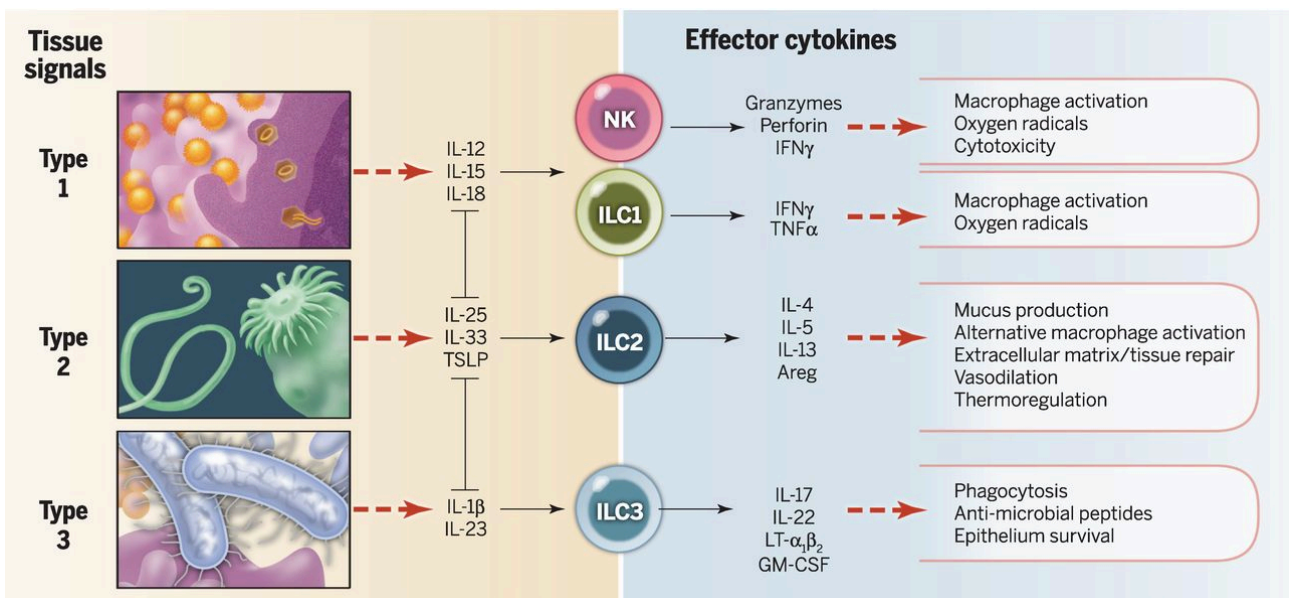


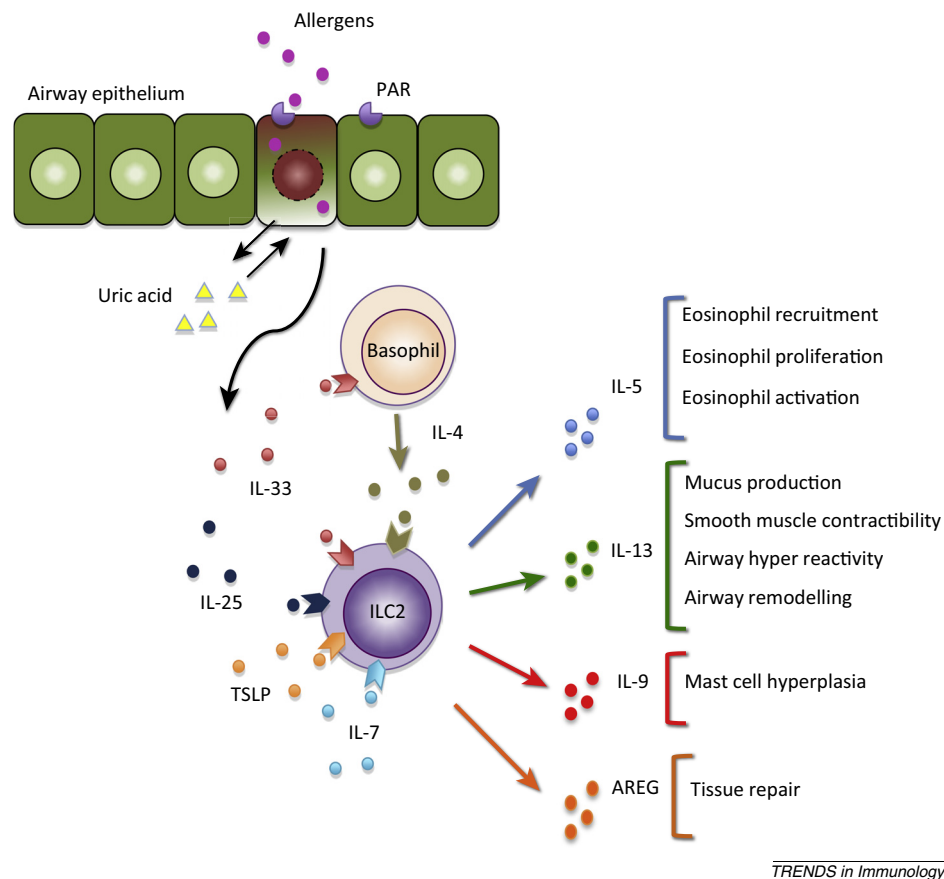
**Figure 1: Classification and function of ILC.** Tissue signals like intracellular microbes, viruses or tumors can activate NK cells and ILC1 to produce effector cytokines for macrophage activation, cytotoxicity and oxygen radicals. Parasites like helminth or allergen exposure lead to signals which activate ILC2 and cytokine release for mucus production, alternative macrophage activation, tissue repair, vasodilatation and thermoregulation. Extracellular microbes like bacteria or fungi lead to activation of ILC3 and result in phagocytosis, anti-microbial peptides and epithelium survival (65).

#### **1.4. ILC2 as drivers of allergic lung inflammation**

In industrialized countries the prevalence of allergic diseases has increased dramatically over the past 50 years. 20 – 30% of the world's population are suffering from allergic disorders (66). Allergic pathology such as asthma, allergic rhinitis and atopic dermatitis (AD) are driven by hyper-reactive type 2 immune responses at barrier tissues. The lungs are exposed to many pathogens that have the ability to invade the epithelium and to cause diseases. The innate and adaptive immune system is required to recognize and eliminate these pathogens by promoting an inflammatory reaction. An overproduction of type 2 cytokines, such as IL-4, IL-5, IL-9 and IL-13, which are released in response to inhaled allergens can drive allergic lung inflammation that causes asthma (67) (68) (69). In particular, IL-4 is responsible for B cell stimulation and induces IgE production. As a consequence, IgE production induces the release of inflammatory mediators like histamine, heparin and serotonin (70). These mediators then recruit alternatively activated macrophages (AAM) and neutrophils and they induce smooth muscle contractility and mucus hyper-production. IL-5 plays an important role for eosinophil recruitment and activation. Eosinophils release the lipid mediator leukotriene C<sub>4</sub>, which enhances mucus production and smooth muscle contraction. IL-9 overproduction leads to mast cell hyperplasia and, finally, IL-13 is crucial for mucus production and airway remodeling (49, 71). ILC2 are a source of type 2 cytokines and play an important role during airway inflammation. Furthermore, they represent the predominant ILC population in the lungs in steady state conditions and they are defined as tissue-resident cells. ILC2 are known to be an important source of IL-5 and IL-13 and release little amounts of IL-4 upon activation. However, since IL-4 is known to be crucial for the IgE production by B cells and a hallmark for allergic inflammation, T<sub>H</sub>2 cells are considered to be the source for IL-4. T cells were thought to be the main drivers for allergen induced type 2 immune response for a long time until Oboki et al. (72) could show that the inhalation of a specific papaya fruit-derived protease allergen called papain can induce type 2 lung inflammation in T and B cell deficient mice. In this study they could also show that the intranasal administration of recombinant IL-33 alone induced the same effect. This study further indicated that an unidentified cell population, which was later characterized as ILC2, were indispensable for inducing allergen induced lung inflammation rather than T<sub>H</sub>2 cells. Another study using ILC2-deficient mice generated by transplantation of

ROR $\alpha$ -deficient mouse bone marrow into irradiated host mice showed no eosinophil infiltration after intranasal papain challenge. The adoptive transfer of ILC2 could reverse the phenotype and cause an inflammation. Thus, these experiments were able to show the fundamental role of ILC2 in allergen induced airway inflammation (71) (73). Another interesting feature of ILC2 is their ability to regulate T<sub>H</sub>2 cells, since it was shown that T<sub>H</sub>2 differentiation and IgE production was impaired in ILC2-deficient mice. This effect could be reversed by the adoptive transfer of WT ILC2, but not il13<sup>-/-</sup> ILC2, indicating that ILC2 in general are important for the generation of T<sub>H</sub>2 responses after papain administration and that ILC2-derived IL-13 is crucial in this context (74). IL-13 exerts an activating function in DC, which express the IL-13R on their surface. Upon binding, IL-13 stimulates DC to get activated and migrate from the lung into the draining mediastinal lymph node (mLN). Once they reach the mLN, DC present the antigen to naive CD4<sup>+</sup> T cells and lead to their differentiation into T<sub>H</sub>2 cells. These cells then migrate to the lung where they release their inflammatory cytokines IL-5 and IL-13 inducing airway inflammation (75).

Inhaled allergens like pollen, molds, house dust mites (HDM), proteases, fungals and air pollutants stimulate epithelial cells to produce alarmins like thymic stromal lymphopoietin (TSLP), IL-25 and IL-33. These cytokines are known to promote T<sub>H</sub>2 responses and also ILC2 activation (76). IL-33 has been shown to be the most potent activator of lung ILC2 compared to TSLP and IL-25 (67) (68) (49). Studies have shown that an administration of the protease papain induce high levels of IL-33 mRNA expression in the lung, a rapid IL-33 release into the airway lumen and a strong proliferation of ILC2 (72). The intranasal administration of IL-33 directly activates ILC2 to proliferate and produce IL-5 and IL-13 (77) (71). However, IL-33 alone cannot induce proliferation and cytokine production in ILC2 *in vitro* as strong as in combination with other cytokines such as IL-2, IL-7, IL-4 or TSLP. In fact, IL-33 alone is able to stimulate ILC2 *in vivo* via IL-4 production by IL-33-stimulated basophils or by IL-7 release by stromal and epithelial cells (71).



*TRENDS in Immunology*

**Figure 2: Activation of ILC2 by alarmins release from epithelial cells leading to innate type 2 immunity.** The release of IL-33, IL-25, TSLP and uric acid by the lung epithelium is induced by the contact of allergens with the epithelial barrier. Stimulated ILC2 produce type 2 cytokines including IL-5, IL-13, IL-9 and amphiregulin. These released cytokines influence different cell types leading to a type 2 lung inflammation characterized by eosinophil proliferation, mucus production by goblet cells, smooth muscle contraction and airway hyper-reactivity (78).

IL-33 is a member of the IL-1 family, that is constitutively expressed by the airway epithelial and endothelial cells (79). Alveolar epithelial type II cells, airway smooth muscle and mast cells are the major source for IL-33 and is released upon necrosis or cell damage (80) (81) (82). Recent studies could show that protease-activated receptor-2(PAR2)-deficient mice treated with HDM had lower lung inflammation suggesting the importance of this receptor for IL-33 release (83). Other studies suggest that full length IL-33 can also be released upon cell damage by the enzymatic activity of cysteine protease allergens like papain, which can be cleaved by allergen proteases leading to an amplification of the functional activity of IL-33 (84) (85). Furthermore, as a



result of cell damage uric acid can also be released and act as an alarmin to stimulate DC. Intranasal administration of HDM or papain leads to a strong release of uric acid. By using uricase to remove uric acid, airway inflammation could be inhibited (86). Activated ILC2 can produce high amounts of amphiregulin, a member of EGF family that promotes repair of damaged tissues (50). Due to this, it is hypothesized that IL-33 release and ILC2 stimulation is a feedback repair mechanism in response to cell damage.

Altogether, ILC2 play an important role for the development of type 2 driven pathogenic lung inflammation (50).

### **1.5. Role of metabolism in immune cell function**

In order to maintain basic cellular functions, cells need to generate energy via metabolic pathways like glycolysis and oxidative phosphorylation (OXPHOS). In the last few years several studies could report that immune cells can modify their metabolism from one pathway to another to fuel their growth and effector functions during immune responses. First evidences of metabolic changes were reported in quiescent cells shifting to activated and proliferating cells. Quiescent cells have a relatively low metabolism compared to activated cells which have high fuel needs. By performing this shift, the cell switches from an oxidative metabolism to anaerobic glycolysis (Warburg effect) (87). The pathway of glycolysis requires high glucose uptake, which is further increased when the cell need higher amount of energy to perform proliferation or effector function. This process consists of the conversion of glucose into pyruvate, thereby generating ATP. During Warburg metabolism, the majority of pyruvate is converted into lactate and NADH is oxidized to NAD<sup>+</sup>, which can support continued glycolysis. To fuel OXPHOS, pyruvate can be shuttled into the tricarboxylic acid (TCA) cycle as well. The process of proliferation requires rapid synthesis of macromolecules and biosynthetic intermediates provided by the TCA cycle. Citrate from the TCA cycle can be shuttled into the cytosol and used for lipid synthesis, which also requires reductive power in the form of NADPH. NADPH is generated by the conversion of malate into pyruvate. Alternatively, shuttling glucose-6-phosphate in the pentose phosphate pathway (PPP) also generates NADPH. This latter pathway is important for nucleotide synthesis (88) (89) (90).

T cell activation results in significant changes in cell metabolism, which aim to orchestrate the response of other immune cells and provide protection against pathogens. Before activation, naïve T cells are quiescent and rely mainly on fatty acid oxidation (FAO) and OXPHOS (91). Upon activation by pathogens these cells can rapidly switch to aerobic glycolysis for increased and faster production of biomass required for growth, accumulation and cytokine production (92). After pathogen elimination, remaining T cells turn into memory T cells which mainly rely on FAO, probably by the acquisition of external lipids (93) (94) (95).

### **Metabolic regulation in ILC2**

Besides the essential role in maintaining and protecting the tissue barrier against invading pathogens, ILC2 are regulators of the host metabolism. They can act as dietary sensors and react to nutritional-derived and metabolic circumstances to promote the maintenance of barrier sites and to orchestrate immune responses.

The ILC barrier function is controlled by dietary-derived products. For this sensing function, the expression of the retinoid acid receptors (RAR) and aryl hydrocarbon receptor (AhR) are crucial. Retinoic acid (RA) is important for the development and growth of the organism and is needed for a functional immune system (96) (97) (98) (99). RA downregulates IL-7R $\alpha$  on ILC2, which results in a suppression of their function and survival. On the other hand, RA can also control ILC3. Vitamin A-deficient mice show reduced numbers of ILC3 compared to mice fed a vitamin A diet. The reduced ILC3 number results in a higher susceptibility to infection with *Citrobacter rodentium*. Thus, vitamin A malnutrition has functional consequences for intestinal immunity and is changing the balance between ILC2 and ILC3 in the intestine (100).

Amino acid metabolism seems to play an indispensable role for ILC2 regulation. A recent study could show that the genetic deletion of arginase 1 (Arg1) in a model of allergen-induced airway inflammation could reduce inflammation and the number of proliferating ILC2. This reduction was caused by the decreased conversion of L-arginine into polyamides that impaired aerobic glycolysis and decreased ILC2 proliferation and activation (101). This was the first study showing the importance of glycolysis for the

pathogenic ILC2 response in airway inflammation. On the other hand, other studies report the dependence of intestinal ILC2 on fatty acid oxidation (FAO) (102). Compared to other cell types like regulatory T cells, ILC2 need a high amount of FAs in steady state. Wilhelm et al (102) could demonstrate that intestinal ILC2 proliferation and accumulation caused by vitamin A deficiency was fueled by external fatty acids. Other studies could show that the inhibition of fatty acid oxidation by using etomoxir, a carnitin-acyltransferase-1 (CPT1) inhibitor, as a treatment impaired ILC2 accumulation as well as the release of IL-5 and IL-13 and ablated anti-helminth immune responses. Similar effect could be observed by using the lipase inhibitor orlistat. However, the impairment of systemic glycolysis by using 2-DG showed no effect on ILC2 activation during helminth infection.

#### **1.6. Ketogenic diet - a unique metabolic state**

Immune cell function metabolically depends on nutrient availability, which has changed over time due to modification of dietary habits. Epidemiological studies show that diet is an important risk factor which can influence disease development such as allergic asthma (103) (104) (105). Furthermore, related to dietary changes, the rates of obesity have risen worldwide and the increase in body weight occurred during a time, when it has been recommended to have a low fat diet to lose weight. These recommendations were based on the assumption that high-fat diets are less satiating and that by a low fat diet the risk for cardiovascular diseases due to less circulating fat and cholesterol would decrease (106). As this dietary advice failed, other dietary regimes, like ketogenic diet (KD) came into focus. A KD is a form of a low-carbohydrate diet, which induces a change in metabolism away from carbohydrates towards fatty acid oxidation. It has been shown that mice on KD have a promoted anti-inflammatory state and increased levels of ketone bodies. When the mobilization of fatty acids from the adipose tissue accelerated in a phase of very low carbohydrate intake, the liver converts acetyl-CoA into ketone bodies. As the liver is lacking the mitochondrial enzyme succinyl CoA:3-ketoacid CoA transferase, which is needed to metabolize the ketone bodies, these translocate from the liver to the other tissues, in particular the brain, to use it as an energy source (107).

Studies that applied KD, mice consumed the same amounts of calories of mice fed with high fat diet. Nevertheless, mice on KD did not gain weight, but even lost weight compared to mice fed normal chow. Thus, KD results in a different metabolic and physiological state compared to normal chow or high fat diet. It is characterized by an increased energy expenditure and a low respiratory quotient. Moreover, hormonal changes are also induced by KD diet. Lower insulin levels and lower serum lipid levels along with higher glucagon levels were measured in mice fed with KD. Additionally, gene expression analysis identifies changes in metabolic genes by KD. For example, genes involved in lipid synthesis, like fatty acid synthase (FAS), stearoyl-CoA desaturase-1 (SCD-1) and sterol regulatory element-binding protein-1c (SREBP-1c) were suppressed (108).

Interestingly, changes in dietary lifestyle are coinciding with gut microbiota changes, indicating an alteration of the composition of the gut microbiota upon diet modification (109). Homeostasis of the gut microbiota is crucial in modulation of the host immunity and control of inflammation, as it is shown in germ-free mice, which have abnormal immune systems, including the absence or underdevelopment of lymph nodes systemically and specifically in gut-associated lymphoid tissues (110). Furthermore, several clinical studies show that antibiotic treatments increase the risk of epileptics or symptomatic seizures in epileptic individuals, suggesting a possible role for the gut microbiota influencing this diseases (111) (112).

However, the exact mechanism of how a KD diet is suppressing the outbreak of inflammation is still poorly understood and needs more investigation.

### **1.7. PPAR $\gamma$ - a regulator in energy metabolism**

Cells are constantly exposed to a variety of lipids that can be used for energy generation and as energy storing molecules. The presence or absence of lipids can influence the metabolism of immune cells and therefor their function (113). The control of FA uptake and metabolism is dependent of peroxisome proliferator-activated receptor gamma (PPAR $\gamma$ ), also known as glitazone receptor or NR1C3, which belong to the nuclear receptor superfamily of ligand-inducible transcription factors. Also belonging to this family are PPAR $\alpha$  (NR1C1) and PPAR $\beta/\delta$  (NR1C2) (114). The PPARs control the

expression of genes involved in adipogenesis, lipid metabolism, inflammation and maintenance of homeostasis by binding to PPAR-responsive regulatory elements and form heterodimers with retinoid X receptor (RXR) (115). They are also known to act as receptors for common dietary fats like oleic, linoleic and linolenic acids as well as for diverse lipid metabolites like prostaglandin J<sub>2</sub>, 8S-hydroxyeicosatetraenoic acid and diverse oxidized phospholipids (116) (117) (118). The ligand binding induces a conformational change of the receptor, which leads to a recruitment of cofactors and a modulation of PPAR activity (119). Each PPAR isoform has unique functions *in vivo* due to their distinct tissue distributions, inherent differences in biochemical properties and different responses to ligands. The highest expression of PPAR $\gamma$  is shown in white adipose tissue (WAT) and brown adipose tissue (BAT), where it exerts a crucial regulation of adipogenesis as well as a potent modulation of lipid metabolism and insulin sensitivity (114) (120). Additionally, PPAR $\gamma$  is also involved in controlling genes in glucose homeostasis like glucose transporter type 4 (Glut4) and c-Cbl-associated protein (CAP). Moreover, PPAR $\gamma$  is an important regulator of various factors secreted by adipose tissue such as adiponectin, resistin, leptin and tumor necrosis factor- $\alpha$  (TNF- $\alpha$ ). All these networks also have also an effect on insulin sensitivity (121) (122) (123) (124).

Thiazolidinediones (TZDs) are potent PPAR $\gamma$  agonists, that act as insulin sensitizers and therefore are highly effective medications for type 2 diabetes (125). Yet, besides their beneficial effects, TZD medication shows a higher risk of for fluid retention, weight gain, bone loss and congestive heart failure (126) (127).

The role of PPAR $\gamma$  in immune cells needs to be further explored. Until now studies have shown, that PPAR $\gamma$  is important in antigen-presenting myeloid dendritic cells and macrophages (128) (129) (130) (131). In DC PPAR $\gamma$  is regulating lipid metabolism and lipid transport as well as antigen uptake, maturation, activation, migration, cytokine production and antigen presentation (128) (129). Furthermore, mice lacking PPAR $\gamma$  in macrophages are more prone to insulin resistance, suggesting an important role in anti-inflammation and lipid metabolism (132) (133).

The effect of PPAR $\gamma$  activation on T<sub>H</sub>2 cells remains unclear. Studies have shown an impaired T cell proliferation after PPAR $\gamma$  activation and an increased antigen-specific proliferation after specific deletion of PPAR $\gamma$  in CD4<sup>+</sup> T cells (134) (135), whereas other

studies report a downregulation of T<sub>H</sub>2 cytokines (IL-4, IL-5 and IL-13) as well as c-Maf (a T<sub>H</sub>2 specific transcription factor) (136) (137). Due to these contradictory reports further studies in this field are needed to elucidate the role of PPAR $\gamma$  activation in T<sub>H</sub>2 cells.

### **1.8. Lipid droplets - regulators of lipid metabolism**

An increased FA uptake leads to more free FA in the cell which can have various influences on the cell and its metabolism. Lipid droplets (LD) are organelles acting as cellular storages for neutral lipids and play a crucial role in lipid and energy metabolism as well as membrane synthesis. The process of storing excess fatty acids and sterols in LD is a protection strategy of the cell to avoid lipotoxicity (138) (139) (140). Abnormal LD dynamics are associated with numerous of diseases like metabolic disease, obesity, diabetes, atherosclerosis and cancer (141).

LD are found predominantly in the cytoplasm even though in some cell types they can also be located in the nucleus (142). These organelles are formed of triacylglycerides (TAGs) and sterol esters (SE). LD have unique structure that is different from most other cellular organelles that have aqueous lumens. They are surrounded by a phospholipid monolayer with the hydrophobic phospholipid tail oriented towards the LD core, which confers their hydrophobic nature. They have a characteristic complement of proteins and more than 100 LD-associated proteins have been identified (143) (144). For example, perilipin-2 (PLIN2/ADRP) and other members of the perilipin family are associated with the phospholipid monolayer. These proteins are involved in lipid metabolism and synthesis, lipid trafficking and organelle transport (143).

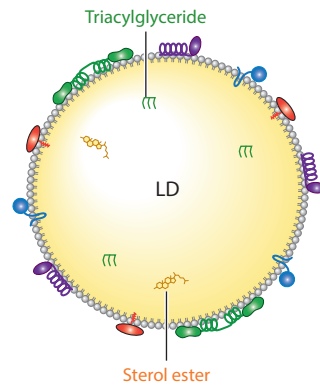


**Figure 3: Schematic representation of the structural composition of an LD.** Colored objects represent LD surface-bound proteins localized to the phospholipid monolayer. Triacylglycerols and sterol esters are found in the neutral lipid core. Figure modified (145).

The life cycle of LD consists of biogenesis, maturation and turnover including fusion and fission. Furthermore they can make close contact to other organelles like mitochondria. The LD machinery is similar in many cell types, however hepatocytes and adipocytes are predominately specialized in the storage of lipids in LD. The formation of these storage organelles take place in the endoplasmic reticulum (ER), where neutral lipids like TAG and SE are synthesized. The final step of TAG synthesis is catalyzed by the DGAT (diacylglycerol) enzymes DGAT1 and DGAT2 (146) (147). These two enzymes differ in their structure, substrate preferences, subcellular localizations, and physiological roles, despite catalyzing the same biochemical reaction. DGAT1, a member of the membrane-bound O-acyltransferase gene family (148), is localized exclusively in the ER. In the ER, DGAT1 encounters its substrates, a fatty acyl-CoA and an acyl acceptor, and catalyzes the esterification reaction to generate neutral lipids. DGAT1 can esterify a variety of substrates like diacylglycerol, retinol, monoacylglycerol, although the main function is the TAG synthesis. It plays an important role in detoxifying excess lipids that are taken up from the cellular environment (149) (150). Otherwise these external free fatty acids can damage the mitochondria membrane leading to a mitochondria dysfunction (151). Additionally, this enzyme is crucial in preventing ER stress due to toxic lipids. In contrast, DGAT2, a member of the DGAT2 gene family, is localized to both the ER and LD. This enzyme seems to be the major enzyme for TAG synthesis from fatty acid substrates derived from *de novo* lipogenesis (152) (153) (154) (149) (155).

DGAT1 or DGAT2 knockout mice have very different phenotypes according to the different biochemical and cell biological properties. Mice lacking DGAT1 are viable, live on average 25% longer than wild type mice and they are lean and resistant to diet-induced obesity, diabetes and liver steatosis (156) (157). In contrast, DGAT2 knockout mice die shortly after birth due to a lipid defect in the skin impairing its barrier function. They have more than 90% reduction in TAG (158).

After the TAG synthesis a lens of neutral lipids is formed within the ER bilayer. Proteins seem to be involved in TAG lens formation. FIT2 is an ER protein which is linked to LD formation (159) (160). It is binding lipids and is suggested to be important for partitioning neutral lipids within the ER for LD formation (161). Overexpression of this protein results in larger LD, although the TAG levels are not altered. This suggests a modified partitioning of newly synthesized TAGs into LD (160).

Next step in LD formation is the budding of the LD into the cytoplasm. This process still remains mainly unclear. Some hypothesis are considering that proteins are involved in the scission of LD from the ER. Additionally, several recent studies indicate that the ER protein seipin may be involved in LD formation and plays a functional role either by helping to generate nascent LD or by facilitating their growth and expansion (162) (163).

In the past decades, the cell biology and the involvement of LD in different diseases has been brought into focus. It is known that LD due to their function as important storage organelles, are acting as regulators of cell metabolism. When energy supply is limited, lipolysis of TAG in LD is promoted. LD-associated neutral lipase, like adipose triglyceride lipase (ATGL), can release large amount of hydrolyzed FAs that can be further used to initiate  $\beta$ -oxidation in the mitochondria for energy generation as well as for the synthesis of new membrane components. (164) (165) (166).



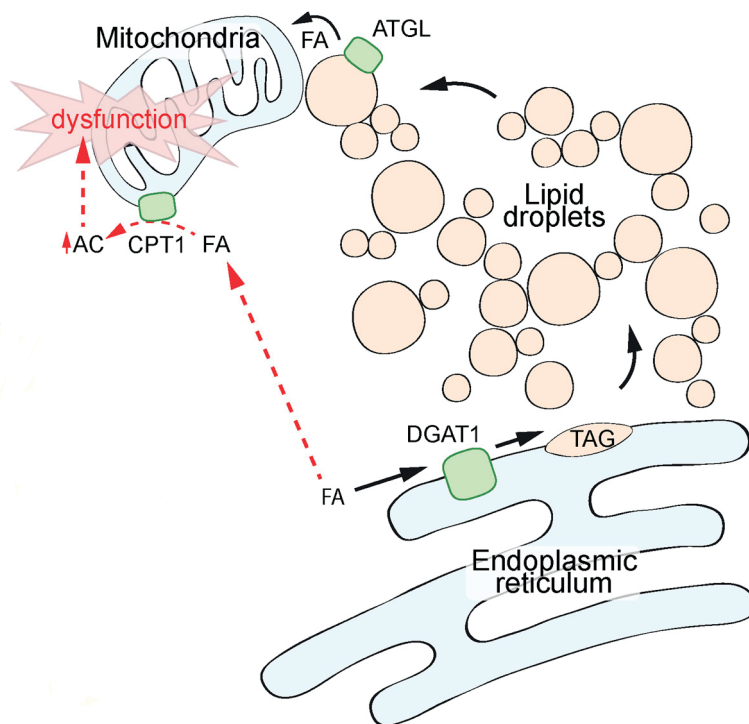


**Figure 4: Lipid droplet biogenesis is a protective response to excess of FFA.** DGAT1 is responsible for detoxification of excess lipids in cells. It generates TAGs stored in lipid droplets. These TAGs can be lipolyzed by ATGL for energy generation in the mitochondria. Excess of FFA in cells can be mitotoxic as they are converted to acylcarnitin (AC) by CPT1. Figure modified (151).

In immune cells LD are considered inflammatory markers (167). They have been mostly studied in macrophages and DC, but their function in immune cells just started to be explored (168). Most aspects of LD dynamics have been studied in non-immune cells and data of LD in immune cells are lacking. However, it is now clear that in inflammatory responses like atherosclerosis, bacterial sepsis, acute respiratory distress syndrome, allergic lung inflammation and arthritis the number of lipid droplets increase. Unlike LD in adipocytes, leukocyte LD store arachidonic acid, a component for the production of inflammatory mediators like eicosanoids. These mediators play a key role in cellular migration, proliferation, activation and apoptosis. Thus, LD play an important role in cellular metabolism and inflammatory responses (169).

### **1.9. Aims of the thesis**

ILC2 are the most dominant ILC population in the lungs and crucial in the initiation and amplification of type 2 immune responses defined by cytokines like IL-5 and IL-13. While T<sub>H</sub>2 responses are protective in context of helminth infection, the inability to initiate tolerance and the aberrant responses to harmless antigens results in allergic diseases, such as asthma.

Studies have already shown that, during steady state conditions and helminth infection, ILC2 rely on FAO and require low amounts of glucose to maintain their protective function. Further studies display the Warburg effect in activated and proliferating immune cells like T cells. Furthermore, expression of Arg1 and arginine metabolism in ILC2 was identified to promote aerobic glycolysis and to support pathogenic ILC2 responses in airway inflammation. The focus of this thesis will be to explore if and how the metabolism of pathogenic ILC2 in the lungs changes during airway inflammation and which signals, nutrients and additional metabolic pathways are needed to induce chronic activation, proliferation and thus lead to pathogenicity.

Overall, the aim of this thesis is to extend the current knowledge on the modification of ILC2 metabolism during airway inflammation and clarify how the pathogenicity of ILC2 is fueled and controlled, in order to identify novel mechanism for potential diet or treatment, which are able to target ILC2 in lung disease.

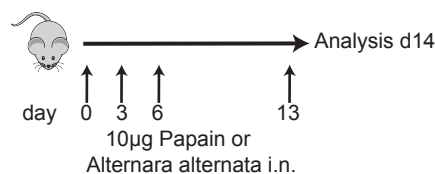
## 2. Material and Methods

### 2.1. Animals

C57Bl/6 (WT) and ST2-deficient mice (C57Bl/6 background, provided by Dr. Andrew McKenzie, MRC Laboratory of Molecular Biology, Cambridge) were bred in-house or purchased from Charles River labs. They were maintained at in-house facilities in Bonn (Germany) under specified pathogen free (SPF) conditions and all procedures were performed according to ethical protocols approved by the local and regional ethical committees. All mice were used for the experiments between 6-10 weeks after date of birth.

### 2.2. Intranasal administration of papain and *alternaria alternata*

C57Bl/6 were anesthetized with isoflurane (5 % Isoflurane, 400-600 ml/min O<sub>2</sub>) and exposed intranasally to 10 µg papain (Callbiochem) or 10 µg of total protein from *alternaria alternata* extract (Greer) in 50 µl PBS on day 0, 3, 6. Seven days later mice were re-challenged intranasally with the same amount of papain or *alternaria alternata* extract in 50 µl PBS. The control group received 50 µl PBS only. Mice were euthanized 18 h after the challenge by cervical dislocation and lung cells were isolated for further analysis.



### 2.3. Intranasal administration of IL-33, IL-25 and TSLP

C57Bl/6 mice were anesthetized with isoflurane (5 % Isoflurane, 400-600 ml/min O<sub>2</sub>) and treated intranasally with 100 ng recombinant mouse IL-33, IL-25 or TSLP (all Biologend) in 50 µl PBS on day 0, 1 and 2. Control mice were challenged with 50 µl PBS only. Control group received 50 µl PBS only. Mice were euthanized 18 h after the challenge by cervical dislocation and lung cells isolated for further analysis.



### 2.4. Cell isolation from tissues

Lung tissues were dissected with a scissor in a small petri dish and digested with 0,25 mg/ml Liberase TL (Roche) and 1 mg/ml DNase I (Sigma) at 37°C for 1 h on a shaker (600 rpm). Digested lung tissues were meshed and filtered through a 70 µm filter and further purified using 5 ml of a 37.5 % Percoll gradient followed by lysis of red blood cells with ACK buffer for 3-4 minutes. Cells were washed and resuspended in complete media with 2 % FCS for further analysis.

### 2.5. Flow cytometry analysis

Single-cell suspensions were stained with anti-CD16/32 (BioXcell) and with fluorochrome-conjugated antibodies against any combinations of the following surface antigens: CD3, CD11b, CD11c, CD49b, CD19, Ter119, NK1.1, Gr-1, CD45, Thy1.2 and ST2. DADP or fixable Zombie UV dye (Biologend) was used to distinguish dead and alive cells. For examination of transcription factors and cellular proliferation, cells were subsequently treated with the Foxp3 fixation/permeabilization kit (eBioscience) in accordance to the manufacturer's instructions and stained for 35 min on ice with fluorochrome-conjugated antibodies against GATA3 and Ki-67.

## **2.6. Re-stimulation of cells for intracellular cytokine staining**

Cells isolated from lung tissues were stimulated for 3 h with Phorbol 12,13-dibutyrate (0.5 µg/ml, PdBU; Biomol) and ionomycin (0,5 µg/ml, Sigma) in the presence of brefeldin A (1 g/ml, GolgiPlug, BD Biosciences). Stimulated cells were stained for surface markers, fixed with 3.7 % formaldehyde (Sigma), followed by fixation with Foxp3 fixation/permeabilization kit (eBioscience) in accordance to the manufacturer's instructions and stained with antibodies against Gata3, IL-5 and IL-13 for 35 min on ice.

## **2.7. Fluorescence-activated cell sorting**

ILC2 were sorted by flow cytometry (Cell Sorter Aria III) from total lung cells isolated from naive, papain and IL-33-challenged mice based on the absence of lineage markers (CD3, CD11b, CD11c, CD49b, CD19, Ter119, NK1.1 and Gr-1) but expression of Thy1.2, CD45 and ST2.

## **2.8. Purification of ILC2**

Purification of lung ILC2 was performed using a negative selection strategy. Total lung cells were stained with a combination of monoclonal antibodies against CD3, CD11b, CD11c, CD49b, CD19, Ter119, NK1.1 and Gr-1 coupled to biotin followed by incubation with Streptavidin-coupled magnetic microbeads (Biolegend) and negative selection on magnetic columns (Miltenyi).

## **2.9. *In vitro* culture of ILC2**

MACS-Purified ILC2 ( $5 \times 10^3$  cells/well) from papain challenged mice were cultured in 50 µl RPMI 1640 supplemented with 3 % FCS (Thermo Fisher Scientific), penicillin/streptomycin (Thermo Fisher Scientific), 25 mM HEPES (PAN biotech), 2 mM glutamine (Thermo Fisher Scientific), nonessential amino acids (Thermo Fisher Scientific), 50 mM β-mercaptoethanol (PAN biotech), 11 mM glucose (Sigma), 1 mM pyruvate (Sigma) (complete medium) and IL-2 (10 ng/ml, Biolegend) for three days. In some experiments a combination of IL-2 and IL-25, IL-33 or TSLP (10 ng/ml each) was added to the culture medium. To assess the effect of DGAT1 and PPAR $\gamma$  purified ILC2 were cultured with IL-2 in the presence of increasing amounts (10 µM – 40 µM) of DGAT1-Inhibitor (A922500, Targetmol) or PPAR $\gamma$  inhibitor (40 µM, GW9662, Cayman Chemicals). To test

the functionality of FFA ILC2 were cultured in the presence of IL-2 and a mixture of 140 nM linoleic acid/oleic acid-BSA (Sigma) or 20  $\mu$ M palmitic acid-BSA (Sigma and coupled to BSA in house) for three days. 20  $\mu$ M palmitic acid in complete media was added to 0.5 % BSA media in a 1:1 ratio and warmed up to 37°C for 5 minutes. The mixture was sonicated for 5 minutes and then used for further experiments. In some experiments addition of FFA was tested in the presence of 20  $\mu$ M Dgat1i A922500. To test the effect of glucose purified cells were cultured with IL-2 with and without glucose/pyruvate.

### **2.10. Cytokine measurements**

For cytokine measurement in the lung homogenate or in the supernatant of cell cultures Biolegend's LEGENDplex bead-based immunoassay was used in accordance to the manufacturer's instructions. The analysis of this assays was done with the associated LEGENDplex data analysis software.

### **2.11. BODIPY<sup>®</sup> 493/503, BODIPY<sup>®</sup> FL C16 and 2-NBDG stainings**

Cultured ILC2 ( $5 \times 10^3$  cells/well) or freshly isolated lung cells ( $2 \times 10^4$  cells/well) were stained with 200 ng/ml BODIPY<sup>®</sup> 493/503 or 25 ng/ml BODIPY<sup>®</sup> FL C16 (both ThermoFisher) for 30 min at 37°C in volume of 200  $\mu$ l complete medium without FCS, washed and analyzed by flow cytometry. Fluorescent BODIPY<sup>®</sup> 493/503 can be used as a stain for neutral lipids like in LD, whether BODIPY<sup>®</sup> FL C16 is a fluorescent fatty acid which can be used to monitor FA uptake. To probe for uptake of 2-NBDG cells were incubated with 16  $\mu$ g/ml 2-NBDG (Cayman) in a volume of 200  $\mu$ l glucose free media for 15 min at 37°C, washed and analyzed by flow cytometry. 2-NBDG is a non-metabolizable glucose analog for monitoring glucose uptake.

### **2.12. Alkyne labeled palmitic acid uptake and staining**

Cells isolated from lung tissues ( $2 \times 10^4$  cells/well) were incubated with 20  $\mu$ M of alkyne labeled palmitic acid (provided by Dr. Thiele, Limes-Institute-Bonn, Germany) coupled with BSA for 30 min at 37°C in a volume of 200  $\mu$ l complete medium without FCS, washed and stained for surface markers. After washing with FACS buffer, the cells were fixed with Formaldehyde (3.7 % in PBS) and permeabilized with Triton X-100 (0.5 % in PBS). Subsequently, the Alkyne-palmitic acids taken up by the cells were detected with

the azide based Click-iT detection kit (Life Technologies) according to manufacturer's instructions. Click chemistry is a robust two-step labeling and detection technique where in the first step the alkyne component fed to cells and can be used in the second step in linking reactions (azide-alkyne bioconjugation reaction). Before analysis cells were intracellularly stained for Gata3 and Ki-67. Alkyne labeled palmitic acid uptake and staining was performed by Dr. Fotios Karagiannis (Institute for Clinical Chemistry and Clinical Pharmacology, University Hospital Bonn).

### **2.13. Flow cytometric determination of apoptosis**

ILC2 ( $5 \times 10^3$  cells/well) were cultured two days in 50  $\mu$ l complete medium with IL-2 (10 ng/ml, Biolegend) and with IL-2 in the presence of DGAT1-Inhibitor (40  $\mu$ M). The culture was analyzed by an annexing V/propidium iodide double staining (Biolegend) following the manufacturer's instructions.

### **2.14. Lipid peroxidation staining**

ILC2 ( $5 \times 10^3$  cells/well) were cultured in 50  $\mu$ l complete medium with IL-2 (10 ng/ml, Biolegend) or with IL-2 in the presence of DGAT1-Inhibitor (40  $\mu$ M). At the same time Image-iT Lipid Peroxidation Sensor BODIPY<sup>®</sup> 581/591 C11(Thermo Fisher) was added. This reagent localizes to membranes in live cells and upon oxidation by lipid hydroperoxides, displays a shift in peak fluorescence emission from 590 nm (red) to 510 nm (green). After two hours cells were analyzed by flow cytometry and ratios of the signal 510 to 590 channels were used to quantify lipid peroxidation.

### **2.15. *In vivo* inhibitor treatment**

To block the activity of DGAT1 or PPAR $\gamma$  30 mg/kg of DGAT1-Inhibitor (A922500, Targetmol) or 1 mg/kg of PPAR $\gamma$  inhibitor (GW9662, Cayman Chemicals) was delivered in 30  $\mu$ l of biotechnology performance certified DMSO and administered intraperitoneally to C57BL/6 WT mice every day for the duration of the experiment. Control mice received 30  $\mu$ l DMSO only.

### **2.16. Diet studies**

Control diet AIN 93G (17.6 % protein, 7.1% fat, 11% sugar) and Ketogenic diet TD.130659 (15 % protein, 72 % fat, 2.4 % sugar) were purchased from Ssniff. Mice were weaned on ketogenic or control diets and maintained on appropriate diets throughout the study.

### **2.17. Antibiotic treatment**

Antibiotic treatment started four days before the first papain treatment (d0). Vancomycin (0.5 g/L, Cayman), Ampicillin (1 g/L, Sigma), Neomycin (1 g/L, Sigma), Metronidazole (1 g/L, Sigma) were provided ad libitum in drinking water for 18 days. After dissolving antibiotics in drinking water the pH was adjusted to 7.4. Amphotericin b (1 g/L, Cayman) was provided the first four days of antibiotic treatment only.

### **2.18. Measurement of free fatty acids, glucose and ketone bodies**

Free fatty acid and glucose levels in the plasma and in the lung homogenates were measured by using Free Fatty Acid Fluorometric Assay Kit (Cayman) or the Gluco-Glo kit (Promega) following the manufacturer's instructions. Ketone body levels were measured using FreeStyle Precision Neo H (Abott).

### **2.19. Histology - PAS staining**

The left lung lobe was fixed in 10 % formaldehyde solution and embedded into paraffin blocks. Sections were stained with periodic acid-Schiff (PAS) stain and airways were assessed for PAS staining as an indication of mucus producing cells.

### **2.20. Confocal microscopy**

For assessment of lipid droplet formation, ILC2 were purified and stained with BODIPY® 493/503 (Thermo Fisher) at a concentration of 500 ng/ml in complete medium without FCS for 30 min at 37°C. To assess external uptake of lipids and storage in lipid droplets, ILC2 were stained with BODIPY® FL C<sub>12</sub> (Thermo Fisher) at a concentration of 1 µg/ml for 30 min at 37°C. Cells were then washed with FACS buffer and cytopspined onto glass slides followed by fixation with Formaldehyde (3.7 %) and two washing steps with PBS.



To determine alkyne-palmitic acid uptake and utilization, purified ILC2 were cultured overnight in complete medium with 3 % FCS containing 2 ng/ml IL-2 and 2  $\mu$ M alkyne-palmitic acid coupled with BSA. Cells were washed and cultured for 24h in medium containing 2  $\mu$ M glucose and 1 % FCS or proceeded directly to immunofluorescence staining. After incubation, cells were washed with FACS buffer and cytopspined onto glass slides followed by fixation with formaldehyde (3.7 %), two washing steps with PBS and permeabilized with Triton X-100 (0.5 % in PBS). Subsequently, the Alkyne-palmitic acids taken up by the cells were detected with the azide based Click-iT detection kit (Life Technologies) according to manufacturer's instructions. The nuclei were counterstained with DAPI, washed once with PBS and coverslips were mounted onto the glass slides with Prolong™ Diamond Antifade Mountant (Life Technologies). Cells were imaged with a LEICA SP5 AOBS confocal microscope. Image analysis was performed with the FIJI software (National Institutes of Health). Confocal microscopy was performed by Dr. Fotios Karagiannis (Institute for Clinical Chemistry and Clinical Pharmacology, University Hospital Bonn).

### **2.21. Real-time PCR.**

RNA was extracted from purified ILC2 using Trizol (Thermo Fisher Scientific) and reverse transcribed with RevertAid Kit (Thermo Fischer Scientific) according to the manufacturer's instructions. The cDNA served as a template for amplification of genes of interest. Target gene expression was calculated using the comparative method for relative quantification upon normalization to  *$\beta$ -actin* gene expression. For analysis on genes expressed by ILC2, TaqMan probes for *acc1*, *fasn*, *hmgcs1*, *srebf*, *ppary*, *pparg*, *cpt1*, *acox1*, *acly*, *dgat1*, *dgat2*, *got1*, *hk1*, *ldha* and *pkm* (IDT) were used and gene expression was normalized to *hprt1*.

### **2.22. Seahorse Analysis**

MACS-Purified ILC2 ( $1.5 \times 10^5$  cells/well) from papain challenged mice were cultured for 2 h with or without a mixture of 140 nM linoleic acid/oleic acid-BSA (Sigma) and 10  $\mu$ M palmitic acid-BSA (Sigma and coupled to BSA in house) and 10 ng/ml IL-2 (Biolegend) in

complete media without FCS. Cells were washed with assay medium transferred into the Seahorse XF Cell Culture Microplate resuspended in 175  $\mu$ l assay medium. Assay medium was prepared supplementing Seahorse XF RPMI with 1mM pyruvate, 2 mM glutamine and 10 mM glucose. Assay medium was warmed to 37°C in an incubator without CO<sub>2</sub> for 35 minutes and pH was adjusted to 7.4. The medium was filtered through a sterile filter. The Seahorse XF Cell Culture Microplate was prepared by coating the plate with cell tak (Fisher Scientific) one day before the assay. A sensor cartridge was hydrated with Seahorse XF Calibrant at 37°C in a non-CO<sub>2</sub> incubator overnight. The Agilent Seahorse XF Cell Mito Stress Test measures key parameters of mitochondrial function by directly measuring the oxygen consumption rate (OCR) of cells. Sequential compound injections measure basal respiration, ATP production, proton leak, maximal respiration, spare respiratory capacity, and non-mitochondrial respiration.

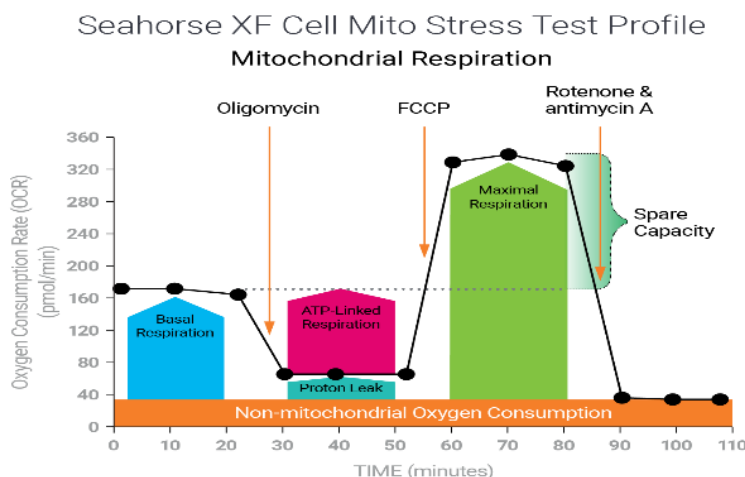


**Figure 5: Agilent Seahorse XF Cell Mito Stress Test profile of the key parameters of mitochondrial respiration.** (Agilent Technologies, 2019; [https://www.agilent.com/cs/library/usermanuals/public/XF\\_Cell\\_Mito\\_Stress\\_Test\\_Kit\\_User\\_Guide.pdf](https://www.agilent.com/cs/library/usermanuals/public/XF_Cell_Mito_Stress_Test_Kit_User_Guide.pdf); 17.11.2019)

The Seahorse XF Cell Mito Stress Test uses modulators of respiration that targets components of the electron transport chain (ETC) in the mitochondria to reveal key parameters of metabolic function. The compounds (Port A: 1.5  $\mu$ M oligomycin, Port B: 0.5  $\mu$ M FCCP, Port C: a mix of 0.5  $\mu$ M rotenone and antimycin A (Rtn/AA) are serially injected (port-loading volume: 25  $\mu$ l) to measure ATP production, maximal respiration,

and nonmitochondrial respiration, respectively. Measurements were done using the Agilent Seahorse XF Analyzer. Proton leak and spare respiratory capacity are then calculated using these parameters and basal respiration.

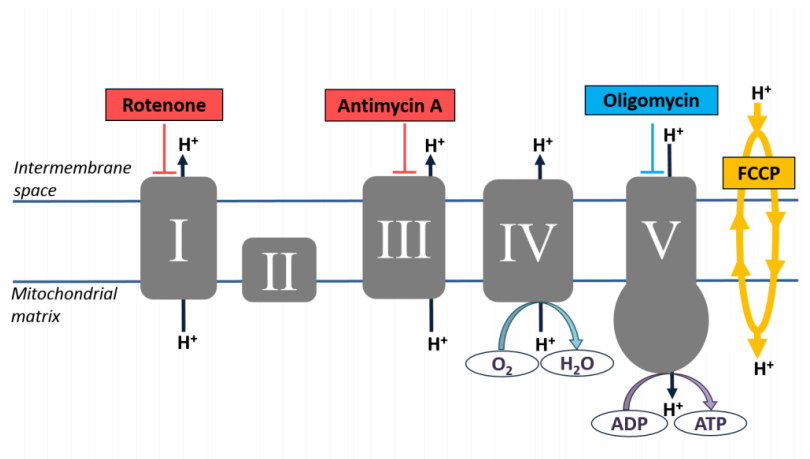


**Figure 6: Agilent Seahorse XF Cell Mito Stress Test modulators of the ETC.**

(Agilent Technologies, 2019; [https://www.agilent.com/cs/library/usermanuals/public/XF\\_Cell\\_Mito\\_Stress\\_Test\\_Kit\\_User\\_Guide.pdf](https://www.agilent.com/cs/library/usermanuals/public/XF_Cell_Mito_Stress_Test_Kit_User_Guide.pdf); 17.11.2019).

**Statistical analysis.** A two-tailed Student's t test was used for all statistical analysis:

\*  $p \leq 0.05$ , \*\* $p \leq 0.01$ , \*\*\*  $p \leq 0.001$ .

### 2.23. Key resources table

REAGENT or RESOURCE	SOURCE	IDENTIFIER
<b>Antibodies</b>		
CD11b mouse/human	Biolegend	Cat# 101204
CD11c mouse	eBioscience	Cat# 25-0114-82
CD25 mouse	eBioscience	Cat# 45-0251-82
CD4 mouse	Biolegend	Cat# 100512
CD45 mouse	Biolegend	Cat# 103116
CD90.2 mouse	Biolegend	Cat# 140310
GATA3 mouse	BD	Cat# 560078
IL-13 mouse	eBioscience	Cat# 53-7133-82
IL-33R	Biolegend	Cat# 145304
IL-5 mouse/human	Biolegend	Cat# 504304
Ki-67 mouse	eBioscience	Cat# 25-5698-82
Ly6G mouse	Biolegend	Cat# 127614
MHC-II mouse	Biolegend	Cat# 107622
Sca-1 mouse	eBioscience	Cat# 56-5981-82
Streptavidin	Biolegend	Cat# 405225
TCR $\beta$ mouse	eBioscience	Cat# 45-5961-82
Siglec F mouse	BD	Cat# 562680
CD3 mouse	Biosciences Biolegend	Cat# 100304
NK1.1 mouse	Biolegend	Cat# 108704
Gr-1 mouse	Biolegend	Cat# 108404
DX5 mouse	Biolegend	Cat# 108904
CD19 mouse	Biolegend	Cat# 115505
Ter119 mouse	Biolegend	Cat# 116204
CD11b mouse	Biolegend	Cat# 101204
CD11c mouse	Biolegend	Cat# 117304
<b>Chemicals, Peptides, and Recombinant Proteins</b>		
2-NBDG	Cayman	Cat# 11046
2-Propanol > 99,8% Rotipuran 2,5 Liter	Roth	Cat# 9866.2

<b>Alternaria alternata</b>	<b>Greer</b>	<b>Cat# XPMID3A25</b>
<b>BODIPY® 493/503</b>	<b>Thermo Fisher Scientific</b>	<b>Cat# D3922</b>
<b>BODIPY® FL C16</b>	<b>Thermo Fisher Scientific</b>	<b>Cat# D3821</b>
<b>Chloroform</b>	<b>Amresco</b>	<b>Cat# 0757-500mL</b>
<b>DAPI</b>	<b>Roth</b>	<b>Cat#6335.1</b>
<b>DMSO - Dimethyl sulfoxide</b>	<b>Biozol</b>	<b>Cat# EMR385250</b>
<b>Ethanol ≥99,5 %, Ph.Eur., reinst</b>	<b>Roth</b>	<b>Cat# 5054.4</b>
<b>Fatty Acid Supplement</b>	<b>Sigma Aldrich</b>	<b>Cat# F7050</b>
<b>Fetal Bovine Serum</b>	<b>Thermo Fisher Scientific</b>	<b>Cat# 10270106</b>
<b>FoxP3/Transcription Staining Set</b>	<b>Thermo Fisher Scientific</b>	<b>Cat# 00-5523-00</b>
<b>Golgi Plug</b>	<b>BD Bioscience</b>	<b>Cat# 51-2301KZ</b>
<b>HEPES Buffer 1M</b>	<b>PAN Biotech</b>	<b>Cat# P05-01100</b>
<b>Tween</b>	<b>Sigma</b>	<b>Cat# P1379</b>
<b>IL-2</b>	<b>Biologend</b>	<b>Cat# 575404</b>
<b>IL-25</b>	<b>Biologend</b>	<b>Cat# 587304</b>
<b>IL-33</b>	<b>Biologend</b>	<b>Cat# 580502</b>
<b>IL-7</b>	<b>Biologend</b>	<b>Cat# 577802</b>
<b>TSLP</b>	<b>R&amp;D Systems</b>	<b>Cat# 555-TS/CF</b>
<b>Ionomycin</b>	<b>Sigma</b>	<b>Cat# I0634-1MG</b>
<b>L-Glutamine (200 mM)</b>	<b>Thermo Fisher Scientific</b>	<b>Cat# A2916801</b>
<b>Liberase™ TL Research Grade</b>	<b>Sigma</b>	<b>Cat# 5401020001</b>
<b>MojoSort Strptavidin Nanobeads</b>	<b>Biologend</b>	<b>Cat# 480016</b>
<b>Papain</b>	<b>Merck</b>	<b>Cat# 5125</b>
<b>Penicillin-Streptomycin</b>	<b>Thermo Fisher Scientific</b>	<b>Cat# 15140122</b>
<b>Percoll</b>	<b>GE Healthcare</b>	<b>Cat# 17-0891-01</b>
<b>Phorbol-12-myristate-13-acetate</b>	<b>Biomol</b>	<b>Cat# LKT- P2857.5</b>
<b>RPMI Medium 1640</b>	<b>Thermo Fisher Scientific</b>	<b>Cat# 21875-091</b>

Sodium pyruvate	Sigma	Cat# P2256-25G
$\beta$ -Mercaptoethanol	PAN Biotech	Cat# P07-05020
Trizol	Thermo Fisher Scientific	Cat# 15596018
A922500	Targetmol	Cat# T6365
GW9662	Cayman Chemicals	Cat# 70785
Linoleic oleic acid BSA	Sigma	Cat# L9655
Palmitic acid	Cayman Chemicals	Cat# 10006627
Palmitic acid click	Prof. Dr. Christoph Thiele	Cat# N.A.
PF06424439	Tocris	Cat# 6348
Vancomycin	Cayman Chemicals	Cat# 15327
Ampicillin	Sigma	Cat# 10835242001
Neomycin	Sigma	Cat# N6386
Metronidazol	Sigma	Cat# M3761
Amphotericin b	Cayman Chemicals	Cat# 11636
Oligomycin	Sigma	Cat# 75351
FCCP	Sigma	Cat# C2920
Rotenone	Sigma	Cat# R8875
Antimycin	Sigma	Cat# A8674
<b>Critical Commercial Assays</b>		
FoxP3/Transcription staining set	Thermo Fisher Scientific	Cat# 00-5523-00
Free Fatty Acid Fluorometric Assay Kit	Cayman	Cat# 700310
Zombie UV Viability Kit	Biolegend	Cat# 423108
Glucose-Glo Assay	Promega	Cat# J6021
Legendplex	Biolegend	Cat# 740446
Annexin V / propidium iodid staining	Biolegend	Cat# 640914
Lipid peroxidation kit	Thermo Fisher Scientific	Cat# C10445

<b>Experimental Models:</b>		
<b>Organisms/Strains</b>		
Mouse: C57BL/6N	Charles River	N/A
ST2 KO	MRC-LMB (A. McKenzie)	N/A
<b>Oligonucleotides</b>		
Acaca	IDT	Mm. PT. 58.12492865 Exon 28-29
Acly	IDT	Mm. PT. 58.33265203 Exon 16-17
Acox1	IDT	Mm. PT. 58.46346115 Exon 7-8
Cpt1a	IDT	Mm. PT. 58.10147164 Exon 12-13
Dgat1	IDT	Mm. PT. 58.32759507 Exon 2-4
Dgat2	IDT	Mm. PT. 58.28629966 Exon 7-8
Fasn	IDT	Mm. PT. 58.14276063 Exon 1-2
Got1	IDT	Mm. PT. 58.10848799 Exon 2-3
Hk1	IDT	Mm. PT. 58.9947184 Exon 15-16
Hmgcs1	IDT	Mm. PT. 58.11355121 Exon 5-6
Hprt	IDT	Mm. PT. 39a.22214828 Exon 6-7

<b>Ldha</b>	<b>IDT</b>	<b>Mm. PT.</b> <b>58.29860774</b> <b>Exon 3-4</b>
<b>Pkm</b>	<b>IDT</b>	<b>Mm. PT.</b> <b>58.6642152</b> <b>Exon 3-4</b>
<b>Ppara</b>	<b>IDT</b>	<b>MM. PT.</b> <b>58.9374886</b> <b>Exon 8-9</b>
<b>Pparg</b>	<b>IDT</b>	<b>Mm. PT.</b> <b>58.31161924</b> <b>Exon 4-5</b>
<b>Slc27a6</b>	<b>IDT</b>	<b>Mm. PT.</b> <b>58.9548097</b> <b>Exon 1-2</b>
<b>Srebf1</b>	<b>IDT</b>	<b>Mm. PT.</b> <b>58.7535355</b> <b>Exon 6-7</b>
<b>Ucp2</b>	<b>IDT</b>	<b>Mm. PT.</b> <b>58.11226903</b> <b>Exon 2-3</b>
<b>Software and Algorithms</b>		
<b>Adobe Illustrator CC</b>	<b>Adobe</b>	<a href="https://www.adobe.com/de/products/illustrator.html">https://www.adobe.com/de/products/illustrator.html</a>
<b>Prism Graphpad 6</b>	<b>GraphPad Software</b>	<a href="https://www.graphpad.com/scientific-software/prism/">https://www.graphpad.com/scientific-software/prism/</a>
<b>QuantStudio Design &amp; Analysis Software</b>	<b>Applied Biosystems by Thermo Fischer Scientific</b>	<a href="https://www.thermofisher.com/de/de/home/technical-resources/software-downloads/ab-quantstudio-3-and-5-real-time-pcr-system.html">https://www.thermofisher.com/de/de/home/technical-resources/software-downloads/ab-quantstudio-3-and-5-real-time-pcr-system.html</a>



<b>Gen5 Microplate reader and imager software</b>	<b>BioTek</b>	<a href="https://www.biotek.com/products/software-robotics-software/gen5-microplate-reader-and-imager-software/">https://www.biotek.com/products/software-robotics-software/gen5-microplate-reader-and-imager-software/</a>
<b>Legenplex Data Analysis Software</b>	<b>Biolegend</b>	<a href="https://www.biolegend.com/legendplex">https://www.biolegend.com/legendplex</a>
<b>FlowJo V10</b>	<b>FlowJO</b>	<a href="https://www.flowjo.com/solutions/flowjo/downloads/">https://www.flowjo.com/solutions/flowjo/downloads/</a>
<b>FIJI Software</b>	<b>National Institutes of Health</b>	<a href="http://fiji.sc/">http://fiji.sc/</a>
<b>Other</b>		
<b>ClustVis</b>	<b>ClustVis</b>	<a href="https://biit.cs.ut.ee/clustvis/">https://biit.cs.ut.ee/clustvis/</a>

### 3. Results

#### 3.1. Activation of ILC2 increased external glucose and FA uptake and induces lipid droplet formation

To study the metabolism of activated ILC2, mice were challenged with the allergen papain on d0, 3, 6 and 13 and lung ILC2 analyzed on d14. Papain is a cysteine protease present in papaya and is able to induce a type 2 immune response (170) (71). As shown in Figure 7A papain challenged mice have an increased percentage of ILC2 and Ki-67<sup>+</sup> ILC2 in total lung. The analysis of Ki-67, commonly known as a proliferation marker, allowed the determination of the growth fraction of a cell population (171). Furthermore, total numbers of ILC2 and Ki-67<sup>+</sup> ILC2 are increased indicating the initiation of a type 2 immunity response (Figure 7B).

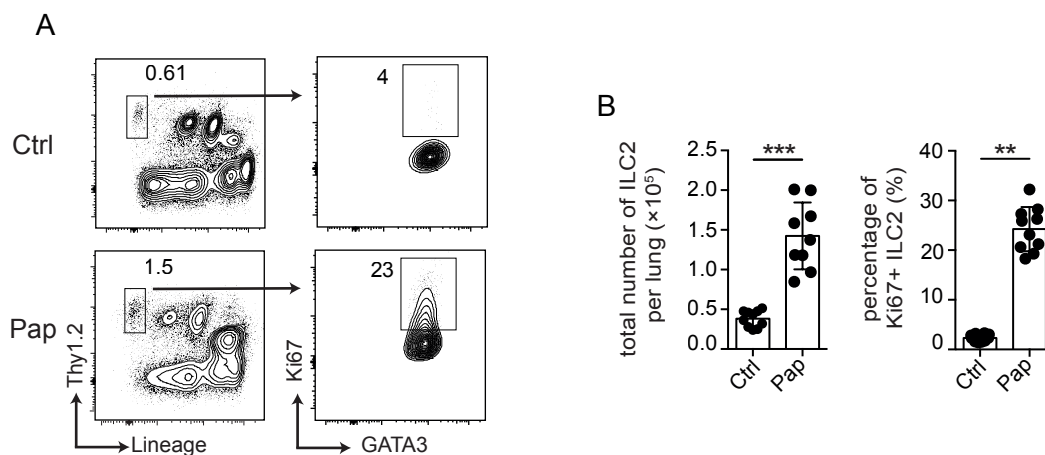


**Figure 7. Papain activates ILC2.** (A) Gating strategy for ILC2 in the lung. C57Bl/6 mice were challenged intranasally with PBS (Ctrl) or papain (Pap) on day 0, 3, 6 and 13. Flow cytometric analysis of cells isolated from the lung of PBS and papain challenged mice at day 14. Panels represent live CD45<sup>+</sup> cells stained with Thy1.2 and lineage (Lin) markers. ILC gated on Lin<sup>-</sup> and Thy1.2<sup>+</sup> expression (ILC) were stained for GATA3 (ILC2) and Ki-67 and (B) total numbers of ILC2 and Ki-67<sup>+</sup> ILC2 in the lung were quantified. Results are representative of two pooled experiments (B) or one representative experiment (A) from at least three independent experiments with three to five mice in each experimental group. All graphs display means SEM; \* p ≤ 0.05, \*\* p ≤ 0.01, \*\*\* p ≤ 0.001.

Glucose uptake analysis was performed by analyzing the uptake of the fluorescent glucose analog 2-NBDG. This analysis showed that upon activation ILC2 take up more 2-NBDG (Figure 8A). In order to test the FA uptake two different methods were used. By using the synthetic, green fluorescent fatty acid palmitate 4,4-difluoro-5,7-dimethyl-4-

bora-3a,4a-diaza-s-indacene-3-hexadecanoic acid (BODIPY® FL C16) it is possible to track the FA uptake, which is drastically higher after papain challenge (Figure 8B). This observation was additionally confirmed by adopting a second approach based on alkyne labeled palmitic acid (Click-Palmitic acid; see section 2.12), which can be detected upon click reaction with an azide-coupled fluorescent reporter (172) (Figure 8C).

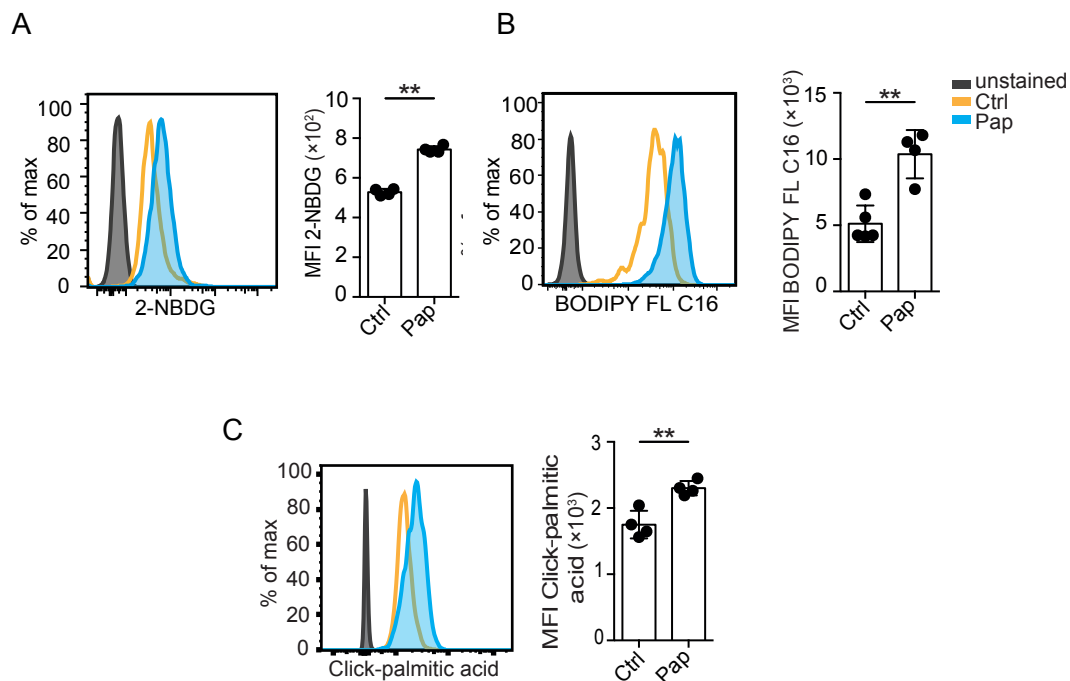


**Figure 8. Papain challenge leads to more glucose and FA uptake in ILC2.** (A) Representative histograms and mean fluorescence intensity (MFI) values of 2-NBDG in lung ILC2 (Lin<sup>-</sup> Thy1.2<sup>+</sup> ST2<sup>+</sup>), (B) MFI values of BODIPY® FL C16 uptake and (C) MFI values of alkyne labeled palmitic acid (Click-Palmitic acid) uptake by lung ILC2 (Lin<sup>-</sup> Thy1.2<sup>+</sup> Gata3<sup>+</sup>) after PBS or papain (Pap) challenge (Click-palmitic acid uptake performed by Dr. Fotios Karagiannis). Results are representative of one representative experiment (A-C) from at least two (C) or three (A, B) independent experiments with three to five mice in each experimental group. All graphs display means SEM; \* p ≤ 0.05, \*\*p ≤ 0.01, \*\*\* p ≤ 0.001.

Furthermore, the availability of glucose in the lung tissue of mice challenged with papain was reduced compared to levels measured in the plasma during steady state conditions. The papain challenge promoted an increase in the glucose level (Figure 9A). as well as the amount of FFA (Figure 9B).

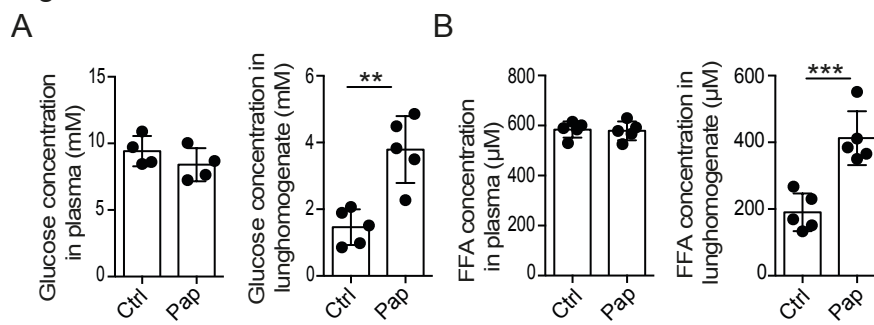


**Figure 9. Papain increases glucose and FFA concentrations in lung homogenate but not in the circulation. (A)** Glucose concentration and **(B)** FFA concentrations in plasma and lung homogenate from PBS (Ctrl) or papain (Pap) challenged mice. Results are representative of at least three independent experiments with three to five mice in each experimental group. All graphs display means SEM; \*  $p \leq 0.05$ , \*\*  $p \leq 0.01$ , \*\*\*  $p \leq 0.001$ .

To further test whether increased uptake of glucose and FA is a general characteristic of chronically activated ILC2 in the context of allergen-driven airway inflammation, the analysis was extended to a model of fungal allergens. Similar to mice challenged with the protease allergen papain, also in this second model ILC2 accumulated in mice treated with the fungal allergen *Alternaria alternata* (*a. alternata*) and displayed increased uptake of exogenous FA and glucose (Figure 10A-C).

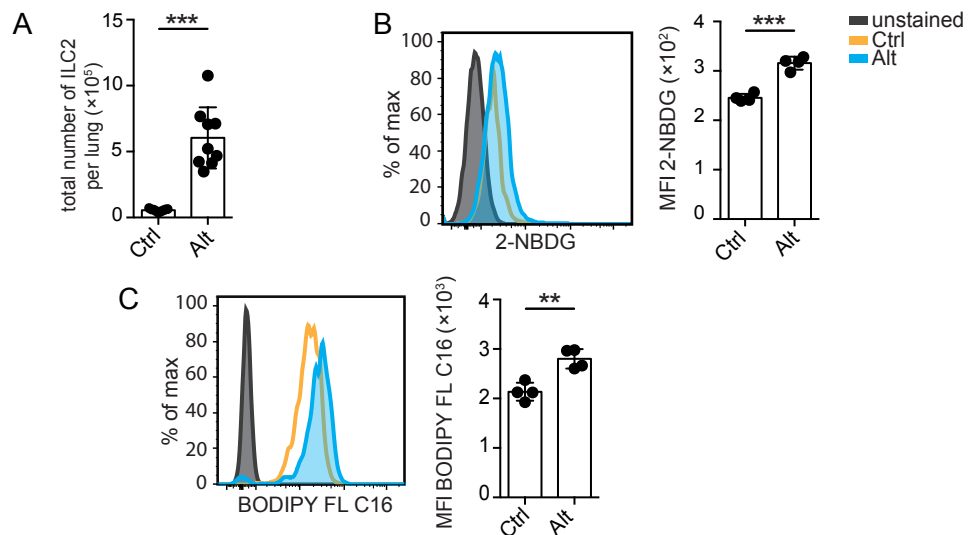


**Figure 10. *Alternaria alternata* induced airway inflammation leads to lipid droplet formation. (A)** C57Bl/6 mice were challenged intranasally with PBS (Ctrl) or *a. alternata* (Alt) on day 0, 3, 6 and 13. Flow cytometric analysis of cells isolated from the lung of *a. alternata* and PBS challenged animals at day 14. Total numbers of ILC2 were analyzed by flow cytometry and compared to PBS challenged controls on day 14. **(B)** Representative histograms and mean fluorescence intensity (MFI) values of 2-NBDG in lung ILC2 (Lin<sup>-</sup> Thy1.2<sup>+</sup> ST2<sup>+</sup>) and **(C)** MFI values of BODIPY<sup>®</sup> FL C16 uptake by lung ILC2 (Lin<sup>-</sup> Thy1.2<sup>+</sup> Gata3<sup>+</sup>). Results are representative of two pooled experiment (A) or one representative experiment (B, C) from at least three independent experiments with three to five mice in each experimental group. All graphs display means SEM; \*  $p \leq 0.05$ , \*\*  $p \leq 0.01$ , \*\*\*  $p \leq 0.001$ .

To test metabolic changes on the transcriptional level ILC2 were isolated to a purity of more than 98% as described in section 2 (Figure 11).

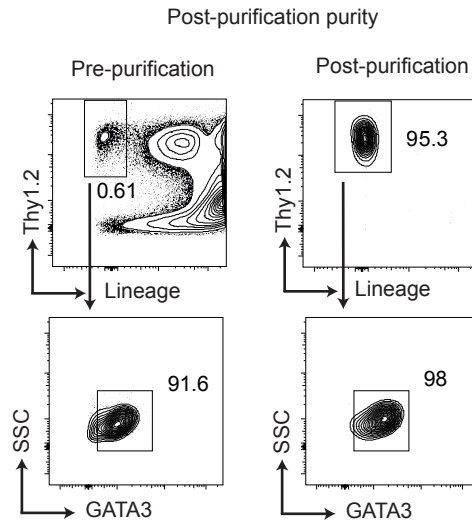


**Figure 11. Purification strategy of ILC2.** Total lung cells were stained with antibodies against CD3, CD11b, CD11c, CD49b, CD19, Ter119, NK1.1 and Gr-1 coupled to biotin followed by incubation with Streptavidin-coupled magnetic microbeads (Biolegend) and negative selection on magnetic columns (Miltenyi). Post-purification measurements indicating a purity greater than 98%.

To test how activation of ILC2 changes metabolism on the gene level, an analysis of the relative gene expression was performed via qPCRs. After Papain challenge ILC2 show changes in different metabolic genes. Genes for fatty acid synthesis, cholesterol synthesis and  $\beta$ -oxidation are downregulated (*Acc1*, *Fasn*, *Acly*, *Hmgcs1*, *Srebf*, *Ppara*, *Cpt1*, *Acox1*), whereas other genes that regulate the triglyceridesynthesis (TGS) (*Dgat1*, *Dgat2*) are highly upregulated. Furthermore genes involved in glycolysis (*Hk1*, *Ldha*, *Pkm*) are upregulated as well as genes involved in FA uptake (*Pparg*, *Slc27a6*).

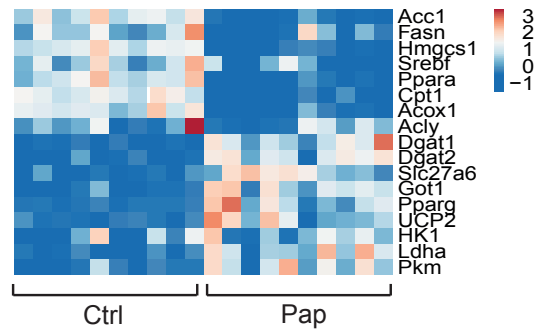


**Figure 12. Papain upregulates genes for triglyceridesynthesis.** Gene expression analysis relative to HPRT of purified lung ILC2 isolated from PBS (Ctrl) or papain (Pap) challenged mice. Results are representative of two pooled experiment from at least three independent experiments with three to five mice in each experimental group.

Since fuel uptake data and qPCR data have shown a higher glucose and fatty acid uptake and an upregulation of genes involved in TGS and FA uptake, another analysis was performed by FACS in order to quantify neutral lipid content, such as triglycerides. Here, cells were stained with the neutral lipid dye 4,4-difluoro-1,3,5,7,8-pentamethyl-4-bora-3a,4a-diaza-s-indacene (BODIPY® 493/503) and lung ILC2 from papain and *a. alternata* challenged mice displayed increased staining with BODIPY® 493/503, indicating an increased LD formation, when compared to ILC2 isolated from control mice (Figure 13A and C). A second approach using confocal microscopy confirmed an increased LD formation in ILC2 activated by papain challenge (Figure 13B).

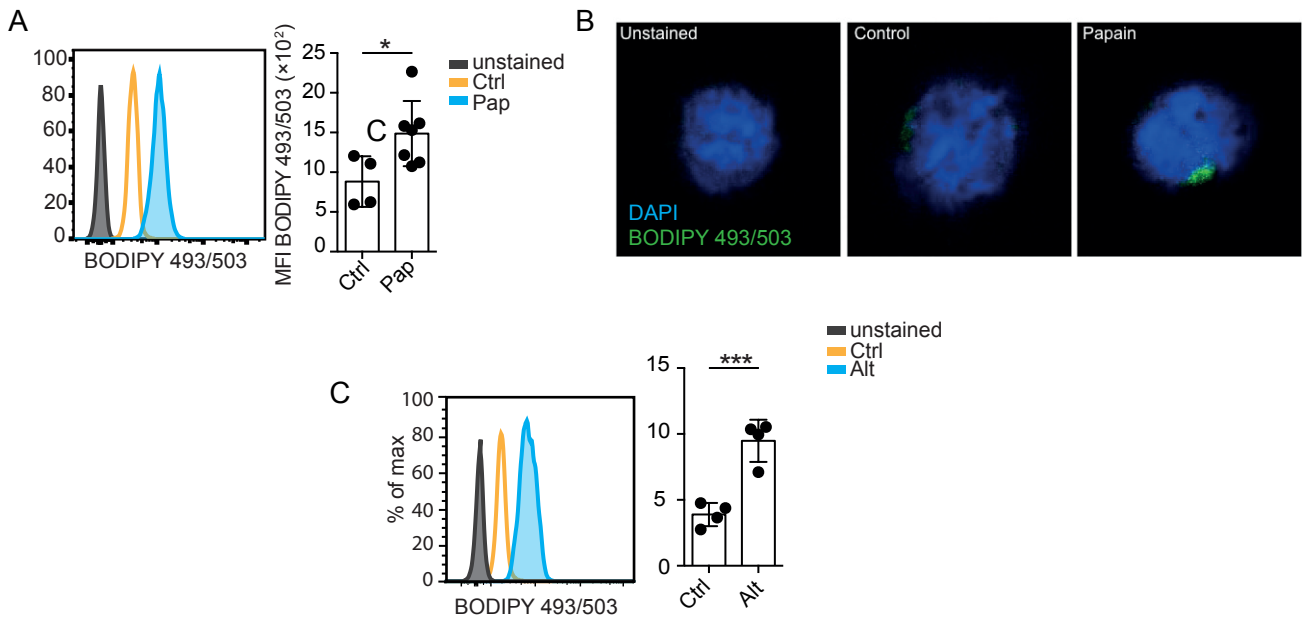


**Figure 13. Activation of pulmonary ILC2 induces lipid droplet formation.** (A) Representative histograms and MFI values of BODIPY® 493/503 (Lin<sup>-</sup> Thy1.2<sup>+</sup> Gata3<sup>+</sup>) and (B) representative microscope images of BODIPY® 493/503 staining in lung ILC2 (Lin<sup>-</sup> Thy1.2<sup>+</sup> Gata3<sup>+</sup>) after PBS or papain challenge. (C) Representative histograms and MFI values of BODIPY® 493/503 (Lin<sup>-</sup> Thy1.2<sup>+</sup> Gata3<sup>+</sup>) from ILC2 isolated from mice challenged with *a. alternata* (confocal microscopy performed by Dr. Fotios Karagiannis). Results are representative of one representative experiment (A-C) from at least two (B) or three (A,C) independent experiments with three to five mice in each experimental group. All graphs display means SEM; \* p ≤ 0.05, \*\*p ≤ 0.01, \*\*\* p ≤ 0.001.

### 3.2. IL-33 promotes acquisition of external FA and LD formation in activated ILC2

Naive ILC2 lung tissue cells were sorted and a cell culture was performed as described in section 2. The purity post-sorting was greater than 99% (Figure 14).

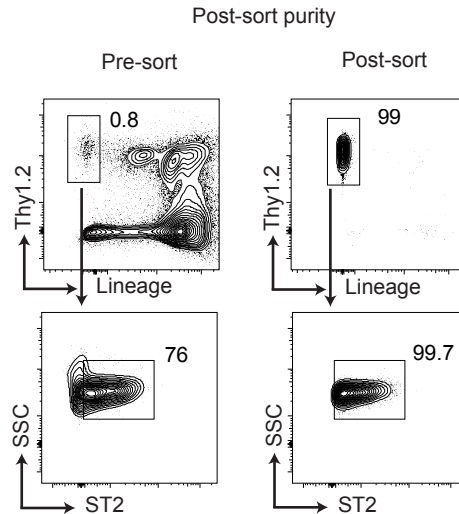


**Figure 14. Sorting strategy of ILC2.** Cells were stained with lineage markers (CD3, CD11b, CD11c, CD49b, CD19, Ter119, NK1.1 and Gr-1) and Thy1.2 and gated on live and CD45<sup>+</sup> cells. ILC2 were sorted as Thy1<sup>+</sup>, Lineage<sup>-</sup>, ST2<sup>+</sup>. Post-sort measurements indicating a purity greater than 99%.

ILC2 are activated by epithelial alarmins such as IL-33, IL-25 and TSLP (76). In order to study the effect of these alarmins on ILC2 and to test if this stimuli can lead to LD formation in ILC2, sorted ILC2 were cultured in the presence of IL-7 alone or in combination with IL-33, IL-25 or TSLP to imitate steady-state conditions or activation of ILC2. Strikingly, only the combination of IL-7 and IL-33 but not IL-7 alone could induce the proliferation of ILC2 and increase their glucose and external FA uptake (Figure 15 A-C). Increased acquisition of FA caused by activation with a combination of IL-7 and IL-33 resulted in the simultaneous increase in LD formation (Figure 15 D). This effect was exclusive for IL-7 and IL-33 stimulation and it could not be observed in other combinations.



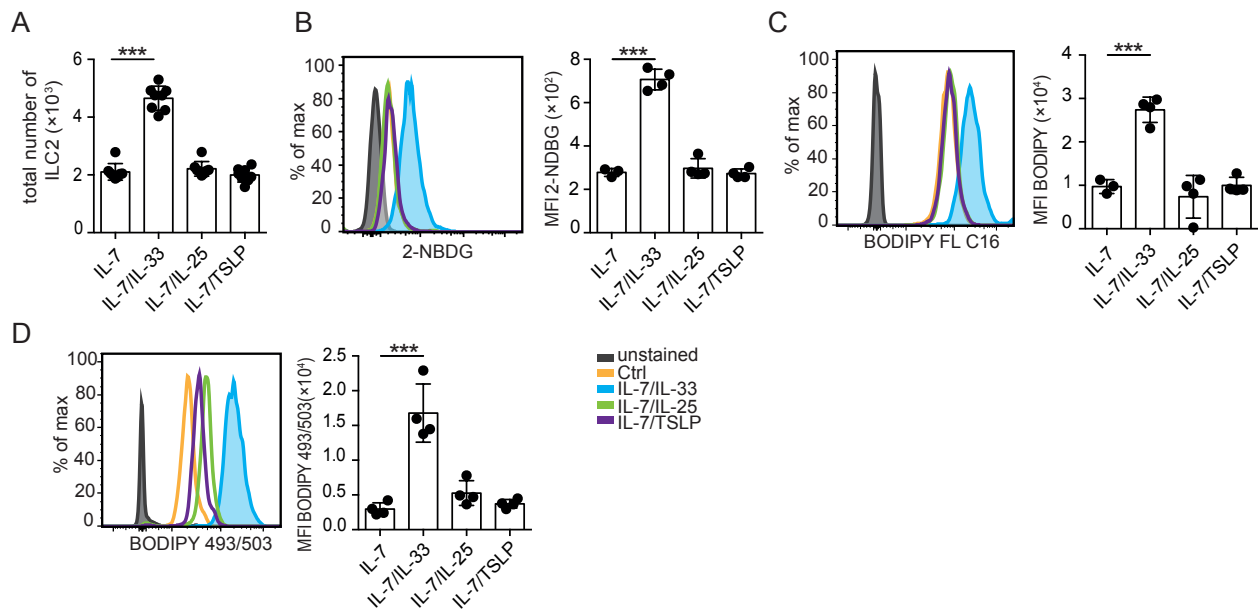


**Figure 15. IL-33 promotes lipid uptake and droplet formation in activated ILC2 *in vitro*.** ILC2 were sort purified from naive C57BL/6 mice and cultured for 3 days in the presence of IL-7, or a combination of IL-7 and IL-33, IL-7 and IL-25 and IL-7 and TSLP. **(A)** Total numbers of purified ILC2 after three days of culture. **(B)** Representative histograms and MFI values of 2-NBDG (Lin<sup>-</sup> Thy1.2<sup>+</sup> ST2<sup>+</sup>) and **(C)** BODIPY<sup>®</sup> FL C<sub>16</sub> uptake by cultured ILC2 (Lin<sup>-</sup> Thy1.2<sup>+</sup> Gata3<sup>+</sup>). **(D)** Representative histograms and MFI values of BODIPY<sup>®</sup> 493/503 staining in cultured ILC2 (Lin<sup>-</sup> Thy1.2<sup>+</sup> Gata3<sup>+</sup>). Results are representative of two pooled experiment (A) or one representative experiment (B-D) from at least three independent experiments with three to five mice in each experimental group. All graphs display means SEM; \* p $\leq$  0.05, \*\*p  $\leq$  0.01, \*\*\* p $\leq$ 0.001.

To further examine the importance of IL-33 in activating a unique metabolic program driving pathogenic ILC2 responses *in vivo*, mice were treated intranasally with the cytokines IL-33, IL-25 or TSLP. In accordance with the *in vitro* findings, only the challenge with IL-33 showed an accumulation of ILC2 in the lung. The challenge with IL-25 or TSLP did not induce this accumulation. IL-33 challenged mice showed an increased acquisition of external glucose and FA, which resulted in increased LD formation in lung ILC2 (Figure 16).

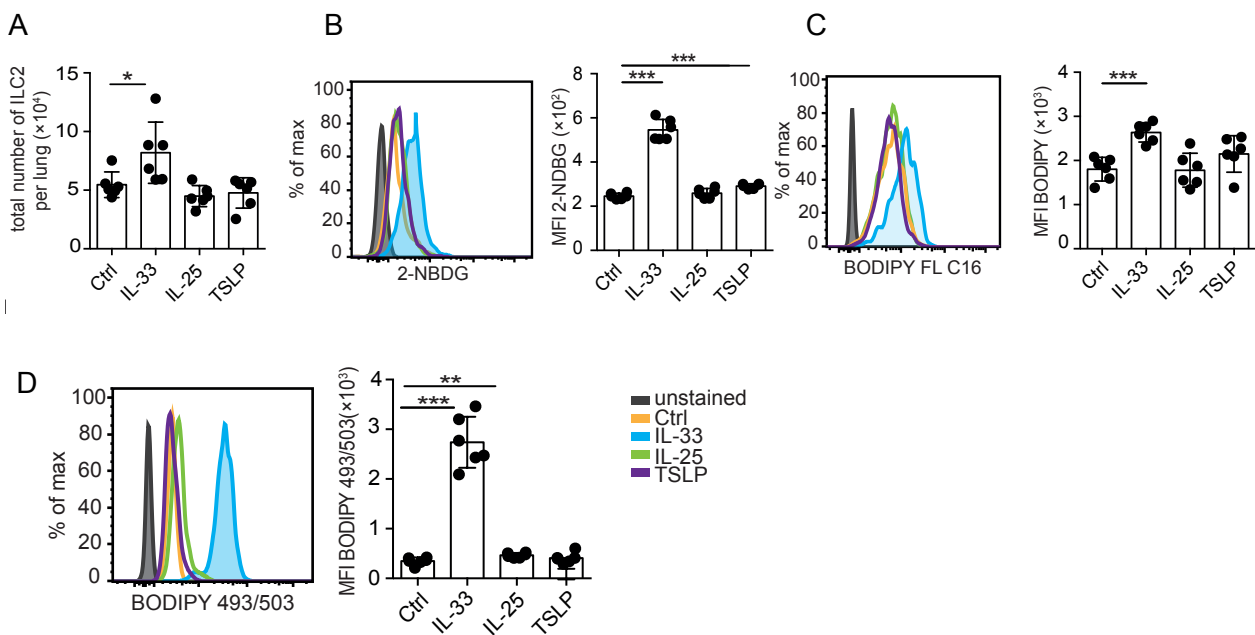


**Figure 16. IL-33 promotes lipid uptake and droplet formation in activated ILC2 *in vivo*.** C57BL/6 mice were challenged intranasally with IL-33, IL-25, TSLP or PBS (Ctrl) on d0, 1 and 2. At d3 cells isolated from the lung of cytokine and PBS challenged animals. **(A)** Total numbers were analyzed by flow cytometry. **(B)** Representative histograms and MFI values of 2-NBDG in lung ILC2 (Lin<sup>-</sup> Thy1.2<sup>+</sup> ST2<sup>+</sup>) and **(C)** BODIPY<sup>®</sup> FL C<sub>16</sub> uptake and **(D)** BODIPY<sup>®</sup> 493/503 staining of lung ILC2 (Lin<sup>-</sup> Thy1.2<sup>+</sup> Gata3<sup>+</sup>). Results are representative of two pooled experiment (A-D) from at least three independent experiments with three to five mice in each experimental group. All graphs display means SEM; \*  $p \leq 0.05$ , \*\* $p \leq 0.01$ , \*\*\*  $p \leq 0.001$ .

Challenge with IL-33 resulted in a change in the expression of genes encoding a metabolic profile. In particular, IL-33 upregulated key genes involved in glycolysis (*Hk1*, *Ldha* and *Pkm*), FA metabolism (*Pparg*, *Slc27a6*) and LD droplet formation (*Dgat1*) (Figure 17). Hence, the *in vitro* and *in vivo* experiments suggest that IL-33 imprints a metabolic program in ILC2, which results in increased glucose and FA uptake, upregulation of glycolysis and LD formation.

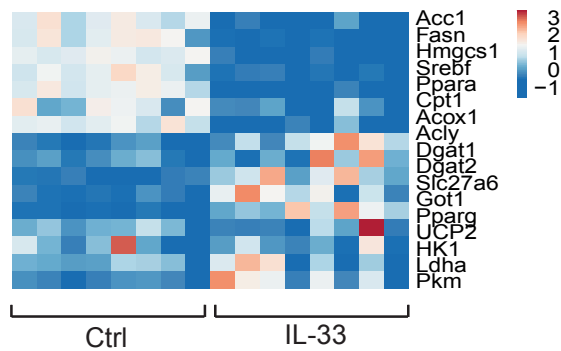


**Figure 17. IL-33 challenge leads to an increase of genes involved in TAG synthesis and FA uptake.** Gene expression analysis relative to HPRT of purified lung ILC2 isolated from IL-33 or PBS (Ctrl) challenged mice. Results are representative of two pooled experiment from at least three independent experiments with three to five mice in each experimental group.

To further test this hypothesis, mice genetically deficient for the IL-33 receptor (ST2 KO mice) (173) were challenged with papain. In accordance to the previous results ILC2 isolated from ST2 KO mice displayed drastically reduced uptake of glucose and FA and failed to increase the formation of LD compared to wild-type (WT) mice (Figure 18A-D). Taken together these data suggest that the epithelial derived cytokine IL-33 shapes a metabolic program in ILC2, which results in increased uptake of glucose and FA, the upregulation of glycolysis and the formation of LD.

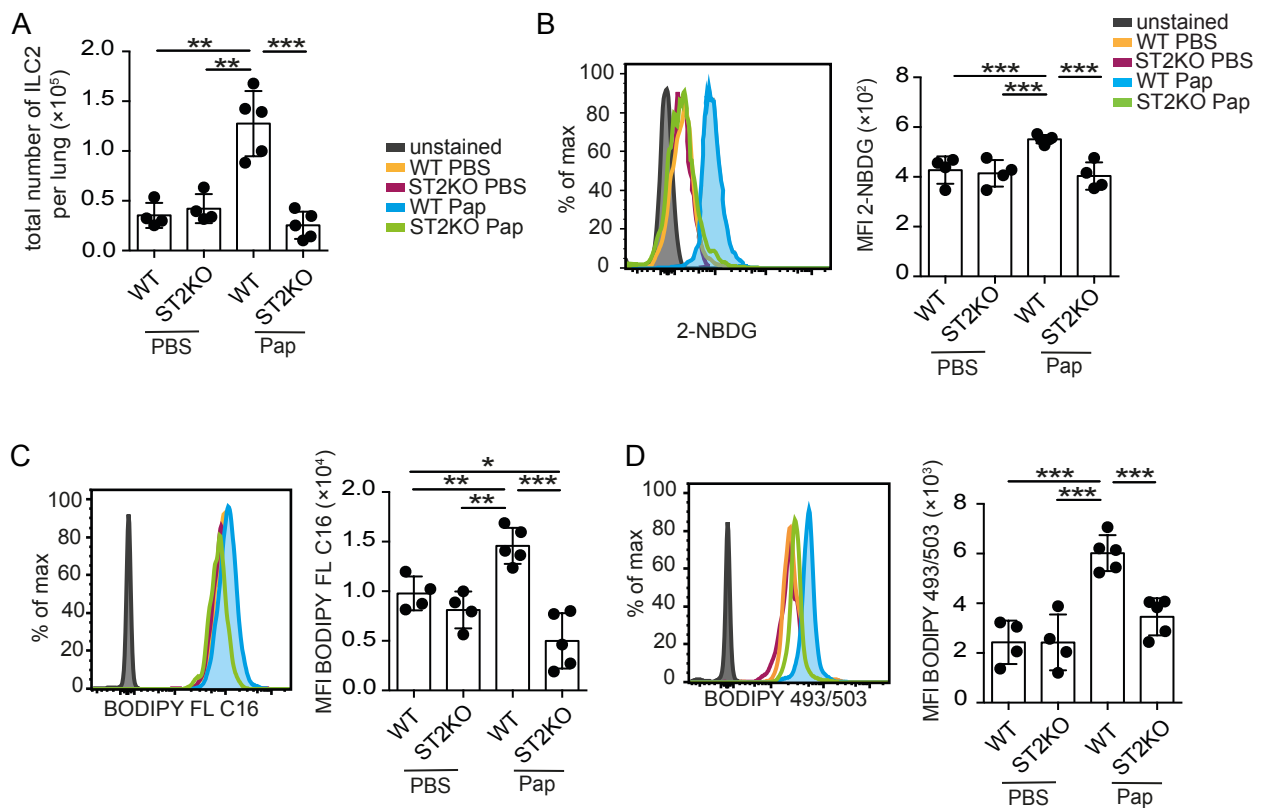


**Figure 18. IL-33 is essential for acquisition of external lipids and lipid droplet formation in ILC2.** (A) WT and ST2 KO mice were challenged intranasally with papain (Pap) or PBS (Ctrl) on day 0, 3, 6 and 13 and total numbers of ILC2 were analyzed by flow cytometry and compared to PBS challenged controls on day 14. (B) Representative histograms and MFI values of 2-NBDG (Lin<sup>-</sup> Thy1.2<sup>+</sup> CD25<sup>+</sup> Sca1<sup>+</sup>), BODIPY<sup>®</sup> FL C<sub>16</sub> (C) and BODIPY<sup>®</sup> 493/503 (D) in lung ILC2 (Lin<sup>-</sup> Thy1.2<sup>+</sup> Gata3<sup>+</sup>) from C57BL/6 and ST2 KO mice challenged with papain (Pap) or PBS (Ctrl). Results are representative of one representative experiment (A-D) from one experiment with four to five mice in each experimental group. All graphs display means SEM; \* p ≤ 0.05, \*\* p ≤ 0.01, \*\*\* p ≤ 0.001.

### 3.3 DGAT1 dependent LD formation protects ILC2 from lipotoxicity and allows for increased uptake of external lipids

As described in section 1.8. excess of FFA in the cytoplasm of cells can generate bioactive lipids or disrupt the integrity of mitochondrial membranes promoting lipotoxicity (149). In this context, the formation of LD is considered as an essential step to prevent FFA from causing lipotoxicity (150, 151). Here, DGAT1, an enzyme that catalyzes the esterification of diacylglycerides and FA into triglycerides is crucial in the process of LD formation. Storage of FFA in LD prevents lipotoxicity caused by either excessive uptake of external lipids or the mobilization of FFA during lipolysis (151). To confirm that external lipids indeed are stored in LD, ILC2 isolated from PBS or papain challenged mice were

cultured with BODIPY® FL C<sub>12</sub>, a saturated FA analog covalently bound to the BODIPY® fluorophore. BODIPY®-FA have been previously used to study lipid trafficking and can be esterified into neutral lipids stored in LD (174) (175) (176). Culturing ILC2 with BODIPY® FL C<sub>12</sub> revealed a rapid uptake of fluorescently labeled FA and subsequent storage in LD as assessed by confocal microscopy (Figure 19).

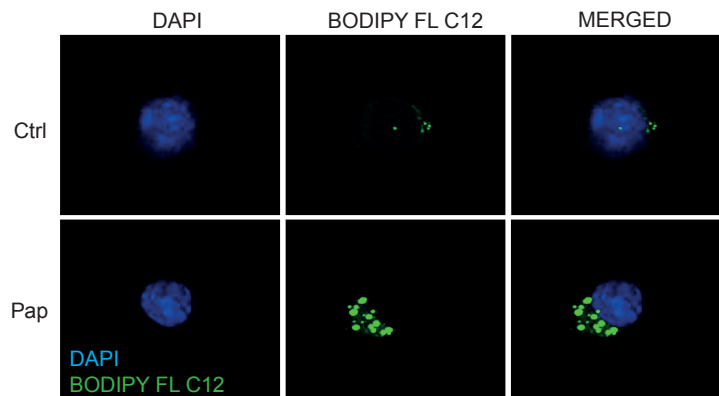


**Figure 19. DGAT1 dependent LD formation protects ILC2 from lipotoxicity and allows for increased uptake of external lipids.** Representative microscope images of purified ILC2 isolated from papain (Pap) or PBS (Ctrl) challenged mice cultured in the presence of IL-7 and BODIPY® FL C<sub>12</sub> (performed by Dr. Fotios Karagiannis). Results are representative of one representative experiment from at least two independent experiments with three to five mice in each experimental group. All graphs display means SEM; \*  $p \leq 0.05$ , \*\* $p \leq 0.01$ , \*\*\*  $p \leq 0.001$ .

To further test if expression of DGAT1 prevents lipotoxicity and allows the acquisition of external lipids in activated ILC2, purified ILC2 were isolated from papain challenged mice treated with increasing concentrations of the DGAT1 inhibitor (DGAT1i), A922500 (177). In agreement with the already known function of DGAT1, 40  $\mu\text{M}$  of DGAT1i *in vitro* cause lipotoxicity and reduce the survival of ILC2 (Figure 20A-B). In line with the essential role of DGAT1 in the formation of lipid droplets, even non-toxic concentrations of A922500 reduced the capacity of ILC2 to form LD (Figure 20C).

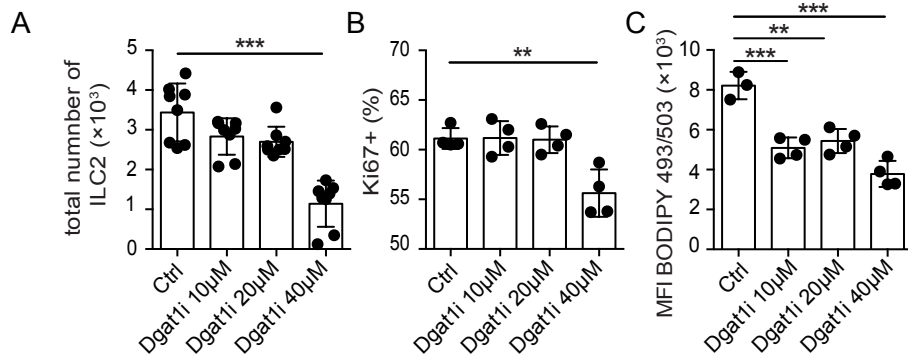


**Figure 20. DGAT1-Inhibitor A922500 decreases ILC2 proliferation and lipid droplet formation.** ILC2 were purified from papain challenged C57BL/6 mice and cultured for 3 days in the presence of IL-2 only (Ctrl) or a combination of IL-2 with increasing concentrations of the DGAT1-Inhibitor A922500 (DGAT1i). **(A)** Total numbers of ILC2 in culture, **(B)** expression of Ki-67 and **(C)** MFI values of BODIPY® 493/503. Results are representative of two pooled experiment (A) or one representative experiment (B-C) from at least three independent experiments with three to five mice in each experimental group. All graphs display means SEM; \* p≤ 0.05, \*\*p ≤ 0.01, \*\*\* p≤0.001.

To prove if DGAT1i A922500 leads to cell death or to limited proliferation, ILC2 were purified and cultured. The cell number on d0 was determined without the addition of any cytokines (input d0). The cell numbers of ILC2 cultured with or without A922500 and the addition of IL-2 was determined on d3. Interestingly, DGAT1i not only reduced the accumulation of ILC2 but also reduced the ILC2 numbers compared to the starting numbers of cultured cells. With these observations it seems clear that DGAT1 inhibition is not only preventing the proliferation and accumulation of ILC2 *in vitro* but also result in cell death (Figure 21).

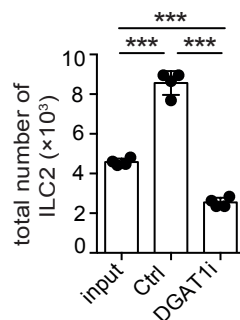


**Figure 21. DGAT1-Inhibitor A922500 leads to cell death in ILC2 *in vitro*.** ILC2 were purified from papain challenged C57BL/6 mice and cultured for three days in the presence of IL-2 only (Ctrl) or with a combination of IL-2 and DGAT1-Inhibitor A922500 (DGAT1i). ILC2 numbers were determined on d0 and d3. Results are representative of one representative experiment from at least two independent experiments with three to five mice in each experimental group. All graphs display means SEM; \* p≤ 0.05, \*\*p ≤ 0.01, \*\*\* p≤0.001.

In order to test cell death via apoptosis, an Annexin V / propidium iodid double stain was performed and analyzed by FACS. Strikingly, ILC2 cultured with A922500 have more apoptotic cells compared to control, which explains the low cell number after three days of culture (Figure 22).

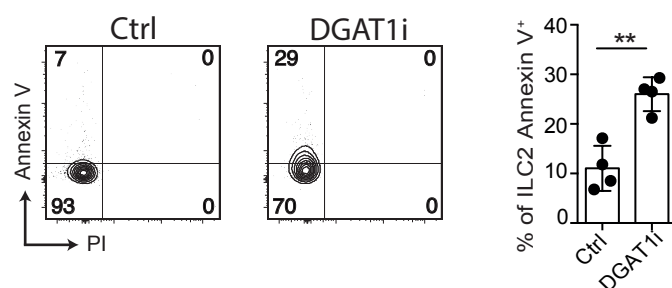


**Figure 22. DGAT1-Inhibitor A922500 leads to apoptosis in ILC2 *in vitro*.** ILC2 were purified from papain challenged C57BL/6 mice and cultured for three days in the presence of IL-2 with increasing concentrations of the DGAT1-Inhibitor A922500 (DGAT1i). Results are representative of one representative experiment from at least two independent experiments with three to five mice in each experimental group. All graphs display means SEM; \*  $p \leq 0.05$ , \*\*  $p \leq 0.01$ , \*\*\*  $p \leq 0.001$ .

As it is known that DGAT1 is important to detoxify cells from extra FA, lipid peroxidation was determined by using a fluorescent reporter BODIPY® 581/591 C11 (Figure 23). This reagent localizes to membranes in living cells and upon oxidation by lipid hydroperoxides, displays a shift in the peak of fluorescence emission. It was verified that A922500 leads to more oxidative degeneration of cellular lipids by reactive oxygen species, which can affect membrane properties, signal transduction pathways and apoptosis. Increased lipid peroxidation induced by DGAT1 inhibition might be one reason of the increased cell death reported in the previous assay.

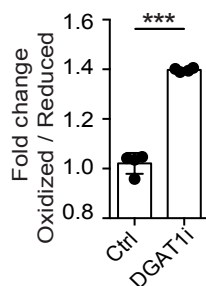


**Figure 23. DGAT1-Inhibitor A922500 leads lipid peroxidation.** ILC2 were purified from papain challenged C57BL/6 mice and cultured for two hours in the presence of IL-2 only (Ctrl) or IL IL-2 and with DGAT1-Inhibitor A922500 (DGAT1i). Results are representative of one representative experiment from at least two independent experiments with three to five mice in each experimental group. All graphs display means SEM; \*  $p \leq 0.05$ , \*\*  $p \leq 0.01$ , \*\*\*  $p \leq 0.001$ .

In contrast, the blocking of DGAT2, another isoform of diacylglycerol O-acyltransferase, which is highly expressed in ILC2 (178), with the specific inhibitor PF06424439 (DGAT2i) (179) had no effect on ILC2 viability, proliferation or LD formation in culture (Figure 24A-B). This suggests that expression of DGAT1 but not DGAT2 may be essential for ILC2 to acquire and store high amounts of external lipids from the environment.

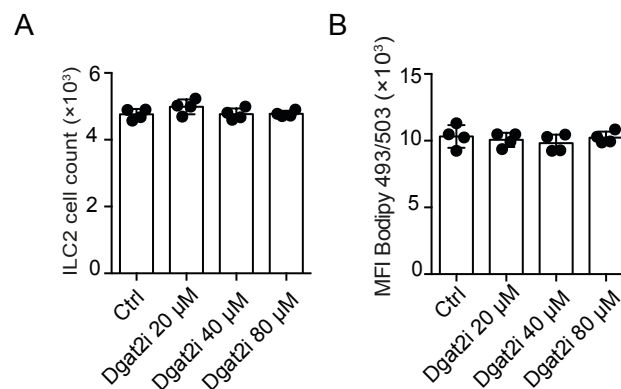


**Figure 24. DGAT2-Inhibitor PF06424439 has no effect on ILC2 numbers and lipid droplet formation.** (A) Total numbers of purified ILC2 after three days of culture. Cells are cultured with IL-2 only (Ctrl) or IL-2 and increasing concentrations of DGAT2-Inhibitor PF06424439. (B) BODIPY® 493/503 staining of cultured ILC2. Results are representative of one representative experiment from at least two independent experiments with three to five mice in each experimental group. All graphs display means SEM; \* p≤ 0.05, \*\*p ≤ 0.01, \*\*\* p≤0.001.

Furthermore, high concentrations of extracellular lipids may cause toxicity (150). Consequently, the upregulation of DGAT1 in the context of airway inflammation may induce ILC2 to be less sensitive to the presence of excess amounts of external lipids. Indeed, DGAT1 function was important for ILC2 to use increased amounts of external lipids since treatment with a non-toxic concentration of DGAT1i impaired their capability to use oleic/linoleic acid or palmitic acid and to proliferate in culture (Figure 25).



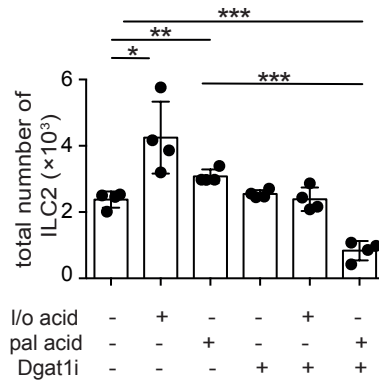


**Figure 25. DGAT1 dependent LD formation protects ILC2 from lipotoxicity and allows for increased uptake of external lipids.** Culture of ILC2 with linoleic acid/oleic acid-BSA (l/o) or palmitic acid-BSA (pal) and a combination of non-toxic concentration of DGAT1i (20  $\mu$ M). Results are representative of one representative experiment from at least two independent experiments with three to five mice in each experimental group. All graphs display means SEM; \*  $p \leq 0.05$ , \*\* $p \leq 0.01$ , \*\*\* $p \leq 0.001$ .

The *in vitro* results suggest that the function of DGAT1 may be essential for chronically activated ILC2 to utilize external lipids. In order to test the importance of LD formation for the functionality of ILC2 in the inflamed tissue microenvironment papain challenged mice were treated with DGAT1i to ablate the formation of LD *in vivo*. Remarkably, inhibition of DGAT1 almost completely ablated the accumulation of ILC2 in the lungs of papain-challenged mice (Figure 26A). Furthermore, while ILC2 isolated from papain challenged mice treated with DGAT1i showed no difference in their capacity to acquire glucose and FA from the environment, ILC2 failed to increase the formation of LD and showed drastically reduced capacity to proliferate (Figure 26B-D). Thus, DGAT1 expression in ILC2 mediates the formation of LD, which act as an essential nutrient buffering system in activated ILC2 to allow the acquisition of high amounts of external FA.

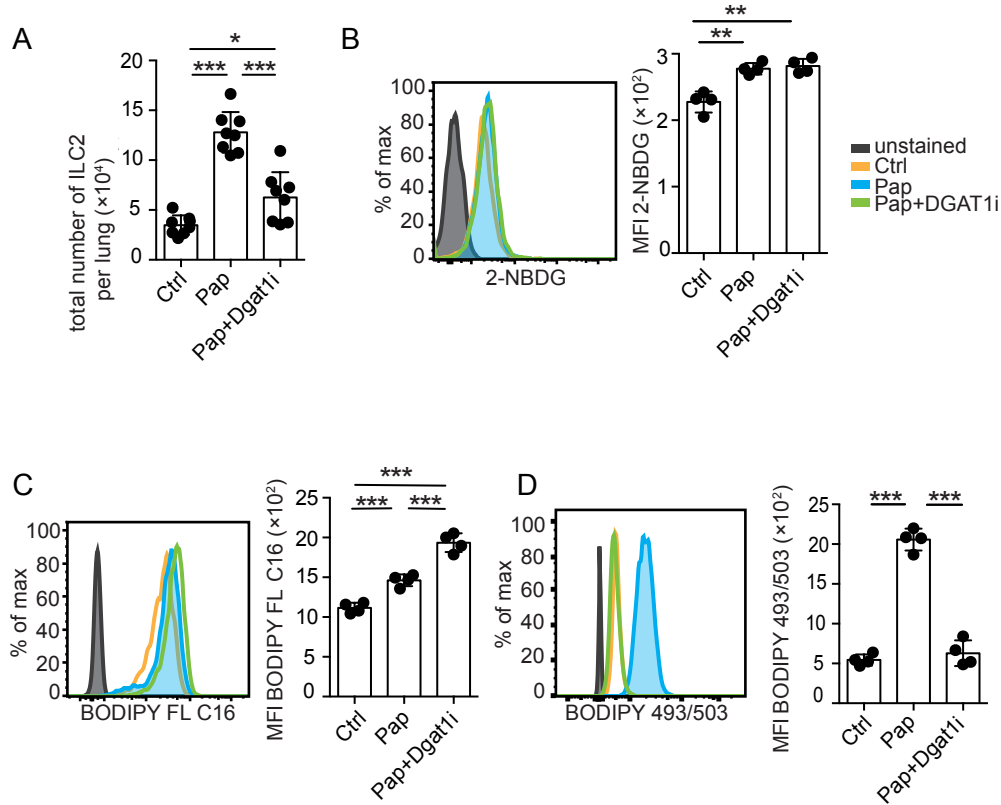


**Figure 26. DGAT1i inhibits ILC2 accumulation in airway inflammation.** C57BL/6 mice were challenged intranasally with papain (Pap) or PBS (Ctrl) on day 0, 3, 6 and 13 and simultaneously treated i.p. daily with DGAT1-Inhibitor A922500 (DGAT1i), control animals were treated with DMSO only. **(A)** Total numbers of ILC2 from PBS (Ctrl), papain (Pap) or papain challenged mice treated with DGAT1i (Pap+DGAT1i) **(B)** Representative histograms and MFI values of 2-NBDG in lung ILC2 (Lin<sup>-</sup> Thy1.2<sup>+</sup> ST2<sup>+</sup>) and **(C)** MFI values of BODIPY<sup>®</sup> FL C<sub>16</sub> uptake and **(D)** BODIPY<sup>®</sup> 493/503 in ILC2 (Lin<sup>-</sup> Thy1.2<sup>+</sup> Gata3<sup>+</sup>). Results are representative of two pooled experiments (A) or one representative experiment (B-D) from at least two independent experiments with three to five mice in each experimental group. All graphs display means SEM; \* p $\leq$  0.05, \*\*p  $\leq$  0.01, \*\*\* p $\leq$ 0.001.

### 3.4 PPAR $\gamma$ regulated FA uptake fuels proliferation and cytokine production

To directly test the effect of external FA on ILC2 the long chain fatty acids linoleic/oleic acid and palmitic acid have been added to cultured ILC2. The addition of external FA substantially increased the proliferation and accumulation in culture (Figure 27).

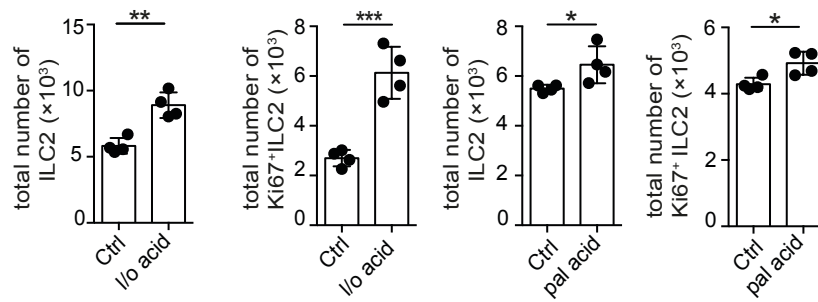


**Figure 27. External FA increased proliferation and accumulation of ILC2 *in vitro*.** (A) Total numbers of purified lung ILC2 and Ki-67<sup>+</sup> ILC2 isolated from papain challenged C57BL/6 mice cultured for three days with IL-2 in the presence or absence of linoleic acid/oleic acid-BSA (I/o) and (B) total numbers of ILC2 and of Ki-67<sup>+</sup> ILC2 cultured with IL-2 in the presence or absence of palmitic acid-BSA (pal). Results are representative of one representative experiment from at least two independent experiments with three to five mice in each experimental group. All graphs display means SEM; \*  $p \leq 0.05$ , \*\*  $p \leq 0.01$ , \*\*\*  $p \leq 0.001$ .

In addition, highly proliferative cells, assessed by intracellular Ki-67 staining, are able to store and acquire more external lipids in LD than non-proliferating cells (Figure 28A-B). Increased lipid acquisition in highly proliferative cells was confirmed by assessing uptake of Click-Palmitic acids in ILC2 isolated from papain challenged mice (Figure 28C).

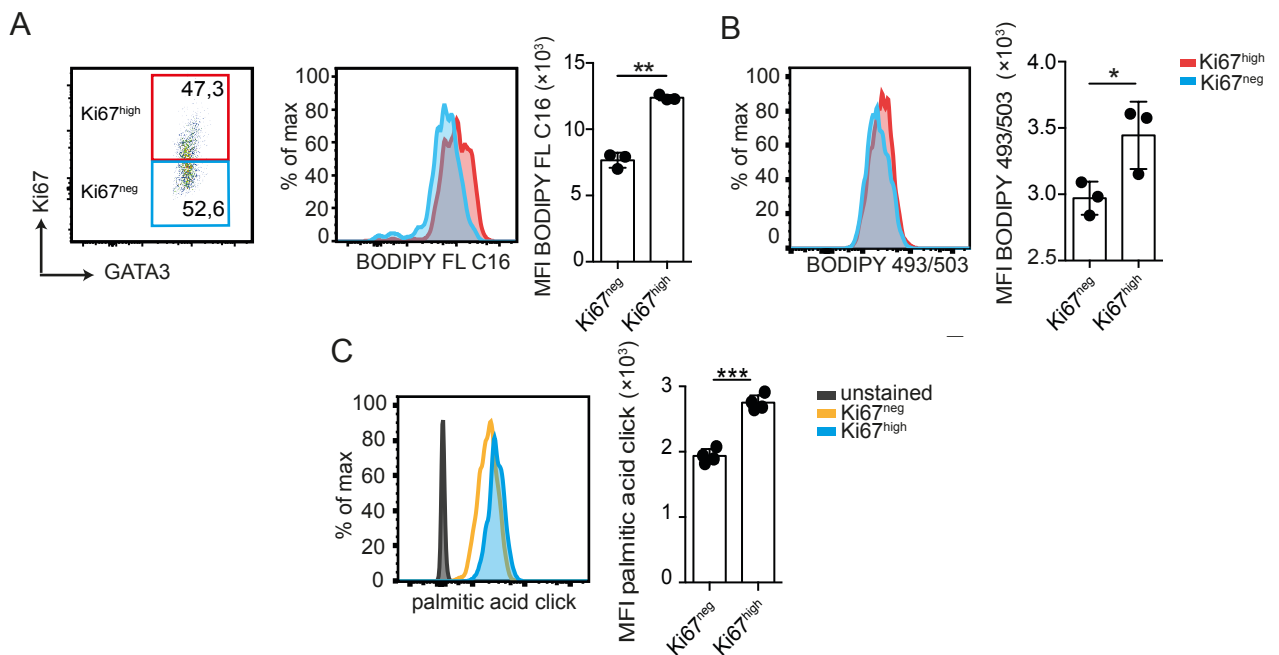


**Figure 28. Proliferating ILC2 take up more fatty acids and build up more lipid droplets compared to non proliferating ILC2.** Representative histograms and MFI values of BODIPY<sup>®</sup> FL C16 (A), BODIPY<sup>®</sup> 493/503 (B) and click-palmitic acid (C) in Ki-67 positive and negative lung ILC2 from mice challenged with papain (Click-palmitic acid uptake performed by Dr. Fotios Karagiannis). Results are representative of one representative experiment from at least two independent experiments with three to five mice in each experimental group. All graphs display means SEM; \*  $p \leq 0.05$ , \*\*  $p \leq 0.01$ , \*\*\*  $p \leq 0.001$ .

These data indicate that exogenous FA increased the proliferation of ILC2. In addition, the gene expression analysis of papain-activated ILC2 did not reveal any substantial upregulation of genes involved in *de novo* lipid synthesis. Hence, it was hypothesized that externally acquired FA may be directly funneled into membrane lipids to support proliferation. To test this assumption a pulse-chase experiment after addition of Click-Palmitic acid to cultured ILC2 was performed and Click-Palmitic acid was shown to accumulate in lipid droplets upon overnight culture, as depicted in confocal microscopy analysis (Figure 29 upper panel). However, after an additional 24 hours of culture, the signal in LD was weaned and Click-Palmitic acid was found localized at the cellular membrane, indicative of a potential conversion of exogenous acquired palmitic acid into membranous phospholipids (Figure 29 middle panel).

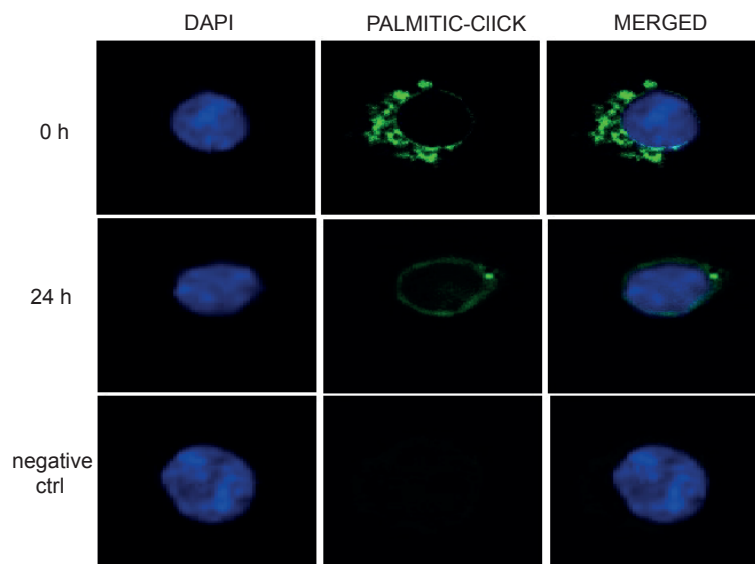


**Figure 29. External FA are directly funneled into membrane lipids for proliferation.** Representative microscope images of purified ILC2 isolated from papain challenged mice cultured with IL-2 and Click-palmitic acid-BSA o.n. Cells were washed and cultured for 24h (performed by Dr. Fotios Karagiannis). Results are representative of one representative experiment from at least two independent experiments with three to five mice in each experimental group. All graphs display means SEM; \*  $p \leq 0.05$ , \*\* $p \leq 0.01$ , \*\*\*  $p \leq 0.001$ .

To show that external FA mainly are used for proliferation and not for  $\beta$ -oxidation, an Agilent Seahorse XF Cell Mito Stress assay was performed with ILC2 isolated from papain challenged mice and cultured with or without FFA (Figure 30). The comparison of the OCRs with baseline values shows no difference between ILC2 cultured with or

without FFA. The further addition of oligomycin, an ATP synthase (complex V) inhibitor, leads to a strong decrease of the OCR in both conditions. Cells cultured with FFA have a higher OCR after addition of the uncoupling agent FCCP compared to ILC2 cultured with no FFA, which results in a higher respiratory capacity and higher spare respiratory capacity. Spare respiratory capacity is defined as the difference between maximal respiration and basal respiration and is a measure of the ability of the cell to respond to an increased energy demand or under stressing conditions (180). Injection of Rotenone/Antimycin A (complex I/complex III inhibitors) results in a strong decrease of the OCR for both conditions. Taken together, these results show, that the addition of FFA had no significant effects on the basal respiration, but it could increase the spare respiratory capacity.

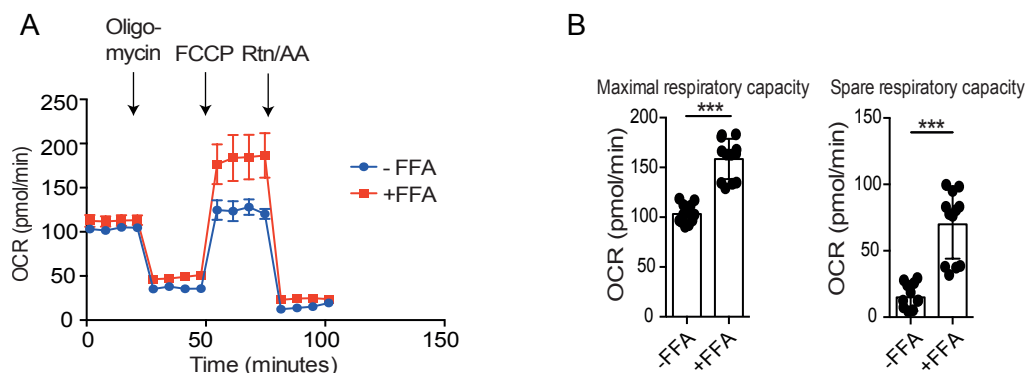


**Figure 30. External FA have no impact on the oxygen consumption rate.** ILC2 were isolated from papain challenged mice and cultured for 2 h with or without FFA. The compounds (oligomycin, FCCP, and a mix of rotenone and antimycin A (Rtn/AA) are serially injected. **(A)** The Agilent Seahorse XF Cell Mito Stress Test was performed to measure key parameters of mitochondrial function by directly measuring the oxygen consumption rate (OCR) of cells. **(B)** Maximal respiratory capacity and spare respiratory capacity were calculated. Results are representative of one representative experiment from at least two independent experiments with three to five mice in each experimental group. All graphs display means SEM; \*  $p \leq 0.05$ , \*\*  $p \leq 0.01$ , \*\*\*  $p \leq 0.001$ .

This data, together with the results of the pulse-chase experiment, lead to the assumption that lipids are probably mainly used for proliferation and less for energy generation through  $\beta$ -oxidation.

As described in section 1.7., PPAR $\gamma$  is an essential regulator of FA metabolism including FA uptake and LD formation in adipose tissue and liver (181), additionally, papain

challenge leads to upregulation of PPAR $\gamma$  in ILC2 (Figure 12). To test the function of PPAR $\gamma$  as an essential factor driving lipid metabolism in papain elicited ILC2, ILC2 isolated from the lung were cultured in the presence or absence of GW9662, a specific inhibitor of PPAR $\gamma$  (182). The ablation of PPAR $\gamma$  in purified ILC2 could drastically reduce the uptake of external lipids and the formation of LD (Figure 31A-B), leading to a compromised capacity of ILC2 to proliferate and expand in culture and a reduction in the production of effector cytokines (Figure 31C-D). Hence, uptake of external FA in ILC2 mediated by PPAR $\gamma$  may be important to fuel proliferation and cytokine production.

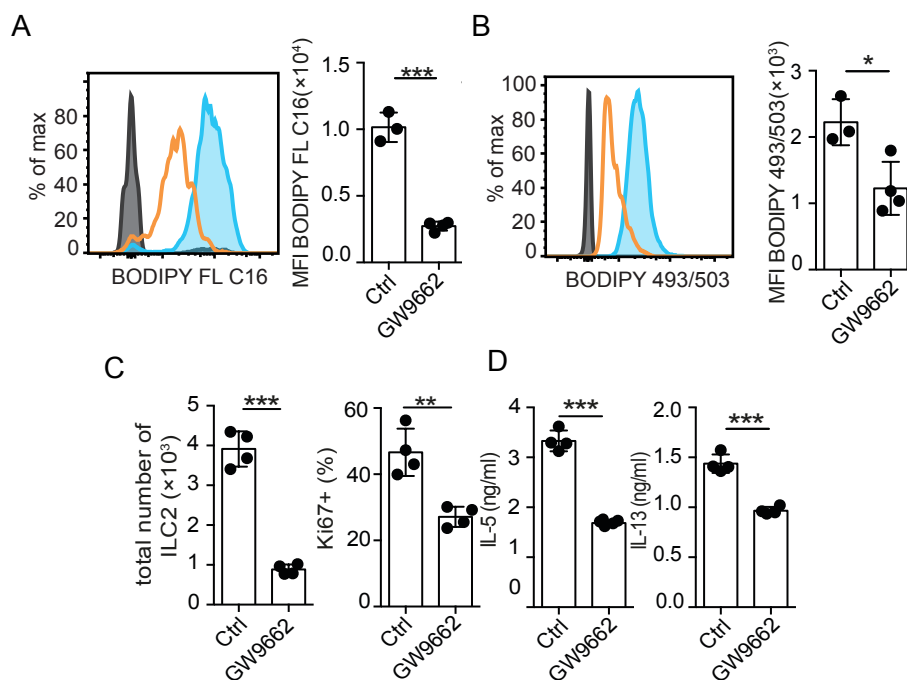


**Figure 31. PPAR $\gamma$  regulates FA uptake *in vitro*.** Purified ILC2 were cultured in the presence or absence of the PPAR $\gamma$  inhibitor GW9662. **(A)** Representative histograms and MFI values of BODIPY<sup>®</sup> FL C<sub>16</sub> uptake and **(B)** MFI values of BODIPY<sup>®</sup> 493/503 in cultured ILC2 **(C)** Total numbers of ILC2, Ki-67 expressing ILC2 and **(D)** cytokines in the supernatant after three days of culture. Results are representative of one representative experiment from at least three independent experiments with three to five mice in each experimental group. All graphs display means SEM; \*  $p \leq 0.05$ , \*\*  $p \leq 0.01$ , \*\*\*  $p \leq 0.001$ .

Interestingly, GW9662 leads to a lower expression of *Dgat1*, and PPAR $\gamma$  is regulating *Dgat1* expression (Figure 32). The decreased expression of *Dgat1* explains the reduced amount of LD in the culture.

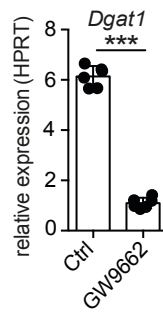


**Figure 32. GW9662 downregulates expression of *Dgat1* in vitro.** Gene expression analysis of ILC2 cultured in the presence or absence of glucose relative to HPRT. Results are representative of one representative experiment from at least two independent experiments with two to five mice in each experimental group. All graphs display means SEM; \*  $p \leq 0.05$ , \*\*  $p \leq 0.01$ , \*\*\*  $p \leq 0.001$ .

To test the importance of PPAR $\gamma$  in ILC2 effector function, papain-challenged mice were treated with GW9662 to impair the uptake of external lipids and the FA metabolism in the context of allergen induced airway inflammation. Strikingly, inhibition of PPAR $\gamma$  drastically reduced the accumulation of papain-induced ILC2 in the airways (Figure 33A). Furthermore, this reduction in pulmonary ILC2 was accompanied by a reduced capacity of ILC2 to take up and store FA in LD, while their capacity to acquire glucose from the environment was unchanged (Figure 33B-D).

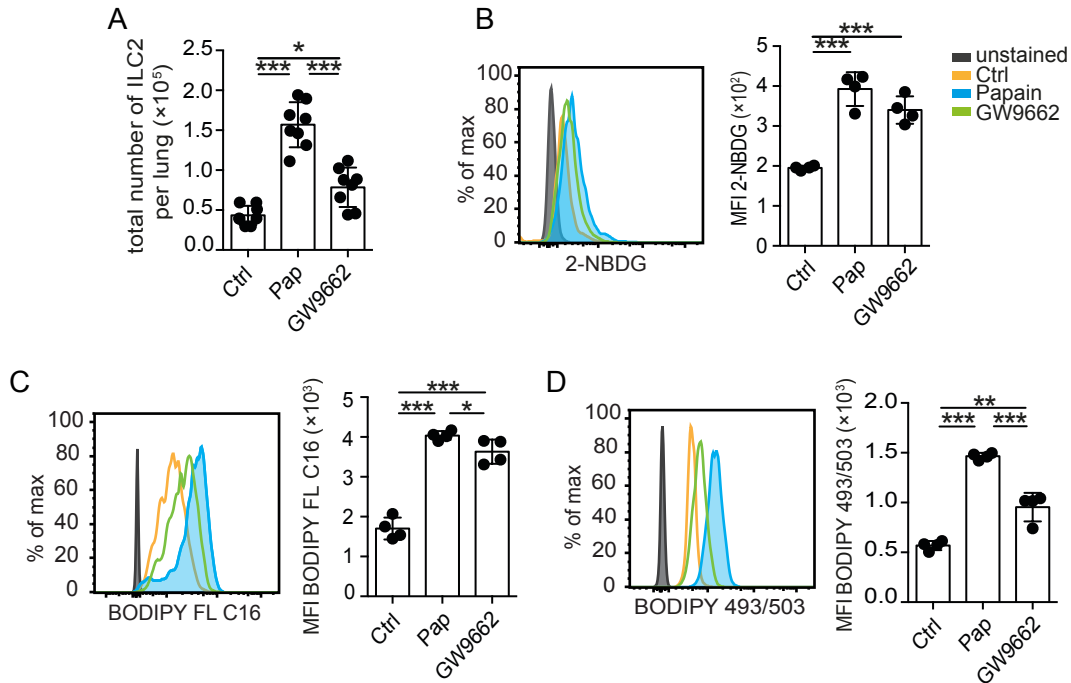


**Figure 33. PPAR $\gamma$  regulates FA uptake and accumulation and proliferation of ILC2 *in vivo*.** C57BL/6 mice were challenged intranasally with papain or PBS on day 0, 3, 6 and 13 and simultaneously treated i.p. with PPAR $\gamma$ -Inhibitor GW9662, control animals were treated with DMSO only. **(A)** Total numbers of ILC2 from PBS (Ctrl), papain (Pap) or papain challenged mice treated with GW9662 (Pap+GW9662). **(B)** Representative histograms and MFI values of 2-NBDG in lung ILC2 (Lin<sup>-</sup> Thy1.2<sup>+</sup> ST2<sup>+</sup>) and **(C)** MFI values of BODIPY<sup>®</sup> FL C16 uptake and **(D)** BODIPY<sup>®</sup> 493/503 in ILC2 (Lin<sup>-</sup> Thy1.2<sup>+</sup> Gata3<sup>+</sup>). Results are representative of two pooled experiments (A) or one representative experiment (B-D) from at least two independent experiments with three to five mice in each experimental group. All graphs display means SEM; \*  $p \leq 0.05$ , \*\* $p \leq 0.01$ , \*\*\* $p \leq 0.001$ .

Additionally, PPAR $\gamma$  inhibition drastically reduced the production of the ILC2 effector cytokines IL-5 and IL-13 in the lung tissue (Figure 34).

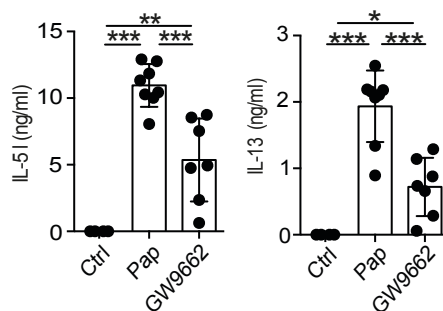


**Figure 34. Inhibition of PPAR $\gamma$  reduces inflammatory cytokine release.** Cytokine concentration of IL-5 and IL-13 in the lung homogenate. Results are representative of two pooled experiments from at least two independent experiments with three to five mice in each experimental group. All graphs display means SEM; \*  $p \leq 0.05$ , \*\* $p \leq 0.01$ , \*\*\* $p \leq 0.001$ .



Thus, the acquisition of external FA by ILC2 appears to fuel proliferation and this process is controlled by PPAR $\gamma$  regulating the uptake of external lipids and the subsequent storage in LD to prevent lipotoxicity. In summary, the inhibition of PPAR $\gamma$  largely impairs the metabolic pathways fueling the accumulation and effector functions of ILC2 in the inflamed airways.

### **3.5 Glucose and external FA cooperate to control fatty acid metabolism in ILC2**

Since previous described observations show an increase in glucose and FA metabolism in activated ILC2, the presence of glucose may play an essential role in the ability of ILC2 to acquire FA from the environment. To test this hypothesis, the ability of ILC2 to obtain FFA from the environment and their capacity to store acquired lipids in LD in the absence of glucose/pyruvate was assessed. In this analysis, ILC2 cultured in the absence of glucose/pyruvate drastically reduced the uptake of external lipids and the formation of LD (Figure 35A-B). The reduced capacity to acquire external lipids led to a reduction of the overall amount of cultured ILC2 and a reduction in the cytokines produced from these cells (Figure 35C-D). Altogether this data suggest, that both glucose and FA may cooperate to fuel the survival and function of pathogenic ILC2 and that glucose availability allows for the increased uptake of external lipids.

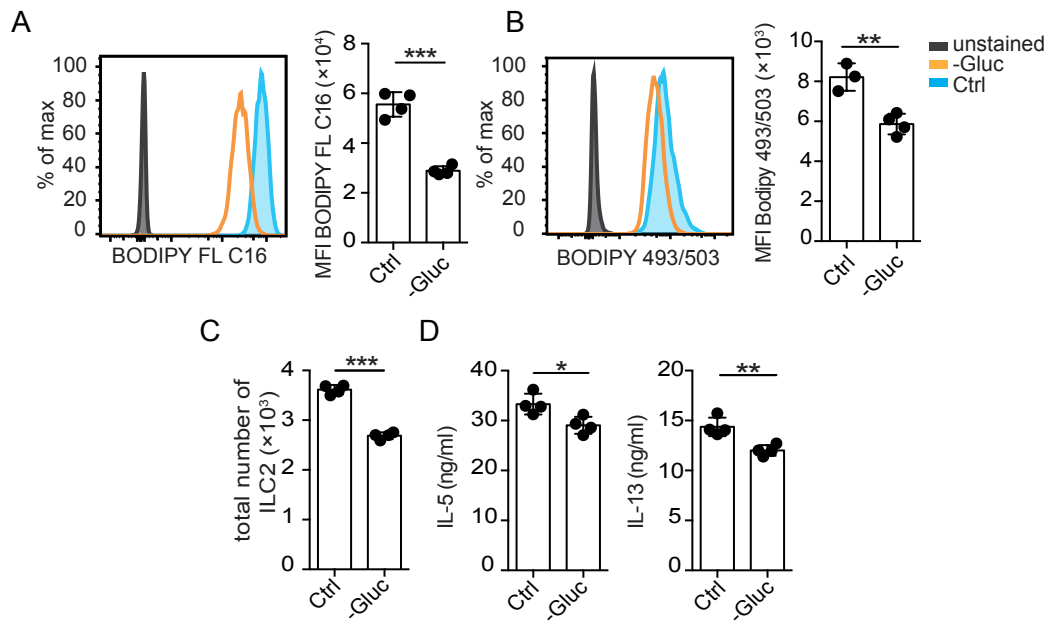


**Figure 35. Glucose and external FA cooperate to fuel fatty acid metabolism in ILC2.** Representative histograms and MFI values of **(A)** BODIPY® FL C<sub>16</sub> uptake and **(B)** MFI values of BODIPY® 493/503 staining in cultured ILC2. **(C)** Total numbers of purified lung ILC2 from papain challenged C57BL/6 mice cultured for three days with IL-2 in the presence (Ctrl) or absence of glucose/pyruvate (-Gluc) and **(D)** cytokines in the culture supernatant. Results are representative of one representative experiment from at least two independent experiments with three to five mice in each experimental group. All graphs display means SEM; \*  $p \leq 0.05$ , \*\*  $p \leq 0.01$ , \*\*\*  $p \leq 0.001$ .

To investigate whether the absence of glucose leads to cell death or limited proliferation, ILC2 were purified, cultured and the cell number was analyzed either without addition of any cytokines (input d0), or with or without glucose/pyruvate and on d3. The cell numbers of ILC2 cultured with or without glucose/pyruvate and the addition of IL-2 was determined on d3. Interestingly, the cell number on d3 without glucose/pyruvate was higher than on d0, which suggests that cells are still proliferating and accumulating but they show a compromised capacity in proliferation (Figure 36).

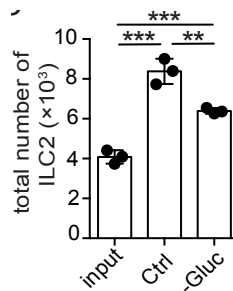


**Figure 36. Absence of glucose leads to limited proliferation.** ILC2 numbers determined on d0 and d3 cultured with or without glucose/pyruvate. Results are representative of one representative experiment from at least two independent experiments with three to five mice in each experimental group. All graphs display means SEM; \*  $p \leq 0.05$ , \*\*  $p \leq 0.01$ , \*\*\*  $p \leq 0.001$ .

Furthermore, ILC2 cultured in absence of glucose/pyruvate showed marked downregulation of *Dgat1* and *Pparg* (Figure 37).

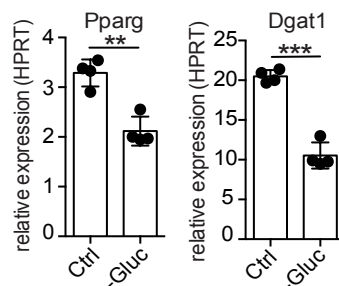


**Figure 37. Presence of glucose regulates expression of *Pparg* and *Dgat1*.** Gene expression analysis of ILC2 cultured in the presence or absence of glucose/pyruvate relative to HPRT. Results are representative of one representative experiment from at least two independent experiments with three to five mice in each experimental group. All graphs display means SEM; \*  $p \leq 0.05$ , \*\*  $p \leq 0.01$ , \*\*\*  $p \leq 0.001$ .

This analysis strongly suggests that glucose availability may regulate expression of *Dgat1* and thus the capacity to form LD, while the reduced expression of *Pparg* controls the capacity to acquire external lipids. In summary, these data strongly suggest a mechanism by which the availability of glucose is coupled to the ability to acquire FA from the environment to fuel activation of pathogenic ILC2 via the expression of *Pparg* and *Dgat1*.

### 3.6 Ketogenic diet abrogates ILC2-driven airway inflammation

Altogether these findings suggest that the pathogenic function of ILC2 may be controlled by the simultaneous increased capacity of ILC2 to utilize glucose and FA as energy sources. Hence it has been hypothesized that actively influencing the metabolic status of the host by restraining the availability of dietary glucose may simultaneously ablate the capacity of ILC2 to increase the acquisition of external FA to fuel airway inflammation. A reduction in glucose availability can be achieved by feeding mice a ketogenic diet (KD) containing a fat to protein and carbohydrate ratio of approximately 4:1 (108) (183).

In order to rule out that ketogenic diet itself has an effect on ILC2 numbers mice were put on control and ketogenic diet for 5 weeks starting at the age of 3 weeks and analyzed via flow cytometry. In steady state conditions no changes in ILC2 and eosinophil numbers were observed between mice fed with control diet (CD) and ketogenic diet (KD) in ILC2 (Figure 38).

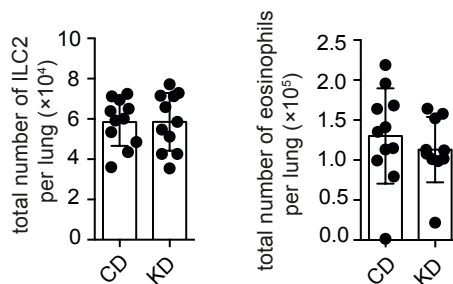


**Figure 38. Ketogenic diet has no effect on ILC2 number in steady state.** C57BL/6 mice were placed on control diet (CD) or ketogenic diet (KD) for five weeks at the age of 3 weeks. Flow cytometric analysis of total numbers of ILC2, Ki-67<sup>+</sup> ILC2 and eosinophils in the lung tissue. Results are representative of one representative experiment from at least two independent experiments with three to five mice in each experimental group. All graphs display means SEM; \*  $p \leq 0.05$ , \*\*  $p \leq 0.01$ , \*\*\*  $p \leq 0.001$ .

Strikingly, mice fed with KD show a drastic reduction in cellular infiltrates and a decreased number of eosinophils. They also almost completely failed to accumulate ILC2 in the airways upon papain challenge (Figure 39A). This effect was restricted to chronically activated ILC2, since dietary restriction of glucose had no effect on ILC2 or eosinophils numbers recovered from the lungs in steady state conditions (Figure 38).

Indeed, animals fed with KD increased the amounts of ketone bodies in the circulation (Figure 39B).

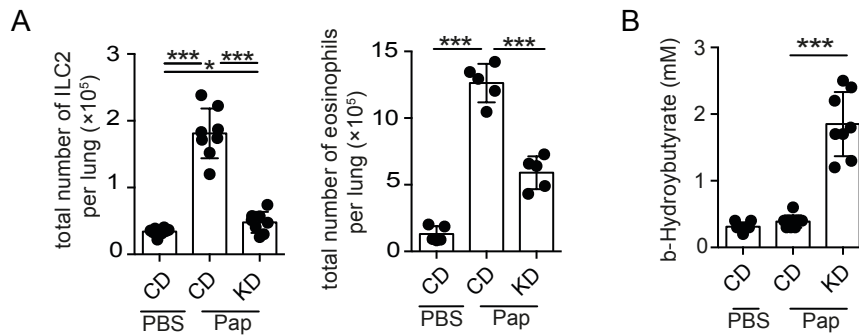


**Figure 39. Ketogenic diet leads to an increase of ketone body concentration in the blood. (A)** C57BL/6 mice were placed on control diet (CD) or ketogenic diet (KD) at the age of three weeks and challenged intranasally with papain or PBS on day 0, 3, 6 and 13. Total numbers of ILC2 and eosinophils were analyzed by flow cytometry on d14. **(B)** Ketone body concentrations in the blood of papain challenged mice on control diet and papain challenged mice on ketogenic diet. Results are representative of two pooled experiments (A) from at least three independent experiments with three to five mice in each experimental group. All graphs display means SEM; \* p ≤ 0.05, \*\*p ≤ 0.01, \*\*\* p ≤ 0.001.

In addition, less proliferating ILC2 and a pronounced reduction in ILC2-derived cytokines IL-5 and IL-13 in the lung tissue could be observed (Figure 40A-B).

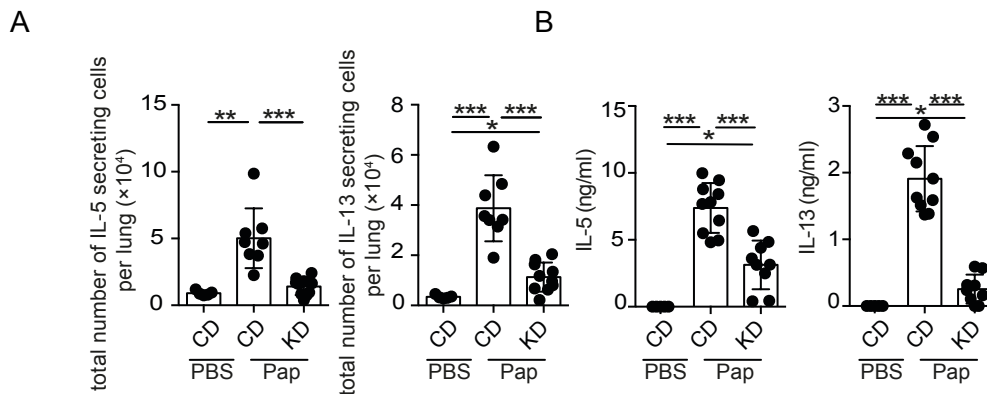


**Figure 40. Ketogenic diet inhibits ILC2-driven airway inflammation.** C57BL/6 mice were placed on control diet (CD) or ketogenic diet (KD) and challenged intranasally with papain or PBS on day 0, 3, 6 and 13. **(A)** total numbers of IL-5 and IL-13 producing ILC2 in the lung tissue of PBS challenged mice fed a control diet (CD), mice fed a control diet (CD+Pap) or ketogenic diet (KD+Pap) and challenged with papain. **(B)** Cytokine concentration of IL-5 and IL-13 in the lung homogenate. Results are representative of two pooled experiments from at least three independent experiments with three to five mice in each experimental group. All graphs display means SEM; \* p ≤ 0.05, \*\*p ≤ 0.01, \*\*\* p ≤ 0.001.

Histological analysis and staining of mucus producing cells by periodic acid-shift assay (PAS) revealed that papain challenged mice dramatically increased cellular infiltrates and mucus producing cells, which are known to be two signs of airway pathology. In contrast, KD entirely abrogated mucus production and cellular infiltration in mouse airways (Figure 41).

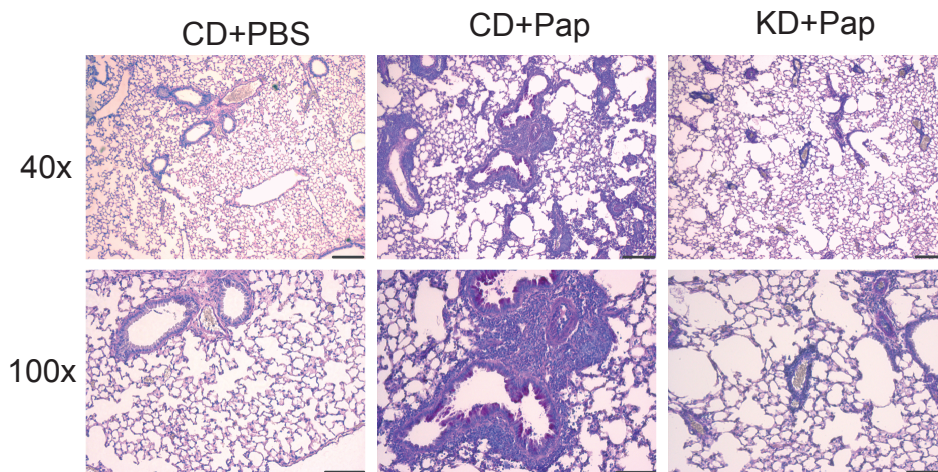


**Figure 41. Ketogenic diet inhibits cell infiltration and mucus production in papain challenged mice.** Histology and PAS staining to identify mucus-producing cells in the lung tissue. Results are representative of one representative experiment from at least two independent experiments with three to five mice in each experimental group. All graphs display means SEM; \*  $p \leq 0.05$ , \*\* $p \leq 0.01$ , \*\*\*  $p \leq 0.001$ .

On a cellular level, while the capacity of ILC2 to acquire glucose was not altered, FA uptake and LD formation was reduced (Figure 42A-C).

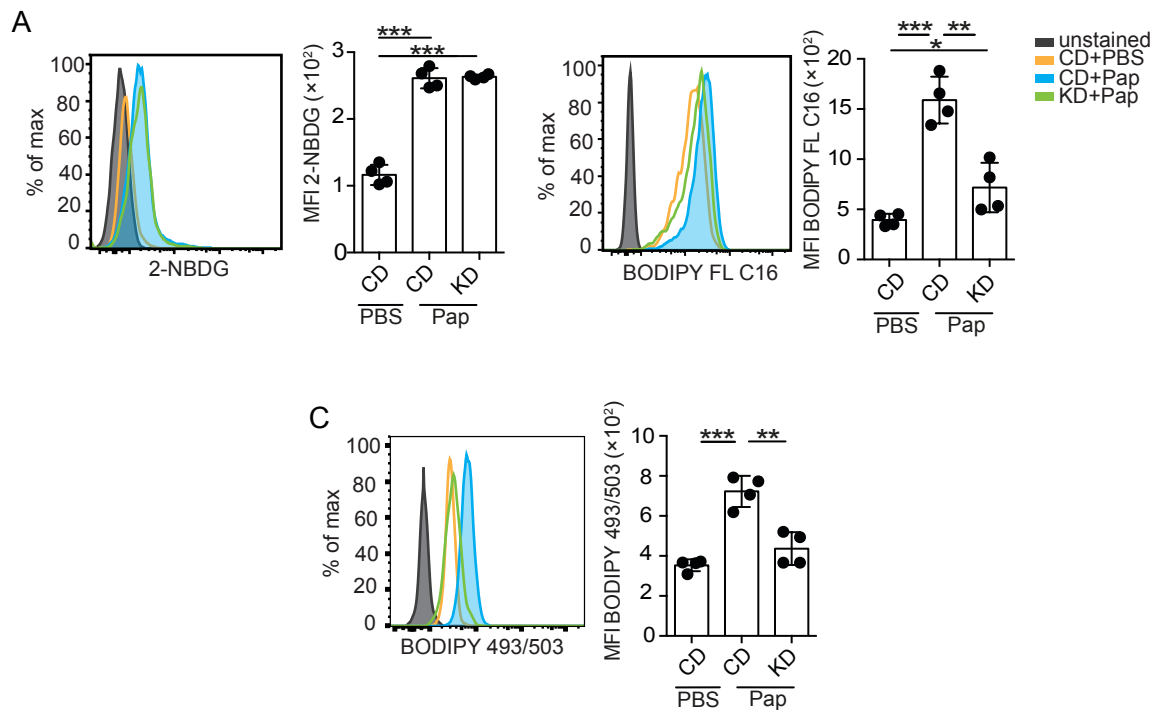


**Figure 42. Ketogenic diet lead to lower FA uptake and less LD formation.** Representative histograms and mean fluorescence intensity (MFI) values of 2-NBDG (**A**) in lung ILC2 (Lin<sup>-</sup> Thy1.2<sup>+</sup> ST2<sup>+</sup>) and (**B**) MFI values of BODIPY<sup>®</sup> FL C<sub>16</sub> uptake and (**C**) MFI values of BODIPY<sup>®</sup> 493/503 analyzed in lung ILC2 (Lin<sup>-</sup> Thy1.2<sup>+</sup> Gata3<sup>+</sup>). Results are representative of one representative experiment from at least two independent experiments with three to five mice in each experimental group. All graphs display means SEM; \* p ≤ 0.05, \*\*p ≤ 0.01, \*\*\* p ≤ 0.001.

In accordance with an overall reduction of glucose availability, KD induced a reduction in the expression of genes involved in glycolysis (*Hk1*, *Ldha* and *Pkm*) were reduced. Additionally, the expression of *Pparγ* and *Dgat1* was reduced, which is in agreement with reduced FA uptake and LD formation shown before (Figure 43).

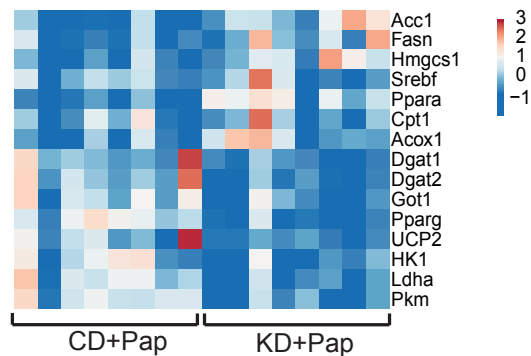


**Figure 43. Ketogenic diet increases expression of *Ppara* and *Dgat1*.** Gene expression analysis relative to HPRT of purified lung ILC2 isolated from papain challenged mice on control diet and papain challenged mice on ketogenic diet. Results are representative of two pooled experiments from at least three independent experiments with three to five mice in each experimental group.

Thus, ketogenic programs potentially restrain ILC2-mediated airway inflammation by lowering the availability of glucose and as a consequence impaired FA metabolism in ILC2.

Considering that several studies previously showed, that KD might effect the microbiota in the gut and this can effect the immune response (109), the role of microbiota in this context was investigated by treating ketogenic-fed mice and control mice with antibiotics (184). Results show that the total number of ILC2 and eosinophils in mice fed with KD was reduced despite antibiotic treatment (section 2.17.) Furthermore, 2-NBDG and BODIPY® FL C16 uptake was also reduced, as well as LD formation (Figure 44).

These results indicate, that the suppressive capacity of ketogenic diet is unaltered by antibiotic treatment, suggesting a microbiota-independent mechanism.



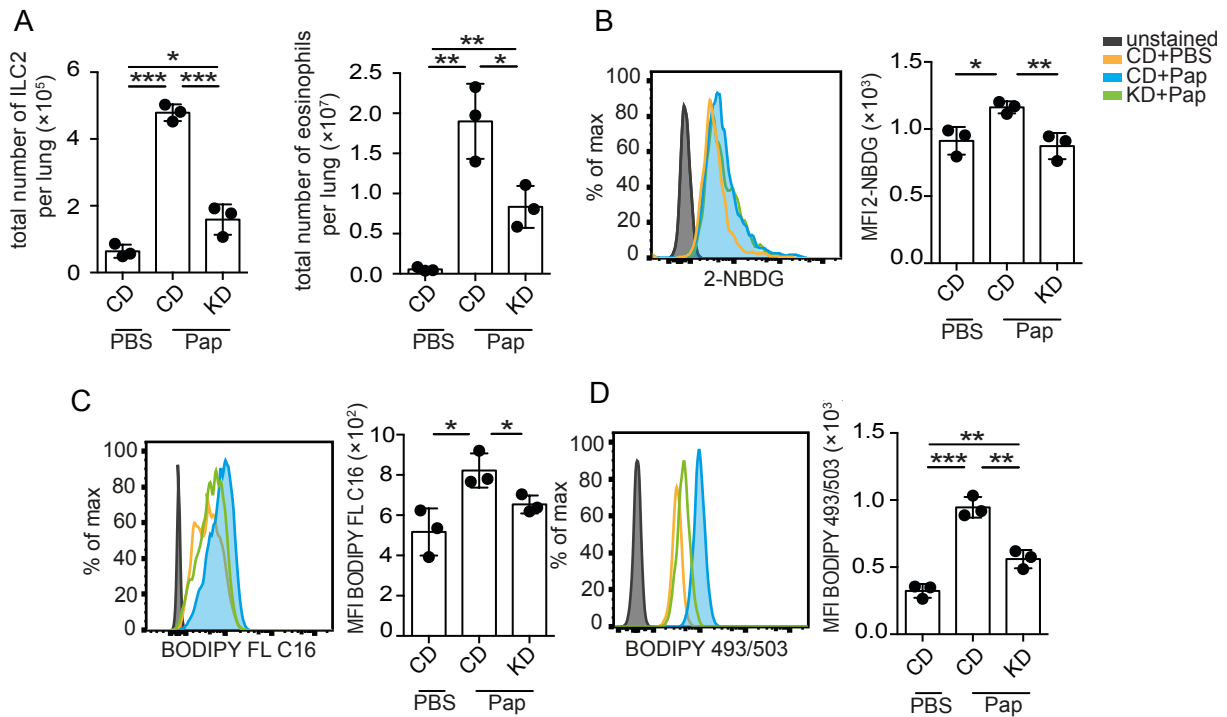


**Figure 44: Microbiota has no impact on inhibition of airway inflammation by using ketogenic diet.** (A) Antibiotics treated C57BL/6 mice were placed on control diet or ketogenic diet for three weeks at the age of 3 weeks and challenged intranasally with papain or PBS on day 0, 3, 6 and 13. Flow cytometric analysis of total numbers of ILC2, Ki-67<sup>+</sup> ILC2 and eosinophils in the lung tissue. Representative histograms and mean fluorescence intensity (MFI) values of 2-NBDG (B) in lung ILC2 (Lin<sup>-</sup> Thy1.2<sup>+</sup> ST2<sup>+</sup>) and (C) MFI values of BODIPY<sup>®</sup> FL C<sub>16</sub> uptake and (D) MFI values of BODIPY<sup>®</sup> 493/503 analyzed in lung ILC2 (Lin<sup>-</sup> Thy1.2<sup>+</sup> Gata3<sup>+</sup>). Results are representative of one representative experiment from at least two independent experiments with three to five mice in each experimental group. All graphs display means SEM; \* p $\leq$  0.05, \*\*p  $\leq$  0.01, \*\*\* p $\leq$ 0.001.

In addition, less proliferating ILC2 and a pronounced reduction in the ILC2-derived cytokines IL-5 and IL-13 could be observed (Figure 45).

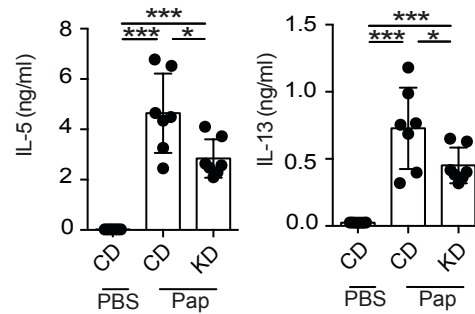


**Figure 45. Ketogenic diet inhibits ILC2-driven inflammatory cytokine release.** Antibiotics treated C57BL/6 mice were placed on control diet or ketogenic diet for three weeks at the age of 3 weeks and challenged intranasally with papain or PBS on day 0, 3, 6 and 13. Cytokine concentration of IL-5 and IL-13 in the lung homogenate. Results are representative of one representative experiment from at least two independent experiments with three to five mice in each experimental group. All graphs display means SEM; \*  $p \leq 0.05$ , \*\*  $p \leq 0.01$ , \*\*\*  $p \leq 0.001$ .

In summary, papain treatment leads to a strong accumulation of ILC2, which goes along with higher glucose and FA uptake. The FA are stored as lipid droplets and used for the generation of new membrane components. *In vitro* and *in vivo* studies could successfully show that IL-33 is the main cytokine which activates ILC2 in the lung and leads to LD formation. The selective inhibition of DGAT1, which is important for LD formation, or PPAR $\gamma$ , which is regulating FA uptake can inhibit ILC2 proliferation and thus ameliorate airway inflammation. The presence of glucose probably plays an important role for the regulation of PPAR $\gamma$  and FA uptake. Altogether these data strongly indicate that dietary restriction of glucose through ketogenic diet can lead to a reduced ILC2 accumulation and inflammatory cytokine release.

## 4. Discussion

ILC are important players in the innate immune response and they exert a key role in lymphoid tissue formation, tissue remodeling and maintenance of homeostasis at the barrier surface: they play these fundamental functions by forming a complex network not only with stromal cells in the tissue, but also with microbiota, nutrients and metabolites (50) (185) (102) (186) (187). However, besides their protective functions, ILC can have an inflammatory role once they are chronically activated: this status promotes local inflammation, which can be favored by changes in nutrient availability or life-style changes coinciding with industrialization (188).

Recent studies have revealed that in steady state conditions and in the context of helminth infection, ILC2 rely on FAO and do not require glucose (102). On the other hand, further studies display the Warburg effect in activated and proliferative immune cells, which is defined as a change in glucose metabolism and increased glucose uptake (87). In this context, this thesis aims to explore how the metabolism of ILC2 in the lung changes during airway inflammation and to identify signals and nutrients needed to induce potential metabolic shifts that lead to immunopathology.

The experiments performed in this thesis provide evidence that pathogenic functions of ILC2 rely on the uptake of extracellular glucose and FA for proliferation and accumulation in the inflamed lung tissue. The study supports the hypothesis that glucose alone is not sufficient for expansion of ILC2 in the context of airway inflammation. Data suggests that increased uptake of exogenous FA by tissue resident ILC2 may be important to mediate proliferation, probably by providing lipids for the generation of membrane phospholipids. The increased FA uptake is linked to increased LD formation in the cell and excess lipids are stored as neutral lipids in LD to avoid lipotoxicity. In this study it is shown that these metabolic changes during airway inflammation can be induced by papain and *Alternaria alternata*. The availability of glucose and FFA increase after papain challenge in the lung tissue which show an increased need of nutrients in the inflamed lung tissue. On the transcriptional level ILC2 display changes in different metabolic genes after papain challenge. Genes that regulate for fatty acid synthesis, cholesterol synthesis and  $\beta$ -oxidation are downregulated (*Acc1*, *Fasn*, *Acly*, *Hmgcs1*, *Srebf*, *Ppara*, *Cpt1*, *Acox1*), whereas genes for triglyceridesynthesis (TGS) (*Dgat1*,

*Dgat2*) are highly upregulated. Furthermore, other genes involved in glycolysis (*Hk1*, *Ldha*, *Pkm*) are upregulated as a consequence of the higher glucose uptake. Also genes involved in FA uptake (*Ppar $\gamma$* , *Slc27a6*) were significantly upregulated. For a cell it may be more efficient to directly use exogenous lipids for building up membrane components, rather than using glucose for *de novo* FA synthesis. Indeed, recent reports suggest that highly proliferating cells rely on external FA to build complex lipids for cellular membranes (189).

Previous studies revealed that papain exposure leads to IL-33 release from the lung epithelium (84). In this thesis *in vitro* and *in vivo* experiments using IL-33, IL-25 and TSLP as stimuli could show ILC2 proliferation and significant changes in nutrient uptake upon IL-33 stimulation alone. Experiments using ST2 KO were performed to test whether IL-33 signaling is important for ILC2 activation, proliferation and higher nutrient uptake. As result, similar changes on the transcriptional level were observed in papain challenged mice. Thus, these data suggested that the stimulation with IL-33 alone is necessary and sufficient for the acquisition of external FFA and glucose for LD formation in the lung. Considering that ILC2 have a different responsiveness to cytokines depending on the tissue, it is important to discriminate between lung and intestinal ILC2. Lung ILC2 have a very low expression of the receptor of IL-25 (IL-17BR) compared to intestinal ILC2 (190) (191), which can explain why only IL-33 leads to ILC2 activation in the lung. Mechanistically IL-33 seems to upregulate PPAR $\gamma$  which then leads to increased FA uptake. As previously shown in Tregs, IL-33 stimulation resulted in binding of basic leucine zipper AFT-like transcription factor (BATF) and interferon regulatory factor 4 (IRF4) to the PPAR $\gamma$  locus (192). The possibility that the same mechanism takes place in ILC2 has to be further investigated.

The formation of LD in ILC2 is an essential process that allows continuous and high uptake of FA from the tissue environment by preventing lipotoxicity otherwise caused by excess intracellular FFA. This study suggests that esterification of FFA into triglycerides, a process mediated by the enzyme DGAT1, is also critical to fuel pathogenic ILC2 elicited in airway inflammation. Culturing lung ILC2 from papain challenged mice with BODIPY<sup>®</sup> FL C<sub>12</sub> revealed a rapid uptake of fluorescently labeled FA and subsequent storage in LD as assessed by confocal microscopy. Blocking the function of DGAT1 with DGAT1 Inhibitor A922500 (DGAT1i) severely impaired the viability of ILC2 *in vitro* and

reduced LD formation. Additionally, *In vitro* survival experiments and Annexin V/propidium iodide double stain show that higher percentage of ILC2 cultured with DGAT1i display increased apoptosis compared to control. In line with this finding, peroxidation staining revealed that using DGAT1i leads to more oxidative degeneration of cellular lipids which can result in cell death. In contrast blocking the activity of DGAT2 with the specific inhibitor PF06424439 (DGAT2i) had no effect on ILC2 viability, proliferation or LD formation in culture. This suggests that expression of DGAT1 but not DGAT2 may be essential in ILC2 to acquire and store high amounts of external lipids from the surrounding environment. This observation is in agreement with the hypothesis that DGAT1 esterifies external FA and DGAT2 is responsible for TAG synthesis from fatty acid substrates derived from *de novo* lipogenesis (155). Furthermore, *in vivo* studies could show a decrease in ILC2 and eosinophil accumulation when mice were treated with DGAT1i. Here, LD formation was highly reduced, although glucose and FA uptake was unchanged or even higher. These findings confirm the initial hypothesis, that considers activated ILC2 to undergo apoptosis due to an excess of FFA which cannot be stored into LD. Evolutionary LD are the main nutrient buffering system, allowing the efficient storage of highly energetic fuel molecules a process that is mainly performed in adipose tissue (193). This mechanism seems to be essential to fuel ILC2 in airway inflammation. The capability of ILC2 and other immune cells to store nutrients may have different functions: On one hand ILC2, which are acting as central effector immune cells responsible for tissue maintenance and repair, are required to operate in variable states of nutrient availability and their capability to store FA in LD may allow them to function also in circumstances of dietary restriction. On the other hand, the glucose levels in tissues are low while FA may be more abundantly available. In this context, the process of tissue remodeling induced upon injury not only requires activation of ILC2 but may also supply FA released from membranes of dying cells (194). Interestingly, a recent report suggests that the mobilization of FFA from phospholipids by the phospholipase Pla2g5 expressed on macrophages is important to support ILC2-driven airway inflammation (195). This further confirms that, the microenvironment in the context of injury and remodeling may provide abundant supply of FA, which required the temporal storage in LD to prevent lipotoxicity. Concerning the specificity of DGAT1 inhibition in ILC2, *in vivo* experiments using DGAT1i was performed in order to target DGAT1 in all

tissues and cell types. To address the specific function of DGAT1 in ILC2 it would be necessary to employ specific genetic models for *in vitro* and *in vivo* studies. In this context the specific deletion of DGAT1 in ILC2 *in vitro* could be reached through siRNA or shRNA. For *in vivo* assessment of DGAT1 animal models using specific DGAT1 deletion in ILC2 can be used. Specific deletion of DGAT1 in ILC2 might be able to reduce LD formation, proliferation and accumulation of ILC2. Alternatively, transfer experiments with DGAT1-depleted ILC2 compared to wild type (WT) ILC2 into RAG2<sup>-/-</sup>/gamma c- double mutant mice can be performed.

Since fuel uptake experiments have shown more FA uptake upon ILC2 activation *in vitro*, the function of extra lipids during ILC2 proliferation was performed by adding external linoleic/oleic acid and palmitic acid in context of proliferation. The addition of these lipids could lead to higher ILC2 accumulation and proliferation (Ki-67<sup>+</sup> ILC2) which strongly suggests that lipids promote the proliferation of activated ILC2. The analysis of Ki-67<sup>+</sup> and Ki-67<sup>-</sup> ILC2 revealed that proliferating ILC2 (Ki-67<sup>+</sup>) take up more FA and have more LD compared to non proliferative ILC2 (Ki-67<sup>-</sup>) which underlines the importance of lipids to promote proliferation. A pulse chase experiment with added Click-Palmitic acid to cultured ILC2 argues for the usage of external lipids as components of cellular membrane. Here the signal in LD had weaned and Click-Palmitic acid localized at the cellular membrane, indicating a possible conversion of exogenous acquired palmitic acid into membranous phospholipids.

To assess if external FA are mainly used for proliferation rather than for  $\beta$ -oxidation an Agilent Seahorse XF Cell Mito Stress test has been performed with ILC2 isolated from papain challenged mice and cultured in the presence or absence of FFA. The comparison of the OCRs at baseline shows no difference between ILC2 cultured with or without FFA which leads to the conclusion that external lipids have no significant effect on basal respiration. Indeed, cells cultured with FFA have a higher OCR after addition of the uncoupling agent FCCP compared to ILC2 cultured with no FFA. This difference results in a higher respiratory capacity and higher spare respiratory capacity, which is a measure of the ability of the cell to respond to increased energy demand or stress, concluding that, external FA are used for energy generation under stress. To verify this assumption, Lipidomics analysis could be performed to investigate the complete lipid

profile and fate within the cell. This detailed analysis would allow to test if external FA are converted first into LD and then used for building up membranous phospholipids.

Using the PPAR $\gamma$  inhibitor GW9662 *in vitro* ILC2 show a strong decrease in FA uptake and LD formation, which goes along with less accumulation, proliferation and cytokine release. Similar results are obtained by using GW9662 *in vivo*. Moreover, usage of GW9662 in culture results in a lower expression of *Dgat1* in ILC2, confirming that PPAR $\gamma$  positively regulates *Dgat1*. The data presented in this thesis suggest that lipid uptake and the storage of FFA in LD is regulated by the transcription factor PPAR $\gamma$ , since inhibition of PPAR $\gamma$  directly suppresses the acquisition of FA, LD formation and proliferation and accumulation of ILC2 in airway inflammation. These findings are in line with previous reports that highlight the importance of PPAR $\gamma$  in T cell activation by direct regulation of genes involved in the uptake of external lipids (196). Similar to the *in vivo* experiments performed with DGAT1i, also PPAR $\gamma$ i was applied directly to mice. To confirm the specific function of PPAR $\gamma$  in ILC2 it would be necessary to employ various genetic *in vitro* and *in vivo* models promoting the deletion of PPAR $\gamma$  in ILC2 by siRNA/shRNA or specific PPAR $\gamma$  KO in ILC2. Also in this case a specific deletion of PPAR $\gamma$  in ILC2 might reduce LD formation, proliferation and accumulation of ILC2. Alternatively, transfer experiments with PPAR $\gamma$  depleted ILC2 compared to WT ILC2 into RAG2-/-/gamma c- double mutant mice might be performed.

Since it was observed that FA uptake as well as glucose uptake are increased upon ILC2 activation and proliferation, it has been hypothesized that the presence of glucose may play an essential role in promoting FA uptake in ILC2. To test this assumption, FA uptake and LD formation in the absence of glucose has been assessed *in vitro*. Interestingly, ILC2 cultured in the absence of glucose significantly reduced the uptake of external lipids and the formation of LD. This reduced capacity to acquire external lipids led to a reduction of the overall amount of ILC2 in culture and a reduction in cytokine production. This data suggest, that both glucose and FA may cooperate to fuel the survival and function of pathogenic ILC2 and that glucose availability allows the increased uptake of external lipids. *In vitro* survival experiments show that ILC2 cultured without glucose reduce their capacity to proliferate compared to control and that the expression of *Dgat1* and *Ppar $\gamma$*  seem to be also controlled by the availability of glucose. Thus, reduced amounts of glucose lead to a lower expression of both genes with then

results in lower FA uptake and less proliferation. The exact mechanism by which glucose regulates the FA uptake is still unknown and needs further investigation. Possible explanations could be the activation of the mammalian target of rapamycin (mTOR) through glucose and the further positive regulation and activation of PPAR $\gamma$  (197). Several studies are still required to clarify the importance of glucose metabolism in ILC2 and this can be assessed by inhibiting the glucose transport with inhibitors like Bay876 (198) or using competitive glucose inhibitors such as 2-Deoxy-D-glucose (2-DG) (199). Another possible approach is the application of the anti-diabetic drug metformin, which inhibits the glucose uptake in the intestine and inhibits gluconeogenesis (200). Moreover, the genetic deletion of *Glut1 in vitro* by using siRNA could support the hypothesis of the role of glucose in ILC2 activation and proliferation. To further investigate the metabolic profile of ILC2 cultured in the presence or absence of glucose, an Agilent Seahorse assay can be performed and determine the effects of the glucose on the OCR can be clarified. Additionally, a more detailed analysis of the role of glucose should be performed by  $^{13}\text{C}$  metabolic flux analysis ( $^{13}\text{C}$ -MFA) in future studies.  $^{13}\text{C}$ -MFA is the primary technique for quantifying intracellular fluxes in cells and to generate a quantitative map of cellular metabolism through using stable isotopes such as  $^{13}\text{C}$ . Labeled substrates like 1,2- $^{13}\text{C}$ -glucose can be metabolized by cells resulting in a rearrangement of carbon atoms and specific labeling patterns in downstream metabolites, which can be measured with mass spectrometry (MS) (201).

Taken together, these data suggest that, increased incidence of chronic airway inflammation in the Western World may be largely mediated by a simultaneous rise in the consumption of carbohydrate and fat. Indeed, recent studies have highlighted the expansion of ILC2 responses in the context of high fat diet induced-obesity (202). Increased glucose availability in the Western World may allow an elevated lipid uptake with unexpected consequences. The data in this thesis strongly suggest that dietary interventions and changes induced in host metabolism through ketogenic diet in particular may be an efficient approach to control airway inflammation. In particular it is shown that using a ketogenic diet appears to block all central aspect of disease development, by limiting not only the availability of glucose but also simultaneously reducing the acquisition of exogenous FA and the formation of lipid droplets. Noticeable, ILC2 numbers are not affected by ketogenic diet in steady state. The papain challenge of



mice fed with control or ketogenic diet leads to drastic differences in cell numbers - ILC2 and eosinophils - and cytokine production. The histological analysis of the lungs of papain challenged mice shows that cellular infiltrates and mucus production dramatically increased, whereas mucus production and cellular infiltration is completely abrogated in mice fed a ketogenic diet. On the transcriptional level genes for glycolysis are down regulated as well as *Ppar $\gamma$*  and *Dgat1* which explains the lower FA uptake and LD formation. Dietary changes can have profound effects on microbiota and such changes may also influence the immune response (109) (184). To test the influence of microbiota, experiments using antibiotics were performed: here, the total number of ILC2 and eosinophils in mice on ketogenic diet was lower and 2-NBDG and BODIPY® FL C16 uptake was also reduced, as well as LD formation. These results strongly suggest that the suppressive capacity of ketogenic diet is unaltered by antibiotic treatment, indicating a microbiota-independent effect. Here, the analysis of microbiota profile would be of great interest, in order to rule out any possible differences induced by the diet. The specific role of ILC2 in this model is hard to prove, since dietary changes are effecting the whole organism and not just one specific cell type. Ketogenic diet may affect hormone levels like insulin (203), which can lead to changed glucose uptake of the cells. These hormonal changes can result in overall changes of the metabolism and thus to changed immune responses (204) (205) (206). A prove of unchanged cell numbers of different immune cell types in other organs like the intestine or fat would be beneficial to show the specific effect on the lung. Another way to show ILC2 specificity would be to bypass the impairment of ILC2 by direct delivery of IL-5 or/and IL-13 to rescue the recruitment of goblet cells. Even though here the specific effect on ILC2 could not be proved, ketogenic diet could certainly provide an efficient way to treat airway inflammation in the future as its already used in the clinic to treat epilepsy (207). Furthermore, it would be interesting to test if ketogenic diet can be used as therapeutical intervention to treat established asthma. Such clinical approach, if proven successful could be a cost effective treatment of asthma and allergies, since the monitoring of ketone bodies by blood ketone body tests will allow self medication.

Overall, the results presented and discussed in this thesis show the acquisition and storage of lipids in LD as an essential mechanism mediating pathogenic ILC2 responses. Here we suggest that the inhibition of FA uptake, by using selective PPAR $\gamma$

inhibitors or reducing glucose intake with ketogenic diet, might represent an efficient therapeutic treatment, which can be applied to target allergen-induced airway inflammation in the near future.

## 5. Summary

The Western world is affected by a dramatic increase of chronic inflammatory diseases like asthma, Crohn's disease and psoriasis. Innate lymphoid cells (ILC) play an important role in the control and maintenance of barrier immunity but also in the development of several inflammatory diseases. Chronic activation of ILC results in immune-mediated pathology probably promoted by higher nutrient availability through life style changes coinciding with industrialization.

In this thesis is shown that, in the context of allergen-driven airway inflammation, tissue resident ILC2 increase the uptake of both external lipids and glucose in the lung. Since gene expression analysis of ILC2 activated upon papain challenge did not reveal any substantial upregulation of genes involved in *de novo* lipid synthesis, it was suggested that externally acquired FA may be directly funneled into membrane lipids to support proliferation. Externally acquired fatty acids are transiently stored in lipid droplets to prevent lipotoxicity and promote the proliferation of ILC2 by using external lipids for membrane synthesis. This metabolic program is imprinted upon exposure to IL-33 and it is positively regulated by *Ppar $\gamma$*  and *Dgat1*, both partially controlled by glucose availability. Inhibition of PPAR $\gamma$  or DGAT1 leads to a strong decrease in ILC2 and eosinophil accumulation, as well as to lower inflammatory cytokine release by impacting lipid droplet formation. *In vitro* studies show that absence of glucose resulted in lower external FA uptake, lower lipid droplet formation and a strong downregulation of *Ppar $\gamma$*  and *Dgat1*. Strikingly, restriction of dietary glucose by feeding mice a ketogenic diet largely ablated ILC2-mediated airway inflammation by impairing fatty acid metabolism and the formation of lipid droplets. Taken together, these results reveal that pathogenic ILC2 responses require both lipid and glucose metabolism and identify ketogenic programs as a potent dietary intervention strategy to treat airway inflammation.

## 6. List of figures

Figure 1: Classification and function of ILC	7
Figure 2: Activation of ILC2 by alarmins release from epithelial cells leading to innate type 2 immunity	10
Figure 3: Schematic representation of the structural composition of an LD	17
Figure 4: Lipid droplet biogenesis is a protective response to excess of FFA	19
Figure 5: Agilent Seahorse XF Cell Mito Stress Test profile of the key parameters of mitochondrial respiration	28
Figure 6: Agilent Seahorse XF Cell Mito Stress Test modulators of the ETC	29
Figure 7. Papain activates ILC2	38
Figure 8. Papain challenge leads to more glucose and FA uptake in ILC2	39
Figure 9. Papain increases glucose and FFA concentrations in lunghomogenate but not in the circulation	40
Figure 10. <i>Alternaria alternata</i> induced airway inflammation leads to lipid droplet formation	40
Figure 11. Purification strategy of ILC2	41
Figure 12. Papain upregulates genes for triglyceridesynthesis	42
Figure 13. Activation of pulmonary ILC2 induces lipid droplet formation	43
Figure 14. Sorting strategy of ILC2	44
Figure 15. IL-33 promotes lipid uptake and droplet formation in activated ILC2 <i>in vitro</i>	45
Figure 16. IL-33 promotes lipid uptake and droplet formation in activated ILC2 <i>in vivo</i>	46
Figure 17. IL-33 challenge leads to an increase of genes involved in TAG synthesis and FA uptake	47
Figure 18. IL-33 is essential for acquisition of external lipids and lipid droplet formation in ILC2	48
Figure 19. DGAT1 dependent LD formation protects ILC2 from lipotoxicity and allows for increased uptake of external lipids	49
Figure 20. DGAT1-Inhibitor A922500 decreases ILC2 proliferation and lipid droplet formation	50
Figure 21. DGAT1-Inhibitor A922500 leads to cell death in ILC2 <i>in vitro</i>	50
Figure 22. DGAT1-Inhibitor A922500 leads to apoptosis in ILC2 <i>in vitro</i>	51
Figure 23. DGAT1-Inhibitor A922500 leads lipid peroxidation	51

Figure 24. DGAT2-Inhibitor PF06424439 has no effect on ILC2 numbers and lipid droplet formation	52
Figure 25. DGAT1 dependent LD formation protects ILC2 from lipotoxicity and allows for increased uptake of external lipids	53
Figure 26. DGAT1i inhibits ILC2 accumulation in airway inflammation	54
Figure 27. External FA increased proliferation and accumulation of ILC2 <i>in vitro</i>	55
Figure 28. Proliferating ILC2 take up more fatty acids and build up more lipid droplets compared to non proliferating ILC2	55
Figure 29. External FA are directly funneled into membrane lipids for proliferation	56
Figure 30. External FA have no impact on the oxygen consumption rate	57
Figure 31. PPAR $\gamma$ regulates FA uptake <i>in vitro</i>	58
Figure 32. GW9662 downregulates expression of <i>Dgat1</i> <i>in vitro</i>	59
Figure 33. PPAR $\gamma$ regulates FA uptake and accumulation and proliferation of ILC2 <i>in vivo</i>	60
Figure 34. Inhibition of PPAR $\gamma$ reduces inflammatory cytokine release	60
Figure 35. Glucose and external FA cooperate to fuel fatty acid metabolism in ILC2	62
Figure 36. Absence of glucose leads to limited proliferation	63
Figure 37. Presence of glucose regulates expression of <i>Ppar<math>\gamma</math></i> and <i>Dgat1</i>	63
Figure 38. Ketogenic diet has no effect on ILC2 number in steady state	64
Figure 39. Ketogenic diet leads to an increase of ketone body concentration in the blood	65
Figure 40. Ketogenic diet inhibits ILC2-driven airway inflammation	65
Figure 41. Ketogenic diet inhibits cell infiltration and mucus production in papain challenged mice	66
Figure 42. Ketogenic diet lead to lower FA uptake and less LD formation	67
Figure 43. Ketogenic diet increases expression of <i>Ppar<math>\gamma</math></i> and <i>Dgat1</i>	68
Figure 44. Microbiota has no impact on inhibition of airway inflammation by using ketogenic diet	69
Figure 45. Ketogenic diet inhibits ILC2-driven inflammatory cytokine release	70

## 7. Literature

1. Straub RH, Schradin C. Chronic inflammatory systemic diseases: An evolutionary trade-off between acutely beneficial but chronically harmful programs. *Evol Med Public Health*. 2016;2016(1):37-51.
2. Multhoff G, Molls M, Radons J. Chronic inflammation in cancer development. *Front Immunol*. 2011;2:98.
3. Coussens LM, Werb Z. Inflammation and cancer. *Nature*. 2002;420(6917):860-7.
4. Platts-Mills TA. The allergy epidemics: 1870-2010. *J Allergy Clin Immunol*. 2015;136(1):3-13.
5. Lambrecht BN, Hammad H. The immunology of the allergy epidemic and the hygiene hypothesis. *Nat Immunol*. 2017;18(10):1076-83.
6. Klein J. Are invertebrates capable of anticipatory immune responses? *Scand J Immunol*. 1989;29(5):499-505.
7. Gallo RL, Murakami M, Ohtake T, Zaiou M. Biology and clinical relevance of naturally occurring antimicrobial peptides. *J Allergy Clin Immunol*. 2002;110(6):823-31.
8. Figdor CG, van Kooyk, Y., Adema, G.J. C-type lectin receptors on dendritic cells and Langerhans cells. *Nature Reviews Immunology*. 2002;77.
9. Aderem A, Underhill, D.M. Mechanism of phagocytosis in macrophages. *Annu Rev Immunol*. 1999;17:593-623.
10. Lee WL, Harrison RE, Grinstein S. Phagocytosis by neutrophils. *Microbes Infect*. 2003;5(14):1299-306.
11. Luster AD. The role of chemokines in linking innate and adaptive immunity. *Curr Opin Immunol*. 2002;14(1):129-35.
12. Janeway CA, Jr. The immune system evolved to discriminate infectious nonself from noninfectious self. *Immunol Today*. 1992;13(1):11-6.
13. Heine H, Lien E. Toll-like receptors and their function in innate and adaptive immunity. *Int Arch Allergy Immunol*. 2003;130(3):180-92.
14. Janeway CA, Jr., Medzhitov R. Innate immune recognition. *Annu Rev Immunol*. 2002;20:197-216.
15. Medzhitov R, Preston-Hurlburt P, Janeway CA, Jr. A human homologue of the *Drosophila* Toll protein signals activation of adaptive immunity. *Nature*. 1997;388(6640):394-7.
16. Dutton RW, Bradley LM, Swain SL. T cell memory. *Annu Rev Immunol*. 1998;16:201-23.
17. Germain RN. MHC-dependent antigen processing and peptide presentation: providing ligands for T lymphocyte activation. *Cell*. 1994;76(2):287-99.
18. Germain RN. T-cell development and the CD4-CD8 lineage decision. *Nat Rev Immunol*. 2002;2(5):309-22.

19. Zamojska R. CD4 and CD8: modulators of T-cell receptor recognition of antigen and of immune responses? *Curr Opin Immunol.* 1998;10(1):82-7.
20. Stockinger B, Veldhoen M. Differentiation and function of Th17 T cells. *Curr Opin Immunol.* 2007;19(3):281-6.
21. Abbas AK, Murphy KM, Sher A. Functional diversity of helper T lymphocytes. *Nature.* 1996;383(6603):787-93.
22. Mosmann TR, Cherwinski H, Bond MW, Giedlin MA, Coffman RL. Two types of murine helper T cell clone. I. Definition according to profiles of lymphokine activities and secreted proteins. *J Immunol.* 1986;136(7):2348-57.
23. Harrington LE, Hatton RD, Mangan PR, Turner H, Murphy TL, Murphy KM, et al. Interleukin 17-producing CD4<sup>+</sup> effector T cells develop via a lineage distinct from the T helper type 1 and 2 lineages. *Nat Immunol.* 2005;6(11):1123-32.
24. Sakaguchi S, Sakaguchi N. Regulatory T cells in immunologic self-tolerance and autoimmune disease. *Int Rev Immunol.* 2005;24(3-4):211-26.
25. DeFranco AL. Molecular aspects of B-lymphocyte activation. *Annu Rev Cell Biol.* 1987;3:143-78.
26. Edelman GM. Antibody structure and molecular immunology. *Scand J Immunol.* 1991;34(1):1-22.
27. Sallusto F, Lenig D, Forster R, Lipp M, Lanzavecchia A. Two subsets of memory T lymphocytes with distinct homing potentials and effector functions. *Nature.* 1999;401(6754):708-12.
28. Artis D, Spits H. The biology of innate lymphoid cells. *Nature.* 2015;517(7534):293-301.
29. Spits HaC, T. Innate Lymphoid Cells: Emerging Insights in Development, Lineage Relationships, and Function. *Annu Rev Immunol.* 2011.
30. Spits H, Artis D, Colonna M, Dieffenbach A, Di Santo JP, Eberl G, et al. Innate lymphoid cells--a proposal for uniform nomenclature. *Nat Rev Immunol.* 2013;13(2):145-9.
31. Spits H, Di Santo JP. The expanding family of innate lymphoid cells: regulators and effectors of immunity and tissue remodeling. *Nat Immunol.* 2011;12(1):21-7.
32. Mjosberg J, Spits H. Human innate lymphoid cells. *J Allergy Clin Immunol.* 2016;138(5):1265-76.
33. Mjosberg JM, Trifari S, Crellin NK, Peters CP, van Drunen CM, Piet B, et al. Human IL-25- and IL-33-responsive type 2 innate lymphoid cells are defined by expression of CCR4 and CD161. *Nat Immunol.* 2011;12(11):1055-62.
34. Yang Q, Monticelli LA, Saenz SA, Chi AW, Sonnenberg GF, Tang J, et al. T cell factor 1 is required for group 2 innate lymphoid cell generation. *Immunity.* 2013;38(4):694-704.
35. Constantinides MG, McDonald BD, Verhoef PA, Bendelac A. A committed precursor to innate lymphoid cells. *Nature.* 2014;508(7496):397-401.

36. Moretta F, Petronelli F, Lucarelli B, Pitisci A, Bertaina A, Locatelli F, et al. The generation of human innate lymphoid cells is influenced by the source of hematopoietic stem cells and by the use of G-CSF. *Eur J Immunol.* 2016;46(5):1271-8.
37. Montaldo E, Teixeira-Alves LG, Glatzer T, Durek P, Stervbo U, Hamann W, et al. Human RORgammat(+)CD34(+) cells are lineage-specified progenitors of group 3 RORgammat(+) innate lymphoid cells. *Immunity.* 2014;41(6):988-1000.
38. Scoville SD, Mundy-Bosse BL, Zhang MH, Chen L, Zhang X, Keller KA, et al. A Progenitor Cell Expressing Transcription Factor RORgammat Generates All Human Innate Lymphoid Cell Subsets. *Immunity.* 2016;44(5):1140-50.
39. Bernink JH, Peters CP, Munneke M, te Velde AA, Meijer SL, Weijer K, et al. Human type 1 innate lymphoid cells accumulate in inflamed mucosal tissues. *Nat Immunol.* 2013;14(3):221-9.
40. Klose CSN, Flach M, Mohle L, Rogell L, Hoyler T, Ebert K, et al. Differentiation of type 1 ILCs from a common progenitor to all helper-like innate lymphoid cell lineages. *Cell.* 2014;157(2):340-56.
41. Robinette ML, Bando JK, Song W, Ulland TK, Gilfillan S, Colonna M. IL-15 sustains IL-7R-independent ILC2 and ILC3 development. *Nat Commun.* 2017;8:14601.
42. Fuchs A, Vermi W, Lee JS, Lonardi S, Gilfillan S, Newberry RD, et al. Intraepithelial type 1 innate lymphoid cells are a unique subset of IL-12- and IL-15-responsive IFN-gamma-producing cells. *Immunity.* 2013;38(4):769-81.
43. Kim BS, Wojno ED, Artis D. Innate lymphoid cells and allergic inflammation. *Curr Opin Immunol.* 2013;25(6):738-44.
44. Mjosberg J, Bernink J, Golebski K, Karrich JJ, Peters CP, Blom B, et al. The transcription factor GATA3 is essential for the function of human type 2 innate lymphoid cells. *Immunity.* 2012;37(4):649-59.
45. Oliphant CJ, Barlow JL, McKenzie AN. Insights into the initiation of type 2 immune responses. *Immunology.* 2011;134(4):378-85.
46. Rouvier E, Luciani MF, Mattei MG, Denizot F, Golstein P. CTLA-8, cloned from an activated T cell, bearing AU-rich messenger RNA instability sequences, and homologous to a herpesvirus saimiri gene. *J Immunol.* 1993;150(12):5445-56.
47. Takai T. TSLP expression: cellular sources, triggers, and regulatory mechanisms. *Allergol Int.* 2012;61(1):3-17.
48. Mirchandani AS, Salmond RJ, Liew FY. Interleukin-33 and the function of innate lymphoid cells. *Trends Immunol.* 2012;33(8):389-96.
49. Moro K, Yamada T, Tanabe M, Takeuchi T, Ikawa T, Kawamoto H, et al. Innate production of T(H)2 cytokines by adipose tissue-associated c-Kit(+)Sca-1(+) lymphoid cells. *Nature.* 2010;463(7280):540-4.



50. Monticelli LA, Sonnenberg GF, Abt MC, Alenghat T, Ziegler CG, Doering TA, et al. Innate lymphoid cells promote lung-tissue homeostasis after infection with influenza virus. *Nat Immunol.* 2011;12(11):1045-54.
51. Smith SG, Chen R, Kjarsgaard M, Huang C, Oliveria JP, O'Byrne PM, et al. Increased numbers of activated group 2 innate lymphoid cells in the airways of patients with severe asthma and persistent airway eosinophilia. *J Allergy Clin Immunol.* 2016;137(1):75-86 e8.
52. Salimi M, Barlow JL, Saunders SP, Xue L, Gutowska-Owsiak D, Wang X, et al. A role for IL-25 and IL-33-driven type-2 innate lymphoid cells in atopic dermatitis. *J Exp Med.* 2013;210(13):2939-50.
53. Koyasu S, Moro K, Tanabe M, Takeuchi T. Natural helper cells: a new player in the innate immune response against helminth infection. *Adv Immunol.* 2010;108:21-44.
54. Monticelli LA, Sonnenberg GF, Artis D. Innate lymphoid cells: critical regulators of allergic inflammation and tissue repair in the lung. *Curr Opin Immunol.* 2012;24(3):284-9.
55. Saenz SA, Noti M, Artis D. Innate immune cell populations function as initiators and effectors in Th2 cytokine responses. *Trends Immunol.* 2010;31(11):407-13.
56. Hams E, Locksley RM, McKenzie AN, Fallon PG. Cutting edge: IL-25 elicits innate lymphoid type 2 and type II NKT cells that regulate obesity in mice. *J Immunol.* 2013;191(11):5349-53.
57. Brestoff JR, Kim BS, Saenz SA, Stine RR, Monticelli LA, Sonnenberg GF, et al. Group 2 innate lymphoid cells promote beiging of white adipose tissue and limit obesity. *Nature.* 2015;519(7542):242-6.
58. Diefenbach A, Colonna M, Koyasu S. Development, differentiation, and diversity of innate lymphoid cells. *Immunity.* 2014;41(3):354-65.
59. Teunissen MBM, Munneke JM, Bernink JH, Spuls PI, Res PCM, Te Velde A, et al. Composition of innate lymphoid cell subsets in the human skin: enrichment of NCR(+) ILC3 in lesional skin and blood of psoriasis patients. *J Invest Dermatol.* 2014;134(9):2351-60.
60. Satoh-Takayama N, Vosshenrich CA, Lesjean-Pottier S, Sawa S, Lochner M, Rattis F, et al. Microbial flora drives interleukin 22 production in intestinal NKp46+ cells that provide innate mucosal immune defense. *Immunity.* 2008;29(6):958-70.
61. Cella M, Fuchs A, Vermi W, Facchetti F, Otero K, Lennerz JK, et al. A human natural killer cell subset provides an innate source of IL-22 for mucosal immunity. *Nature.* 2009;457(7230):722-5.
62. Sanos SL, Bui VL, Mortha A, Oberle K, Heners C, Johner C, et al. ROR $\gamma$  and commensal microflora are required for the differentiation of mucosal interleukin 22-producing NKp46+ cells. *Nat Immunol.* 2009;10(1):83-91.
63. Sonnenberg GF, Monticelli LA, Elloso MM, Fouser LA, Artis D. CD4(+) lymphoid tissue-inducer cells promote innate immunity in the gut. *Immunity.* 2011;34(1):122-34.

64. Takatori H, Kanno Y, Watford WT, Tato CM, Weiss G, Ivanov II, et al. Lymphoid tissue inducer-like cells are an innate source of IL-17 and IL-22. *J Exp Med*. 2009;206(1):35-41.
65. Eberl G, Colonna M, Di Santo JP, McKenzie AN. Innate lymphoid cells. Innate lymphoid cells: a new paradigm in immunology. *Science*. 2015;348(6237):aaa6566.
66. Pawankar R, Canonica, GW., Holgate ST., RF Lockey. White book on allergy. World Allergy Organ J. 2011.
67. Fort MM, Cheung J, Yen D, Li J, Zurawski SM, Lo S, et al. IL-25 induces IL-4, IL-5, and IL-13 and Th2-associated pathologies in vivo. *Immunity*. 2001;15(6):985-95.
68. Hurst SD, Muchamuel T, Gorman DM, Gilbert JM, Clifford T, Kwan S, et al. New IL-17 family members promote Th1 or Th2 responses in the lung: in vivo function of the novel cytokine IL-25. *J Immunol*. 2002;169(1):443-53.
69. Price AE, Liang HE, Sullivan BM, Reinhardt RL, Easley CJ, Erle DJ, et al. Systemically dispersed innate IL-13-expressing cells in type 2 immunity. *Proc Natl Acad Sci U S A*. 2010;107(25):11489-94.
70. Wedemeyer J, Tsai M, Galli SJ. Roles of mast cells and basophils in innate and acquired immunity. *Curr Opin Immunol*. 2000;12(6):624-31.
71. Halim TY, Krauss RH, Sun AC, Takei F. Lung natural helper cells are a critical source of Th2 cell-type cytokines in protease allergen-induced airway inflammation. *Immunity*. 2012;36(3):451-63.
72. Oboki K, Ohno T, Kajiwara N, Arae K, Morita H, Ishii A, et al. IL-33 is a crucial amplifier of innate rather than acquired immunity. *Proc Natl Acad Sci U S A*. 2010;107(43):18581-6.
73. Halim TY, MacLaren A, Romanish MT, Gold MJ, McNagny KM, Takei F. Retinoic-acid-receptor-related orphan nuclear receptor alpha is required for natural helper cell development and allergic inflammation. *Immunity*. 2012;37(3):463-74.
74. Yamane H, Paul WE. Cytokines of the gamma(c) family control CD4+ T cell differentiation and function. *Nat Immunol*. 2012;13(11):1037-44.
75. Halim TY, Hwang YY, Scanlon ST, Zaghouani H, Garbi N, Fallon PG, et al. Group 2 innate lymphoid cells license dendritic cells to potentiate memory TH2 cell responses. *Nat Immunol*. 2016;17(1):57-64.
76. Islam SA, Luster AD. T cell homing to epithelial barriers in allergic disease. *Nat Med*. 2012;18(5):705-15.
77. Klein Wolterink RG, Kleinjan A, van Nimwegen M, Bergen I, de Bruijn M, Levani Y, et al. Pulmonary innate lymphoid cells are major producers of IL-5 and IL-13 in murine models of allergic asthma. *Eur J Immunol*. 2012;42(5):1106-16.
78. Martinez-Gonzalez I, Steer CA, Takei F. Lung ILC2s link innate and adaptive responses in allergic inflammation. *Trends Immunol*. 2015;36(3):189-95.

79. Smith DE. IL-33: a tissue derived cytokine pathway involved in allergic inflammation and asthma. *Clin Exp Allergy*. 2010;40(2):200-8.
80. Mohapatra A, Van Dyken SJ, Schneider C, Nussbaum JC, Liang HE, Locksley RM. Group 2 innate lymphoid cells utilize the IRF4-IL-9 module to coordinate epithelial cell maintenance of lung homeostasis. *Mucosal Immunol*. 2016;9(1):275-86.
81. Kaur D, Gomez E, Doe C, Berair R, Woodman L, Saunders R, et al. IL-33 drives airway hyper-responsiveness through IL-13-mediated mast cell: airway smooth muscle crosstalk. *Allergy*. 2015;70(5):556-67.
82. Cayrol C, Girard JP. The IL-1-like cytokine IL-33 is inactivated after maturation by caspase-1. *Proc Natl Acad Sci U S A*. 2009;106(22):9021-6.
83. de Boer JD, Van't Veer C, Stroo I, van der Meer AJ, de Vos AF, van der Zee JS, et al. Protease-activated receptor-2 deficient mice have reduced house dust mite-evoked allergic lung inflammation. *Innate Immun*. 2014;20(6):618-25.
84. Kamijo S, Takeda H, Tokura T, Suzuki M, Inui K, Hara M, et al. IL-33-mediated innate response and adaptive immune cells contribute to maximum responses of protease allergen-induced allergic airway inflammation. *J Immunol*. 2013;190(9):4489-99.
85. Scott IC, Majithiya JB, Sanden C, Thornton P, Sanders PN, Moore T, et al. Interleukin-33 is activated by allergen- and necrosis-associated proteolytic activities to regulate its alarmin activity during epithelial damage. *Sci Rep*. 2018;8(1):3363.
86. Kool M, Willart MA, van Nimwegen M, Bergen I, Pouliot P, Virchow JC, et al. An unexpected role for uric acid as an inducer of T helper 2 cell immunity to inhaled antigens and inflammatory mediator of allergic asthma. *Immunity*. 2011;34(4):527-40.
87. Vander Heiden MG, Cantley LC, Thompson CB. Understanding the Warburg effect: the metabolic requirements of cell proliferation. *Science*. 2009;324(5930):1029-33.
88. Pearce EL, Pearce EJ. Metabolic pathways in immune cell activation and quiescence. *Immunity*. 2013;38(4):633-43.
89. van der Windt GJ, Pearce EL. Metabolic switching and fuel choice during T-cell differentiation and memory development. *Immunol Rev*. 2012;249(1):27-42.
90. Thompson CB. Rethinking the regulation of cellular metabolism. *Cold Spring Harb Symp Quant Biol*. 2011;76:23-9.
91. MacIver NJ, Michalek RD, Rathmell JC. Metabolic regulation of T lymphocytes. *Annu Rev Immunol*. 2013;31:259-83.
92. Pearce EL, Poffenberger MC, Chang CH, Jones RG. Fueling immunity: insights into metabolism and lymphocyte function. *Science*. 2013;342(6155):1242-454.
93. Cui G, Staron MM, Gray SM, Ho PC, Amezcua RA, Wu J, et al. IL-7-Induced Glycerol Transport and TAG Synthesis Promotes Memory CD8+ T Cell Longevity. *Cell*. 2015;161(4):750-61.

94. O'Sullivan D, van der Windt GJ, Huang SC, Curtis JD, Chang CH, Buck MD, et al. Memory CD8(+) T cells use cell-intrinsic lipolysis to support the metabolic programming necessary for development. *Immunity*. 2014;41(1):75-88.
95. Pan Y, Tian T, Park CO, Lofftus SY, Mei S, Liu X, et al. Survival of tissue-resident memory T cells requires exogenous lipid uptake and metabolism. *Nature*. 2017;543(7644):252-6.
96. Duester G. Retinoic acid synthesis and signaling during early organogenesis. *Cell*. 2008;134(6):921-31.
97. Liu ZM, Wang KP, Ma J, Guo Zheng S. The role of all-trans retinoic acid in the biology of Foxp3+ regulatory T cells. *Cell Mol Immunol*. 2015;12(5):553-7.
98. Veldhoen M, Brucklacher-Waldert V. Dietary influences on intestinal immunity. *Nat Rev Immunol*. 2012;12(10):696-708.
99. Hall JA, Grainger JR, Spencer SP, Belkaid Y. The role of retinoic acid in tolerance and immunity. *Immunity*. 2011;35(1):13-22.
100. Spencer SP, Wilhelm C, Yang Q, Hall JA, Bouladoux N, Boyd A, et al. Adaptation of innate lymphoid cells to a micronutrient deficiency promotes type 2 barrier immunity. *Science*. 2014;343(6169):432-7.
101. Monticelli LA, Buck MD, Flamar AL, Saenz SA, Tait Wojno ED, Yudanin NA, et al. Arginase 1 is an innate lymphoid-cell-intrinsic metabolic checkpoint controlling type 2 inflammation. *Nat Immunol*. 2016;17(6):656-65.
102. Wilhelm C, Harrison OJ, Schmitt V, Pelletier M, Spencer SP, Urban JF, Jr., et al. Critical role of fatty acid metabolism in ILC2-mediated barrier protection during malnutrition and helminth infection. *J Exp Med*. 2016;213(8):1409-18.
103. Devereux G, Turner SW, Craig LC, McNeill G, Martindale S, Harbour PJ, et al. Low maternal vitamin E intake during pregnancy is associated with asthma in 5-year-old children. *Am J Respir Crit Care Med*. 2006;174(5):499-507.
104. Devereux G. The increase in the prevalence of asthma and allergy: food for thought. *Nat Rev Immunol*. 2006;6(11):869-74.
105. Chen Y, Bishop M, Liepold H. Increased effect of obesity on asthma in adults with low household income. *J Asthma*. 2010;47(3):263-8.
106. Raben A, Macdonald I, Astrup A. Replacement of dietary fat by sucrose or starch: effects on 14 d ad libitum energy intake, energy expenditure and body weight in formerly obese and never-obese subjects. *Int J Obes Relat Metab Disord*. 1997;21(10):846-59.
107. Cahill GF, Jr. Fuel metabolism in starvation. *Annu Rev Nutr*. 2006;26:1-22.
108. Kennedy AR, Pissios P, Otu H, Roberson R, Xue B, Asakura K, et al. A high-fat, ketogenic diet induces a unique metabolic state in mice. *Am J Physiol Endocrinol Metab*. 2007;292(6):E1724-39.

109. Klein MS, Newell C, Bomhof MR, Reimer RA, Hittel DS, Rho JM, et al. Metabolomic Modeling To Monitor Host Responsiveness to Gut Microbiota Manipulation in the BTBR(T+tf/j) Mouse. *J Proteome Res.* 2016;15(4):1143-50.
110. Saita D, Ferrarese R, Foglieni C, Esposito A, Canu T, Perani L, et al. Adaptive immunity against gut microbiota enhances apoE-mediated immune regulation and reduces atherosclerosis and western-diet-related inflammation. *Sci Rep.* 2016;6:29353.
111. Olson CA, Vuong HE, Yano JM, Liang QY, Nusbaum DJ, Hsiao EY. The Gut Microbiota Mediates the Anti-Seizure Effects of the Ketogenic Diet. *Cell.* 2018;174(2):497.
112. Kwan P, Brodie MJ. Early identification of refractory epilepsy. *N Engl J Med.* 2000;342(5):314-9.
113. Varga T, Czimmerer Z, Nagy L. PPARs are a unique set of fatty acid regulated transcription factors controlling both lipid metabolism and inflammation. *Biochim Biophys Acta.* 2011;1812(8):1007-22.
114. Evans RM, Barish GD, Wang YX. PPARs and the complex journey to obesity. *Nat Med.* 2004;10(4):355-61.
115. Barish GD, Narkar VA, Evans RM. PPAR delta: a dagger in the heart of the metabolic syndrome. *J Clin Invest.* 2006;116(3):590-7.
116. Forman BM, Tontonoz P, Chen J, Brun RP, Spiegelman BM, Evans RM. 15-Deoxy-delta 12, 14-prostaglandin J2 is a ligand for the adipocyte determination factor PPAR gamma. *Cell.* 1995;83(5):803-12.
117. Forman BM, Chen J, Evans RM. Hypolipidemic drugs, polyunsaturated fatty acids, and eicosanoids are ligands for peroxisome proliferator-activated receptors alpha and delta. *Proc Natl Acad Sci U S A.* 1997;94(9):4312-7.
118. Forman BM, Chen J, Evans RM. The peroxisome proliferator-activated receptors: ligands and activators. *Ann N Y Acad Sci.* 1996;804:266-75.
119. Poulsen L, Siersbaek M, Mandrup S. PPARs: fatty acid sensors controlling metabolism. *Semin Cell Dev Biol.* 2012;23(6):631-9.
120. Tontonoz P, Spiegelman BM. Fat and beyond: the diverse biology of PPARgamma. *Annu Rev Biochem.* 2008;77:289-312.
121. Hollenberg AN, Susulic VS, Madura JP, Zhang B, Moller DE, Tontonoz P, et al. Functional antagonism between CCAAT/Enhancer binding protein-alpha and peroxisome proliferator-activated receptor-gamma on the leptin promoter. *J Biol Chem.* 1997;272(8):5283-90.
122. Iwaki M, Matsuda M, Maeda N, Funahashi T, Matsuzawa Y, Makishima M, et al. Induction of adiponectin, a fat-derived antidiabetic and antiatherogenic factor, by nuclear receptors. *Diabetes.* 2003;52(7):1655-63.

123. Hofmann C, Lorenz K, Braithwaite SS, Colca JR, Palazuk BJ, Hotamisligil GS, et al. Altered gene expression for tumor necrosis factor-alpha and its receptors during drug and dietary modulation of insulin resistance. *Endocrinology*. 1994;134(1):264-70.
124. Tomaru T, Steger DJ, Lefterova MI, Schupp M, Lazar MA. Adipocyte-specific expression of murine resistin is mediated by synergism between peroxisome proliferator-activated receptor gamma and CCAAT/enhancer-binding proteins. *J Biol Chem*. 2009;284(10):6116-25.
125. Kung J, Henry RR. Thiazolidinedione safety. *Expert Opin Drug Saf*. 2012;11(4):565-79.
126. Nissen SE, Wolski K. Effect of rosiglitazone on the risk of myocardial infarction and death from cardiovascular causes. *N Engl J Med*. 2007;356(24):2457-71.
127. Graham DJ, Ouellet-Hellstrom R, MaCurdy TE, Ali F, Sholley C, Worrall C, et al. Risk of acute myocardial infarction, stroke, heart failure, and death in elderly Medicare patients treated with rosiglitazone or pioglitazone. *JAMA*. 2010;304(4):411-8.
128. Szatmari I, Rajnavolgyi E, Nagy L. PPARgamma, a lipid-activated transcription factor as a regulator of dendritic cell function. *Ann N Y Acad Sci*. 2006;1088:207-18.
129. Szeles L, Torocsik D, Nagy L. PPARgamma in immunity and inflammation: cell types and diseases. *Biochim Biophys Acta*. 2007;1771(8):1014-30.
130. Szanto A, Balint BL, Nagy ZS, Barta E, Dezso B, Pap A, et al. STAT6 transcription factor is a facilitator of the nuclear receptor PPARgamma-regulated gene expression in macrophages and dendritic cells. *Immunity*. 2010;33(5):699-712.
131. Tontonoz P, Nagy L, Alvarez JG, Thomazy VA, Evans RM. PPARgamma promotes monocyte/macrophage differentiation and uptake of oxidized LDL. *Cell*. 1998;93(2):241-52.
132. Odegaard JI, Ricardo-Gonzalez RR, Goforth MH, Morel CR, Subramanian V, Mukundan L, et al. Macrophage-specific PPARgamma controls alternative activation and improves insulin resistance. *Nature*. 2007;447(7148):1116-20.
133. Sugii S, Evans RM. Epigenetic codes of PPARgamma in metabolic disease. *FEBS Lett*. 2011;585(13):2121-8.
134. Clark RB, Bishop-Bailey D, Estrada-Hernandez T, Hla T, Puddington L, Padula SJ. The nuclear receptor PPAR gamma and immunoregulation: PPAR gamma mediates inhibition of helper T cell responses. *J Immunol*. 2000;164(3):1364-71.
135. Yang XY, Wang LH, Chen T, Hodge DR, Resau JH, DaSilva L, et al. Activation of human T lymphocytes is inhibited by peroxisome proliferator-activated receptor gamma (PPARgamma) agonists. PPARgamma co-association with transcription factor NFAT. *J Biol Chem*. 2000;275(7):4541-4.
136. Chung SW, Kang BY, Kim TS. Inhibition of interleukin-4 production in CD4+ T cells by peroxisome proliferator-activated receptor-gamma (PPAR-gamma) ligands: involvement of physical association between PPAR-gamma and the nuclear factor of activated T cells transcription factor. *Mol Pharmacol*. 2003;64(5):1169-79.

137. Won HY, Min HJ, Ahn JH, Yoo SE, Bae MA, Hong JH, et al. Anti-allergic function and regulatory mechanisms of KR62980 in allergen-induced airway inflammation. *Biochem Pharmacol.* 2010;79(6):888-96.
138. Devries-Seimon T, Li Y, Yao PM, Stone E, Wang Y, Davis RJ, et al. Cholesterol-induced macrophage apoptosis requires ER stress pathways and engagement of the type A scavenger receptor. *J Cell Biol.* 2005;171(1):61-73.
139. Koliwad SK, Streeper RS, Monetti M, Cornelissen I, Chan L, Terayama K, et al. DGAT1-dependent triacylglycerol storage by macrophages protects mice from diet-induced insulin resistance and inflammation. *J Clin Invest.* 2010;120(3):756-67.
140. Listenberger LL, Han X, Lewis SE, Cases S, Farese RV, Jr., Ory DS, et al. Triglyceride accumulation protects against fatty acid-induced lipotoxicity. *Proc Natl Acad Sci U S A.* 2003;100(6):3077-82.
141. Gross DA, Silver DL. Cytosolic lipid droplets: from mechanisms of fat storage to disease. *Crit Rev Biochem Mol Biol.* 2014;49(4):304-26.
142. Ohsaki Y, Kawai T, Yoshikawa Y, Cheng J, Jokitalo E, Fujimoto T. PML isoform II plays a critical role in nuclear lipid droplet formation. *J Cell Biol.* 2016;212(1):29-38.
143. Bersuker K, Olzmann JA. Establishing the lipid droplet proteome: Mechanisms of lipid droplet protein targeting and degradation. *Biochim Biophys Acta Mol Cell Biol Lipids.* 2017;1862(10 Pt B):1166-77.
144. Krahmer N, Farese RV, Jr., Walther TC. Balancing the fat: lipid droplets and human disease. *EMBO Mol Med.* 2013;5(7):973-83.
145. Walther TC, Chung J, Farese RV, Jr. Lipid Droplet Biogenesis. *Annu Rev Cell Dev Biol.* 2017;33:491-510.
146. Cases S, Smith SJ, Zheng YW, Myers HM, Lear SR, Sande E, et al. Identification of a gene encoding an acyl CoA:diacylglycerol acyltransferase, a key enzyme in triacylglycerol synthesis. *Proc Natl Acad Sci U S A.* 1998;95(22):13018-23.
147. Lardizabal KD, Mai JT, Wagner NW, Wyrick A, Voelker T, Hawkins DJ. DGAT2 is a new diacylglycerol acyltransferase gene family: purification, cloning, and expression in insect cells of two polypeptides from *Mortierella ramanniana* with diacylglycerol acyltransferase activity. *J Biol Chem.* 2001;276(42):38862-9.
148. Chan CC SJ, Chang T-Y. Membrane-bound O-acyltransferases (MBOATs). *Frontiers in Biology.* 2011;6:177.
149. Villanueva CJ, Monetti M, Shih M, Zhou P, Watkins SM, Bhanot S, et al. Specific role for acyl CoA:Diacylglycerol acyltransferase 1 (Dgat1) in hepatic steatosis due to exogenous fatty acids. *Hepatology.* 2009;50(2):434-42.
150. Unger RH, Clark GO, Scherer PE, Orci L. Lipid homeostasis, lipotoxicity and the metabolic syndrome. *Biochim Biophys Acta.* 2010;1801(3):209-14.

151. Nguyen TB, Louie SM, Daniele JR, Tran Q, Dillin A, Zoncu R, et al. DGAT1-Dependent Lipid Droplet Biogenesis Protects Mitochondrial Function during Starvation-Induced Autophagy. *Dev Cell*. 2017;42(1):9-21 e5.
152. Irshad Z, Dimitri F, Christian M, Zammit VA. Diacylglycerol acyltransferase 2 links glucose utilization to fatty acid oxidation in the brown adipocytes. *J Lipid Res*. 2017;58(1):15-30.
153. Li C, Li L, Lian J, Watts R, Nelson R, Goodwin B, et al. Roles of Acyl-CoA:Diacylglycerol Acyltransferases 1 and 2 in Triacylglycerol Synthesis and Secretion in Primary Hepatocytes. *Arterioscler Thromb Vasc Biol*. 2015;35(5):1080-91.
154. Qi J, Lang W, Geisler JG, Wang P, Petrounia I, Mai S, et al. The use of stable isotope-labeled glycerol and oleic acid to differentiate the hepatic functions of DGAT1 and -2. *J Lipid Res*. 2012;53(6):1106-16.
155. Wurie HR, Buckett L, Zammit VA. Diacylglycerol acyltransferase 2 acts upstream of diacylglycerol acyltransferase 1 and utilizes nascent diglycerides and de novo synthesized fatty acids in HepG2 cells. *FEBS J*. 2012;279(17):3033-47.
156. Chen HC, Smith SJ, Ladha Z, Jensen DR, Ferreira LD, Pulawa LK, et al. Increased insulin and leptin sensitivity in mice lacking acyl CoA:diacylglycerol acyltransferase 1. *J Clin Invest*. 2002;109(8):1049-55.
157. Smith SJ, Cases S, Jensen DR, Chen HC, Sande E, Tow B, et al. Obesity resistance and multiple mechanisms of triglyceride synthesis in mice lacking Dgat. *Nat Genet*. 2000;25(1):87-90.
158. Stone SJ, Myers HM, Watkins SM, Brown BE, Feingold KR, Elias PM, et al. Lipopenia and skin barrier abnormalities in DGAT2-deficient mice. *J Biol Chem*. 2004;279(12):11767-76.
159. Choudhary V, Ojha N, Golden A, Prinz WA. A conserved family of proteins facilitates nascent lipid droplet budding from the ER. *J Cell Biol*. 2015;211(2):261-71.
160. Kadereit B, Kumar P, Wang WJ, Miranda D, Snapp EL, Severina N, et al. Evolutionarily conserved gene family important for fat storage. *Proc Natl Acad Sci U S A*. 2008;105(1):94-9.
161. Gross DA, Zhan C, Silver DL. Direct binding of triglyceride to fat storage-inducing transmembrane proteins 1 and 2 is important for lipid droplet formation. *Proc Natl Acad Sci U S A*. 2011;108(49):19581-6.
162. Salo VT, Belevich I, Li S, Karhinen L, Vihinen H, Vigouroux C, et al. Seipin regulates ER-lipid droplet contacts and cargo delivery. *EMBO J*. 2016;35(24):2699-716.
163. Wang H, Becuwe M, Housden BE, Chitraju C, Porras AJ, Graham MM, et al. Seipin is required for converting nascent to mature lipid droplets. *Elife*. 2016;5.
164. Brasaemle DL. Thematic review series: adipocyte biology. The perilipin family of structural lipid droplet proteins: stabilization of lipid droplets and control of lipolysis. *J Lipid Res*. 2007;48(12):2547-59.



165. Ducharme NA, Bickel PE. Lipid droplets in lipogenesis and lipolysis. *Endocrinology*. 2008;149(3):942-9.
166. Zechner R, Strauss JG, Haemmerle G, Lass A, Zimmermann R. Lipolysis: pathway under construction. *Curr Opin Lipidol*. 2005;16(3):333-40.
167. Bozza PT, Melo RC, Bandeira-Melo C. Leukocyte lipid bodies regulation and function: contribution to allergy and host defense. *Pharmacol Ther*. 2007;113(1):30-49.
168. Steinman RM, Adams JC, Cohn ZA. Identification of a novel cell type in peripheral lymphoid organs of mice. IV. Identification and distribution in mouse spleen. *J Exp Med*. 1975;141(4):804-20.
169. Bozza PT, Viola JP. Lipid droplets in inflammation and cancer. *Prostaglandins Leukot Essent Fatty Acids*. 2010;82(4-6):243-50.
170. Wilhelm C, Hirota K, Stieglitz B, Van Snick J, Tolaini M, Lahl K, et al. An IL-9 fate reporter demonstrates the induction of an innate IL-9 response in lung inflammation. *Nat Immunol*. 2011;12(11):1071-7.
171. Gerdes J, Schwab U, Lemke H, Stein H. Production of a mouse monoclonal antibody reactive with a human nuclear antigen associated with cell proliferation. *Int J Cancer*. 1983;31(1):13-20.
172. Gaebler A, Penno A, Kuerschner L, Thiele C. A highly sensitive protocol for microscopy of alkyne lipids and fluorescently tagged or immunostained proteins. *J Lipid Res*. 2016;57(10):1934-47.
173. Townsend MJ, Fallon PG, Matthews DJ, Jolin HE, McKenzie AN. T1/ST2-deficient mice demonstrate the importance of T1/ST2 in developing primary T helper cell type 2 responses. *J Exp Med*. 2000;191(6):1069-76.
174. Herms A, Bosch M, Ariotti N, Reddy BJ, Fajardo A, Fernandez-Vidal A, et al. Cell-to-cell heterogeneity in lipid droplets suggests a mechanism to reduce lipotoxicity. *Curr Biol*. 2013;23(15):1489-96.
175. Kassan A, Herms A, Fernandez-Vidal A, Bosch M, Schieber NL, Reddy BJ, et al. Acyl-CoA synthetase 3 promotes lipid droplet biogenesis in ER microdomains. *J Cell Biol*. 2013;203(6):985-1001.
176. Rambold AS, Cohen S, Lippincott-Schwartz J. Fatty acid trafficking in starved cells: regulation by lipid droplet lipolysis, autophagy, and mitochondrial fusion dynamics. *Dev Cell*. 2015;32(6):678-92.
177. King AJ, Segreti JA, Larson KJ, Souers AJ, Kym PR, Reilly RM, et al. In vivo efficacy of acyl CoA: diacylglycerol acyltransferase (DGAT) 1 inhibition in rodent models of postprandial hyperlipidemia. *Eur J Pharmacol*. 2010;637(1-3):155-61.

178. Robinette ML, Fuchs A, Cortez VS, Lee JS, Wang Y, Durum SK, et al. Transcriptional programs define molecular characteristics of innate lymphoid cell classes and subsets. *Nat Immunol.* 2015;16(3):306-17.
179. Futatsugi K, Kung DW, Orr ST, Cabral S, Hepworth D, Aspnes G, et al. Discovery and Optimization of Imidazopyridine-Based Inhibitors of Diacylglycerol Acyltransferase 2 (DGAT2). *J Med Chem.* 2015;58(18):7173-85.
180. Hill BG, Dranka BP, Zou L, Chatham JC, Darley-Usmar VM. Importance of the bioenergetic reserve capacity in response to cardiomyocyte stress induced by 4-hydroxynonenal. *Biochem J.* 2009;424(1):99-107.
181. Ahmadian M, Suh JM, Hah N, Liddle C, Atkins AR, Downes M, et al. PPARgamma signaling and metabolism: the good, the bad and the future. *Nat Med.* 2013;19(5):557-66.
182. Bendixen AC, Shevde NK, Dienger KM, Willson TM, Funk CD, Pike JW. IL-4 inhibits osteoclast formation through a direct action on osteoclast precursors via peroxisome proliferator-activated receptor gamma 1. *Proc Natl Acad Sci U S A.* 2001;98(5):2443-8.
183. Lutas A, Yellen G. The ketogenic diet: metabolic influences on brain excitability and epilepsy. *Trends Neurosci.* 2013;36(1):32-40.
184. Newell C, Bomhof MR, Reimer RA, Hittel DS, Rho JM, Shearer J. Ketogenic diet modifies the gut microbiota in a murine model of autism spectrum disorder. *Mol Autism.* 2016;7(1):37.
185. Ignacio A, Breda CNS, Camara NOS. Innate lymphoid cells in tissue homeostasis and diseases. *World J Hepatol.* 2017;9(23):979-89.
186. Wilhelm C, Kharabi Masouleh S, Kazakov A. Metabolic Regulation of Innate Lymphoid Cell-Mediated Tissue Protection-Linking the Nutritional State to Barrier Immunity. *Front Immunol.* 2017;8:1742.
187. Sonnenberg GF, Artis D. Innate lymphoid cell interactions with microbiota: implications for intestinal health and disease. *Immunity.* 2012;37(4):601-10.
188. Statovci D, Aguilera M, MacSharry J, Melgar S. The Impact of Western Diet and Nutrients on the Microbiota and Immune Response at Mucosal Interfaces. *Front Immunol.* 2017;8:838.
189. Yao CH, Fowle-Grider R, Mahieu NG, Liu GY, Chen YJ, Wang R, et al. Exogenous Fatty Acids Are the Preferred Source of Membrane Lipids in Proliferating Fibroblasts. *Cell Chem Biol.* 2016;23(4):483-93.
190. von Moltke J, Ji M, Liang HE, Locksley RM. Tuft-cell-derived IL-25 regulates an intestinal ILC2-epithelial response circuit. *Nature.* 2016;529(7585):221-5.
191. Ricardo-Gonzalez RR, Van Dyken SJ, Schneider C, Lee J, Nussbaum JC, Liang HE, et al. Tissue signals imprint ILC2 identity with anticipatory function. *Nat Immunol.* 2018;19(10):1093-9.

192. Vasanthakumar A, Moro K, Xin A, Liao Y, Gloury R, Kawamoto S, et al. The transcriptional regulators IRF4, BATF and IL-33 orchestrate development and maintenance of adipose tissue-resident regulatory T cells. *Nat Immunol.* 2015;16(3):276-85.
193. Marcelin G, Chua S, Jr. Contributions of adipocyte lipid metabolism to body fat content and implications for the treatment of obesity. *Curr Opin Pharmacol.* 2010;10(5):588-93.
194. Iturralde M, Gamen S, Pardo J, Bosque A, Pineiro A, Alava MA, et al. Saturated free fatty acid release and intracellular ceramide generation during apoptosis induction are closely related processes. *Biochim Biophys Acta.* 2003;1634(1-2):40-51.
195. Yamaguchi M, Samuchiwal SK, Quehenberger O, Boyce JA, Balestrieri B. Macrophages regulate lung ILC2 activation via Pla2g5-dependent mechanisms. *Mucosal Immunol.* 2018;11(3):615-26.
196. Angela M, Endo Y, Asou HK, Yamamoto T, Tumes DJ, Tokuyama H, et al. Fatty acid metabolic reprogramming via mTOR-mediated inductions of PPARgamma directs early activation of T cells. *Nat Commun.* 2016;7:13683.
197. Blanchard PG, Festuccia WT, Houde VP, St-Pierre P, Brule S, Turcotte V, et al. Major involvement of mTOR in the PPARgamma-induced stimulation of adipose tissue lipid uptake and fat accretion. *J Lipid Res.* 2012;53(6):1117-25.
198. Siebeneicher H, Cleve A, Rehwinkel H, Neuhaus R, Heisler I, Muller T, et al. Identification and Optimization of the First Highly Selective GLUT1 Inhibitor BAY-876. *ChemMedChem.* 2016;11(20):2261-71.
199. Zhang D, Li J, Wang F, Hu J, Wang S, Sun Y. 2-Deoxy-D-glucose targeting of glucose metabolism in cancer cells as a potential therapy. *Cancer Lett.* 2014;355(2):176-83.
200. Rena G, Hardie DG, Pearson ER. The mechanisms of action of metformin. *Diabetologia.* 2017;60(9):1577-85.
201. Antoniewicz MR. A guide to (13)C metabolic flux analysis for the cancer biologist. *Exp Mol Med.* 2018;50(4):19.
202. Everaere L, Ait-Yahia S, Molendi-Coste O, Vorng H, Quemener S, LeVu P, et al. Innate lymphoid cells contribute to allergic airway disease exacerbation by obesity. *J Allergy Clin Immunol.* 2016;138(5):1309-18 e11.
203. Hamdy O, Tasabehji MW, Elseaidy T, Tomah S, Ashrafzadeh S, Mottalib A. Fat Versus Carbohydrate-Based Energy-Restricted Diets for Weight Loss in Patients With Type 2 Diabetes. *Curr Diab Rep.* 2018;18(12):128.
204. Taneja V. Sex Hormones Determine Immune Response. *Front Immunol.* 2018;9:1931.
205. Sunahara KK, Sannomiya P, Martins JO. Briefs on insulin and innate immune response. *Cell Physiol Biochem.* 2012;29(1-2):1-8.
206. Bhalla AK. Hormones and the immune response. *Ann Rheum Dis.* 1989;48(1):1-6.

207. Neal EG, Chaffe H, Schwartz RH, Lawson MS, Edwards N, Fitzsimmons G, et al. A randomized trial of classical and medium-chain triglyceride ketogenic diets in the treatment of childhood epilepsy. *Epilepsia*. 2009;50(5):1109-17.

## 8. Acknowledgements

The last 4 years in Bonn were an experience for which I am very grateful. I have learned a lot, both scientifically and personally. I am glad to have met so many new people and made new friends that made my time here so special. I would like to thank all people that made this thesis possible:

**Prof. Dr. Christoph Wilhelm**, my supervisor, for taking me as your first PhD student and teaching me how to be a scientist. You have always been very supportive and full of ideas which I am grateful for. Thank you for taking time when it was needed and for sometimes pushing me out of my comfort zone. It has been a great and challenging journey.

The whole Wilhelm group (**Marcel Michla, Fotios Karagiannis, Surendar Jayagopi, Vanessa Schmitt, Alexander Kazakov, Larissa Mühlenbeck**) for helping me in the lab and giving me new input and ideas for my work.

The Core Facility (**Andreas Dolf, Peter Wurst, Max Germer, David Kühne**) for your help with the Fortessa and sorting. Thank you for your time and patience and for always being so friendly.

**Mama & Papa & Khati & Bahareh & Shirin & rest of my family**, thank you for being the best family on earth!! Your love and support brought me so far and I am so grateful that I can rely on you always and no matter what. مرسی

**Samira**, for your mental support and for all the partys, cooking sessions or just chilling before my dancing class starts :D, for the great travelings we did together. Sri Lanka will be awesome! :) I hope there will be some more chances to do your make up and to see your scared face :D but you always looked great!

**Marcel**, for all the fun we had together in the lab and everywhere else! I just knew it from the beginning that we were made for each other :D Just have to laugh when I think about our (or my?!) laughter when you turned on your yellow light from Ikea or when I told you the story about the headlamp :D I am happy that I finally found someone who

loves to hear my loud music in the car without turning down the volume...Ich haaaasse es! :D don't forget: #sparplan #srilanka.

**Teresa**, for correcting my miserable english :D, for having great yoga sessions and long deep-talks about everything (while the car battery is draining and we have to wait for the ADAC :D), I am sure at some point we will end up together in Berlin! The universe will do the best for us! :\*

**Natalie**, for always being there for me and the ever-long phone calls :) I had the most relaxing holiday with you in Griechenschlafland! Maybe we can find some time in between in Sri Lanka to sleep when Samira and Marcel are not watching :P I enjoyed the time when you came here for "the project". Btw...wo ist eigentlich Mike?? :D

**Rebecca**, for the long and nice conversations on your cozy sofa, for sharing your party make up, I love your glitter stuff even though I still had it for the next five days in my face :D good glue! We still have to drive to Würzburg!! :) Jan a man is waiting for us! :D

**Charlie**, for being a friend since the day we met in the HET :) I loved all the dinners we had together and the origami night with milk rice! We should definitely repeat it! Maybe we both end up as yoga teachers and have our own studio together :D :)

**Romy**, for always being so positive and funny, even when your face was burnt in Tenerife like hell :D I guess your collected rainwater would have been a good face mask for that!! Next holiday we will take the bottle with us :D I was always happy to see you waving your hand in the BMZ even though I always realized to late that it is you :D :\*

**Helene**, for being the nicest and smartest bachelor student I had. I am happy that we could build up such a friendship even though we live far away from each other. I loved our breakfasts and our Ziegenkäse im Speckmantel :D See you soon in Oxford :) :\*

**Pia**, for accompanying me on my way (first had a typo and wrote "war", would also fit ;)) since 20 years. Omg 20!! :D all starting with our keyboard lessons. Sorry for leaving you alone with Schollmeyer :D This was the beginning of our musical career and I hope there will be a comeback of Nasiwamshi soon :D